U.PORTO

MESTRADO EM METABOLISMO – BIOPATOLOGIA E EXPERIMENTAÇÃO

Bioactivity and regenerative potential of functionalized polycaprolactone-based skin dressings for diabetic wounds management

Frantz Olivier Gojon

M

2024

MASTER IN METABOLISM – BIOPATHOLOGY AND EXPERIMENTAL

Bioactivity and regenerative potential of functionalized polycaprolactone-based skin dressings for diabetic wounds management

MSc Student: Frantz Olivier Gojon

Supervisor and affiliation

Maria Raquel Martins da Costa

Department of Biomedicine – Unit of Biochemistry, Faculty of Medicine of Porto, University of Porto, Porto, Portugal

Centre for Biotechnology and Fine Chemistry (CBQF), Catholic University of Portugal, Porto, Portugal

Co-supervisor and affiliation

Rúben Miguel Pereira Fernandes

Full Professor - University Fernando Pessoa

AGRADECIMENTOS

Quero começar estes agradecimentos por mencionar a pessoa que deu início à minha carreira científica e desde então me tem ajudado a subir cada degrau para que continue a atingir patamares cada vez mais elevados a nível científico e académico. Obrigado Professor Rúben, sem si não estava a entregar hoje uma tese de mestrado. Espero continuar a estar aqui para observar também todas as suas conquistas.

Quero também agradecer à pessoa que completou a outra metade da minha orientação. A pessoa que apesar do seu distinto conhecimento científico e elevada capacidade intelectual, tem uma incrível capacidade humana para descer e se colocar no mesmo patamar que eu e, por ao longo destes 3 longos anos, perceber sempre a minha disponibilidade e demais compromissos, não sendo só uma orientadora, mas acima de tudo uma voz amiga.

Prof. Raquel Soares, obrigado por ter tanta paciência, não só comigo, mas com todos os alunos que passam pelas suas mãos. O nosso mestrado não podia estar em melhores mãos. Finalmente, ao fim de 3 anos já se vai ver livre de mim!

Quero agradecer a todo o staff do departamento de bioquímica da FMUP, UFP e HE-UFP por realmente me terem feito sentido “acolhido” nas minhas instituições de acolhimento.

Agora e com um carinho muito especial, quero agradecer a todos aqueles que sem obrigação, despenderam do seu precioso tempo para garantir que um dia seria mestre.

André Sousa, se tivesse de colocar por palavras toda a ajuda que me deste, não conseguia entregar a tese a tempo. Se estou hoje aqui a entregar a tese, é graças a ti. Para além do trabalho todo que tivemos vindo a desenvolver juntos, sempre com muitos sorrisos à mistura, em especial neste, posso considerar que foste também um dos meus orientadores.

Catarina Rocha, eu sei que ainda não tens filhos, mas durante estes 3 anos acho que tiveste um bom estágio comigo. Obrigado por toda a paciência que tiveste comigo, por todos os ensaios que me ensinaste a fazer, por todos os protocolos que me deste 17 vezes, porque eu não uso cadernos. Segunda-feira vais me aturar outra vez, que tenho que melhorar uns “n” da minha tese.

Liliana Carvalho, acho que senão fosses tu ainda estava a tentar formatar as minhas tabelas. Obrigado por toda a paciência que tens com os estudantes, obrigado por todos os lembretes, obrigado por perderes 4 horas seguidas da tua vida a formatar a minha tese, e acima de tudo por o fazeres com tanto gosto e sempre com um sorriso na cara. No entanto, não vou meter uma foto dos meus porquinhos na tese porque não me deixaste.

Cláudia Sousa-Mendes e Diana Meireles, obrigado por toda a ajuda que me deram, mesmo não estando associado ao piso 6. Mais importante que toda a ajuda, é o à vontade com que me deixam para o fazer e, saber que o fazem de bom grado. Cláudia, prometo que te vou continuar a dizer olá quando passar no piso 6 e Diana espero poder continuar a trabalhar contigo, nem que seja só a levar-te os sangues do Dr. Pedro.

Por último e extratrabalho científico e académico quero também agradecer aqueles que fazem parte da minha vida numa base diária.

A todos os colegas do biotério (Catarina, Flávia, Cristina, Dona Sónia, Joel, Mariana, Carolina, Dona Ginha, Liliana, Prof. Patrícia) obrigado por todos os momentos de carinho e pela constante preocupação em me verem mestre. Obrigado por todas as trocas e liberdade de horários que me permitiram acabar o mestrado. Um grande obrigado ao Dr. Pedro e à agora Dra. Liliana, por serem os melhores "chefes emprestados" que podia ter.

A todos os colegas do Coliseu Porto AGEAS, obrigado por serem a melhor equipa do mundo e por transmitirem o sentimento que juntos conseguimos resolver qualquer problema. Obrigado por transformarem um trabalho num hobbie remunerado. Obrigado Tapeface, por me comprares sempre o jantar para eu poder conciliar os meus 17 trabalhos.

À minha parceira professora da ESS, Cláudia, obrigado por me fazeres gostar de dar aulas.

Obrigado à minha família. Obrigado Tuna TS. Principalmente aqueles com quem tenho o prazer de trabalhar todos os dias. Mesmo com alguma discórdia, emoções à mistura, no final do dia damos conta do recado e reina a música, as tunas e a boémia, pilares que nos mantém unidos ao longo de todos estes anos. No entanto, tenho de deixar uma nota a algumas pessoas. Pedro e Miguel, não é por me ligarem 18 vezes às 03h que vos vou atender. Biclas, quero que saibas que houve momentos que deixei de fazer a tese para ler as tuas opiniões no grupo da direção e, estou arrependido com essa decisão. Estandartes, demorei 3 anos a acabar a tese, mas pelo menos tivemos 15 prémios seguidos. Pandeiretas, com jeitinho também chegamos lá. Especialmente se o Zelensky continuar a ter concertos em Lisboa.

Michelin, Rafa, Gancho e Leonor (sim, Leonor não devias, mas também tens direito) muito obrigado por dizerem sempre "sim" a todos os planos que combinamos em cima da hora e por serem as pessoas mais genuínas que conheço.

Eminem, António, Joel, Diogo e Gustavo. Acabei a licenciatura de férias convosco em Madrid. Agora acabo o mestrado, infelizmente sem vocês todos por perto fisicamente, mas sempre bem perto no pensamento. Agora já me posso juntar ao vosso grupo de mestres.

Joana, obrigado por teres sido um pilar importante da minha vida nestes últimos 3 anos. Obrigado por me acolheres sempre em tua casa, me tratares melhor que ninguém e acima de tudo me compreenderes sempre. Espero que daqui a 4 anos sejas tu a estar a entregar a tua tese de licenciatura em Bioquímica!

Um agradecimento especial a todos os porquinhos dos quais eu cuido e contribuem com a sua vida para o avanço da ciência.

Por último e não menos importante, um obrigado a toda a minha família que mesmo na adversidade me acolheu e me deu um lar, onde não só vivi mas também pude chamar de casa. Obrigado Tia, Rui, Diana. Obrigado Avô por todo o esforço que fazes. Obrigado Tio, por seres um pai para mim. Obrigado Avó, por seres mais do que uma mãe. Obrigado por viveres para eu ser feliz e que não me falte nada.

SUMMARY

Chronic wounds are associated with rising morbidity and mortality rates, placing a considerable strain on healthcare systems worldwide. Diabetic foot ulcers (DFU) and lower limb complications, which frequently lead to amputations, affect 40 to 60 million diabetic individuals globally, posing a significant economic, social, and public health challenge. Despite extensive efforts to develop cellular and molecular therapies aimed at promoting wound healing, achieving complete regeneration that is clinically applicable remains elusive, underscoring the need for innovative treatment strategies.

In this study, we employed both *in vitro* and *in vivo* approaches, using skin cell lines and a diabetic wound model in *db/db* mice, to evaluate the effects of two types of polycaprolactone (PCL) membranes—microporous and macroporous—as skin substitutes for treating diabetic wounds. We further investigated the potential of two bioactive compounds, grape stem extract (GSE) and cannabidiol (CBD), with the aim of functionalizing the PCL membranes to enhance their regenerative capacity.

Our results demonstrated that *in vivo* the PCL membranes alone promoted skin regeneration in the diabetic wound model, with the microporous membrane showing superior regenerative effects compared to the macroporous variant. Additionally, we observed that CBD *in vitro* exhibited promising regenerative potential. These findings suggest that the combination of microporous PCL membranes and CBD could offer a potent strategy for improving diabetic wound healing.

RESUMO

As feridas crónicas estão associadas a taxas crescentes de morbilidade e mortalidade, colocando uma pressão considerável nos sistemas de saúde em todo o mundo. As úlceras do pé diabético (DFU) e as complicações dos membros inferiores, que frequentemente levam a amputações, afetam 40 a 60 milhões de indivíduos diabéticos globalmente, representando um desafio económico, social e de saúde pública significativo. Apesar dos extensos esforços para desenvolver terapias celulares e moleculares direcionadas para promover a cicatrização de feridas, a regeneração completa e clinicamente aplicável ainda não foi alcançada, sublinhando a necessidade de estratégias terapêuticas inovadoras.

Neste estudo, utilizámos abordagens tanto *in vitro* quanto *in vivo*, usando linhas celulares de pele e um modelo de ferida diabética em ratinhos *db/db*, para avaliar os efeitos de dois tipos de membranas de policaprolactona (PCL)—microporosa e macroporosa—como substitutos da pele para o tratamento de feridas diabéticas. Investigámos também o potencial de dois compostos bioativos, extrato de engaço de uva (GSE) e canabidiol (CBD), com o objetivo de funcionalizar as membranas de PCL e aumentar a sua capacidade regenerativa.

Os nossos resultados demonstraram que as membranas de PCL *in vivo*, por si só, promoveram a regeneração da pele no modelo de ferida diabética, com a membrana microporosa a apresentar efeitos regenerativos superiores em comparação com a variante macroporosa. Além disso, observámos que o CBD *in vitro* apresentou um potencial regenerativo promissor. Estes achados sugerem que a combinação de membranas microporosas de PCL e CBD pode representar uma estratégia eficaz para melhorar a cicatrização de feridas diabéticas.

TABLE OF CONTENTS

AGRADECIMENTOS ..... **III**

SUMMARY ..... **VII**

RESUMO ..... **IX**

TABLE OF CONTENTS ..... **XI**

INDEX OF FIGURES ..... **XV**

INDEX OF TABLES ..... **XIX**

ABBREVIATIONS ..... **XXI**

INTRODUCTION **1**

1. DIABETES 1

1.1 Types *1*

1.1.1 Type 1 diabetes 1

1.1.2 Type 2 diabetes 2

1.1.3 MODY (Maturity-onset diabetes of the young) 3

1.1.4 Gestational diabetes 5

1.1.5 Neonatal diabetes 5

1.1.6 Diabetes mellitus secondary to endocrinal pathologies 7

1.2 Diagnosis *9*

1.3 Complications *10*

1.3.1 Cardiovascular System 10

1.3.2 Renal system 11

1.3.3 Ocular system 13

1.3.4 Nervous system 14

1.3.5 Immune system 15

1.3.6 Other systems 16

2. DIABETIC FOOT WOUNDS 16

2.1. Definition and Epidemiology *16*

2.2. Physiopathology *17*

2.3. Classification and Staging *19*

2.4. Complications of diabetic foot *20*

2.5. Diagnosis and clinical evaluation *21*

2.6. Treatment and management of diabetic foot *22*

3. ANIMAL MODELS 23

3.1. Importance of Animal Models in Wound Healing Research *23*

3.2. Commonly Used Animal Models for Diabetic Wound Studies *23*

4. POLYCAPROLACTONE MEMBRANES 25

4.1. Characteristics *25*

4.2. Applications *26*

4.3. Fabrication process *27*

4.4. Advantages and Disadvantages *27*

5. BIOACTIVE COMPOUNDS 27

5.1. Grape stem extract *28*

5.1.1. Introduction 28

5.1.2. Chemical composition 28

5.1.3. Extraction methods 29

5.1.4. Analytical analysis 29

5.1.5. Biological activity 30

5.1.6. Current applications 30

5.1.7. Sustainability 30

5.2. Cannabidiol extract *30*

5.2.1. Chemical composition and pharmacokinetics 31

5.2.2. Extraction methods 31

5.2.3. Biological activity and biomedical applications 32

5.2.4. Commercialized products 33

AIMS **35**

MATERIALS AND METHODS **37**

PCL MEMBRANES 37

Pore size *37*

Electrospinning process *37*

CELL LINES 37
CELL COUNTING 37
Hemocytometer *37*
MEMBRANE ASSAYS 38
CELL VIABILITY 38
MTT assay *38*
CELL MOTILITY 39
Wound healing *39*
ANIMAL MODEL 39
Housing conditions *39*
Skin Wound Healing Model *40*
RNA EXTRACTION 41
RNA extraction from skin rodent samples *41*
RNA QUALITY EVALUATION 42
REVERSE TRANSCRIPTASE POLYMERASE CHAIN REACTION (RT-PCR) 42
Complementary DNA (cDNA) synthesis *42*
Primers used *43*
Thermocycler *43*
HISTOLOGY 44
Hematoxylin-Eosin *44*
Masson´s Trichrome *44*
Verhoeff-Van Gieson *44*
STATISTICAL ANALYSIS 45
RESULTS 47
PCL MEMBRANES 47
MTT assay *47*
Wound Healing *49*
MACROSCOPIC EVALUATION 54
HISTOLOGY 55

RNA EXPRESSION 56

BIOCOMPOUNDS 57

MTT assay *57*

DISCUSSION **59**

CONCLUSIONS **69**

FUTURE PERSPECTIVES **71**

APPENDICES **73**

LIST OF APPENDICES 73

APPENDIX A - ANIMAL WELFARE COMMITTEE OF THE FACULTY OF MEDICINE OF THE UNIVERSITY OF PORTO APPROVAL 74

APPENDIX B – PROJECT "6-WELL PLATE INSERT" 75

APPENDIX C – AWARD "BRAGANÇA PARREIRA" FROM SPD 2023 77

APPENDIX D – SPD 2023 POSTER CERTIFICATE 78

REFERENCES **79**

INDEX OF FIGURES

Figure 1 - Scheme illustrating the pathology of type I Diabetes and type II Diabetes, compared to a healthy individual. 3

Figure 2 - MODY diagnosis flowchart, sourced from [25]. 4

Figure 3 - Illustrating images of endocrine pathologies that lead to diabetes. A) Enlarged hands of an acromegaly patient [187]; B) Round face in a Cushing´s syndrome patient [188]; C) CT scan showing a pheochromocytoma [189]; D) Exophtalmus in a Graves´ disease patient [190]; E) CT scan showing two benign tumors in a primary aldosteronism patient [191]; E) Histological staining of a somatostaninoma [192]. 9

Figure 4 - Anatomy of the blood vessels of the foot, highlighting the dorsal pedis artery in green [193]. 11

Figure 5 - Implications of diabetes in several pathways ultimately leading to DKD, sourced from [67] PKC: protein kinase; AGE: advanced glycation end products; ECM: extracellular matrix; RAGE: receptor for advanced glycation end products, SAPK/JNK: stress-activated protein kinases/Jun amino-terminal kinases, ERK1/2: extracellular signal-regulated kinase 1/2, JAK/STAT: Janus kinase/signal transducers and activators of transcription, ICAM-1: intercellular adhesion molecule 1, VCAM-1: vascular cell adhesion molecule 1, TNF-α: tumor necrosis factor alpha, CTGF: connective tissue growth factor, PAI-1: plasminogen activator inhibitor 1. 12

Figure 6 - Retina location and anatomy [194]. 13

Figure 7 - Four stages of wound healing: hemostasis (coagulation), inflammation, proliferation and remodeling. 18

Figure 8 - NETosis: Formation of Neutrophil Extracellular Traps (NETs), sourced from [195]. 19

Figure 9 - Illustrative figure of gangrenous and healthy tissue in a foot [196]. 21

Figure 10 - Example of rodents used in research: on the left, a C57BL/6 (mice); on the right, a Sprague-Dawley (rat) [202], [203]. 23

Figure 11 - STZ-Induced Diabetes Model. (A) Mechanism of pancreatic β-cell damage through single or multiple doses of STZ. (B) STZ's action mechanism within the nucleus of β-cells, sourced from [204]. 24

Figure 12 - Db/db mice [205]. 25

Figure 13 - Synthesis of poly(e-caprolactone), highlighting the recurring sequence of e-caprolactone units [197]. 26

Figure 14 - Grape stem [199]. 28

Figure 15 - Principle of Folin-Ciocalteu method to assess Total Phenolic Content [200]. 29

Figure 16 - Molecular structure of cannabidiol [201] 31

Figure 17 - CBD mechanism of action on CB2 receptor. 33

Figure 18 - Animal number 1 being monitored and eating corn. 39

Figure 19 - Db/db mice wound healing model with the 3 experimental groups. 40

Figure 20 - Moment of application of the membranes to each experimental group. 41

Figure 21 - Schematic program used in the thermocycler. 43

Figure 22 - MTT direct assay of PCL membranes in HDF cell line (n=2). CN: Control group; Tega: Tegaderm™; Micro: Microporous; Macro: Macroporous. 47

Figure 23 - MTT indirect contact assay of PCL membranes in HDF cell line (n=2). CN: Control group; Tega: Tegaderm™; Micro: Microporous; Macro: Macroporous. 47

Figure 24 - MTT direct assay of PCL membranes in HaCat cell line (n=2). CN: Control group; Tega: Tegaderm™; Micro: Microporous; Macro: Macroporous. 48

Figure 25 - MTT indirect contact assay of PCL membranes in HaCat cell line (n=2). CN: Control group; Tega: Tegaderm™; Micro: Microporous; Macro: Macroporous 48

Figure 26 - Wound Healing assay in HDF cells: control group (n=1). 49

Figure 27 - Wound Healing assay in HDF cells: Tegaderm™ group (n=1). 50

Figure 28 - Wound Healing assay in HDF cells: microporous group (n=1). 51

Figure 29 - Wound Healing assay in HDF cells: macroporous group (n=1). 52

Figure 30 - Macroscopic photos of the wounds after 21 days of regeneration. 54

Figure 31 - Histological staining of skin wounds in db/db mice. A: H&E staining of animal 1 (TEGA group). Magnification 4x. B: H&E staining of animal 9 (MICRO group). Magnification 4x. C: H&E staining of animal 15 (MACRO group). Magnification 4x. D: MT staining of animal 1 (TEGA group). Magnification 4x. E: MT staining of animal 9 (MICRO group). Magnification 4x. F: MT staining of animal 15 (MACRO group). Magnification 4x. G: VVG staining of animal 9 (MICRO group). H: VVG staining of animal 15 (MACRO group). H&E: Hematoxylin and Eosin; MT: Masson's Trichrome; VVG: Verhoeff-Van Gieson; TEGA: Tegaderm™; MICRO: Microporous; MACRO: Macroporous. 55

Figure 32 - RNA expression of VEGFR2. Tega: Tegaderm™; Micro: microporous; Macro: macroporous. 56

Figure 33 - RNA expression of TGF-B2. Tega: Tegaderm™; Micro: microporous; Macro: macroporous. 56

Figure 34 - MTT assay of GSE in HDF cell line (n=2). 57

Figure 35 - MTT assay of GSE in HaCat cell line (n=2). 57

Figure 36 - MTT assay of CBD in HaCat cell line (n=1). 58

Figure 37 - Scheme highlighting the role of TGF-β2 in scar formation, sourced from [185] ... 64

INDEX OF TABLES

Table 1 - Genes responsible for Neonatal Diabetes, sourced from [38]. 6

Table 2 - Reference values, prediabetes, and diabetes values for diagnosis, sourced from [61]. 10

Table 3 - Types of neuropathies, affected axons, symptoms, and pathophysiological mechanisms of neuropathies related to diabetes, sourced from [70], [71], [72], [73], [74] and [75]. 15

Table 4 - PEDIS classification, sourced from [93]. PAD - Peripheral Arterial Disease; CLI - Critical Limb Ischemia; SIRS - Systemic Inflammatory Response Syndrome. 20

Table 5 - Parameter used in cDNA synthesis. 42

Table 6 - List of primers used and respective sequence, both forward and reverse. 43

Table 7 - Parameters used in RT-PCR 43

Table 8 – Percentage of closure of the wound healing assay of the various experimental groups (n=1). 53

ABBREVIATIONS

2H-PG 2 hours plasma glucose

5-HT3 Serotonin

ACTH Adrenocorticotropic hormone

AGE Advanced glycation end products

AGIs Alpha-glucosidase inhibitors

AMPK 5' adenosine monophosphate-activated protein kinase

ATCC American Type Culture Collection

ATP Adenosine triphosphate

BACH1 BTB Domain And CNC Homolog 1

CB1 Type 1 cannabinoid receptor

CB2 Type 2 cannabinoid receptor

CBD Cannabidiol

CBDA Cannabidiolic acid

cDNA Complementary DNA

CLI Critical Limb Ischemia

CMP Cardiomyopathy

CRP C-reactive protein

CT Computed tomography

CTGF Connective tissue growth factor

DFU Diabetic foot ulcers

DGAV Direção-Geral da Alimentação e Veterinária

DKD Diabetic kidney disease

DM Diabetes mellitus

DMEM Dulbecco's Modified Eagle Medium

DMSO Dimethyl sulfoxide

DN Diabetic neuropathy

DR Diabetic retinopathy

ECM Extracellular matrix

EMA European Medicines Agency

ERK1/2 Extracellular signal-regulated kinase ½

ESRD End-stage kidney disease

FBS Fetal Bovine Serum

FDA Food and Drug Administration

FDM Fusion deposition modeling

FMUP Faculty of Medicine – University of Porto

FPG Fasting plasma glucose

FTIR Fourier-Transform Infrared

GC-MS Gas Chromatography-Mass Spectrometry

GDM Gestational diabetes mellitus

GFAT Glutamine:fructose-6-phosphate-amidotransferas

GI Gastrointestinal tract

GLP-1 Glucose-like peptide 1

GLUT-2 Glucose transporter type 2

GLUT-4 Glucose transporter type 4

GRAS Generally Recognized As Safe

GSE Grape stem extract

H&E Hematoxylin and eosin

HaCat Human Keratinocyte

HbA1C Glycated hemoglobin

HDF Human Dermal Fibroblasts

HDL High density lipoprotein

HIF-1 Hypoxia-Inducible Factor 1

HLA Human leukocyte antigen

HMOX1 Heme oxygenase 1

HNF Hepatocyte Nuclear Factor

HPLC High-Performance Liquid Chromatography

ICAM-1 Intercellular adhesion molecule 1

IL Interleukin

JAK/STAT Janus kinase/signal transducers and activators of transcription

K_{ATP} Potassium channels

LC-MS Liquid Chromatography-Mass Spectrometry

LDH Lactate dehydrogenase

LDL Low-density lipoprotein

MCP-1 Monocyte chemoattractant protein-1

MI Myocardial infarction

MODY Maturity-onset diabetes of the young

MRI Magnetic Resonance Imaging

MT Masson's trichrome

MTT 3-(4,5-Dimethylthiazol-2-yl)-2,5-diphenyltetrazolium bromide

NADPH Nicotinamide adenine dinucleotide phosphate hydrogen

NETs Neutrophil Extracellular Traps

NMPA National Medical Products Administration

NMR Nuclear Magnetic Resonance

NO Nitric oxide

NPDR Non-proliferative diabetic retinopathy

NPWT Negative Pressure Wound Therapy

OGTT Oral Glucose Tolerance Test

PA Primary aldosteronism

PAD Peripheral arterial disease

PAI-1 Plasminogen activator inhibitor-1

PBS Phosphate-buffered saline

PCL Polycaprolactone

PCOS Polycystic ovary syndrome

PDGF Platelet-derived growth factor

PDR Proliferative diabetic retinopathy

PEDIS Perfusion, Extent, Depth, Infection and Sensation

PET Positron emission tomography

PK Pyruvate kinase

PKC Protein kinase

PPAR-γ Gamma isoform of peroxisome proliferator-activated receptor

RAGE Receptor for advanced glycation end products

RNA Ribonucleic acid

ROS Reactive oxygen species

SAPK/JNK Stress-activated protein kinases/Jun amino-terminal kinases

SINBAD Site, Ischemia, Bacterial Infection, Area, and Depth

SIRS Systemic Inflammatory Response Syndrome

SPD Sociedade Portuguesa de Diabetologia

SPECT Single-photon emission computed tomography

STZ Streptozotocin

T1DM Type 1 Diabetes mellitus

T2DM Type 2 Diabetes mellitus

T3 Triiodothyronine

T4 Thyroxine

TCC Total contact casting

TFC Total Flavonoid Content

TGF-β1 Transforming growth factor β1

THC Tetrahydrocanabinol

THC Tetrahydrocannabinol

THCA Tetrahydrocannabinolic acid

TIRAP Toll-Interleukin 1 Receptor (TIR) Domain Containing Adaptor Protein

TLR Toll-Like Receptor

TNF-α Tumor necrosis factor alpha

TPC Total Phenolic Content

UFP University Fernando Pessoa

UPR Unfolded protein response

VCAM-1 Vascular cell adhesion molecule 1

VEGF Vascular endothelial growth factor

VEGFR2 Vascular endothelial growth factor receptor 2

VVG Verhoeff-Van Gieson

WHO World Health Organization

INTRODUCTION

1. Diabetes

Diabetes mellitus (DM) is a metabolic disorder defined by impairments in insulin production or function, leading to chronically elevated blood glucose levels and widespread metabolic disturbances. There are several types of diabetes, including type 1 diabetes, type 2 diabetes, maturity-onset diabetes of the young (MODY), gestational diabetes, neonatal diabetes, and diabetes originating from secondary causes due to endocrinal pathologies [1].

1.1 Types

1.1.1 Type 1 diabetes

Type 1 DM is a chronic autoimmune disease that destroys insulin-producing beta cells in the pancreas. Insulin is a hormone that binds to insulin receptors, which are transmembrane receptors that belong to the class of tyrosine kinase receptors. When insulin binds to this receptor, it triggers the translocation of GLUT-4 to the membrane, allowing glucose to be stored. Without insulin, glucose accumulates in the bloodstream leading to diabetes (Figure 1) [2], [3]. The underlying causes that lead to the body's destruction of its beta cells are unknown, although it is believed that this damage results from a balance between genetics and environmental factors [4].

Regarding genetic factors, HLA DR3/DQ2 and HLA DR4/DQ8 (specific genetic markers found in the human leukocyte antigen (HLA) system), increased PTPN22 activity (encodes a protein involved in the regulation of immune system activity), IL2RA variants (encodes a protein that is part of the interleukin-2 (IL-2) receptor complex), and a first-degree relative with type 1 DM are known to be risk factors. The presence of DRB1*15:01, DQA*01:02, DQB1*06:02 (specific genetic variants within the HLA system), and a rare variant of IFIH1 (gene that encodes the MDA5 protein) are known to be protective factors. Concerning environmental factors, group B Coxsackieviruses, early cereal introduction, high latitudes, cold seasons, white ethnicity, and maternal age inferior to 35 years old are risk factors. Longer breastfeeding duration, vitamin D intake supplements, intestinal microbiome, and multiple living siblings are considered protective factors [4].

The treatment includes insulin therapy, glucose monitoring, and diet awareness. Insulin therapy can be performed with lifelong insulin replacement with multiple daily insulin injections, insulin pump therapy, or the use of an automated insulin delivery system [3]. Type 1 DM represents about 5 percent of all diabetes cases worldwide. In 2022, 62% of all new type 1 DM cases were diagnosed in people aged less than 20 years old. As of 2022, there were 8.75 million people

with type 1 diabetes, with one-fifth of those individuals living in low-income and lower-middle-income countries [5], [6], [7].

1.1.2 Type 2 diabetes

Type 2 DM is characterized by two primary factors, a deficient insulin secretion by pancreatic beta cells and tissue insulin resistance – a reduced ability of insulin to exert its biological activity on target tissues, namely adipose tissue, skeletal muscle, and liver (Figure 1) [8]. Although it is not entirely known what causes this insulin resistance, there are some pathways with implications in this process, such as the accumulation of ectopic lipid metabolites, activation of the unfolded protein response (UPR) pathway, and innate immune pathways. The correlation between lipid accumulation and insulin resistance has been widely described and accepted [8], [9].

Weight – being overweight or obese-, fat distribution – main storage of fat being abdominal-, sedentarism– lack of physical activity-, family history – 1st degree-, race and ethnicity – being Black, Hispanic, or Asian-, blood lipid levels – low levels of HDL-, and having polycystic ovary syndrome (PCOS) are risk factors that increase the probability of a certain individual to have type 2 DM [8], [9].

Type 2 DM management requires both behavioral and pharmacological approaches [10]. Changes in dietary intake, exercise, sleep habits, stress management, and reduction of sedentary behavior contribute to the management of type 2 DM [11].

The pharmacological approach is based on the intake of oral antihyperglycemic agents, such as insulin secretagogues, insulin sensitizers, and drugs that delay the absorption of carbohydrates from the gastrointestinal tract [12]. Insulin secretagogues can be divided into two categories: sulfonylureas (glibenclamide, glipizide, glicazide) and meglitinide analogues (nateglinide and repaglinide) [13]. Sulfonylureas function by closing ATP-sensitive potassium channels on the pancreatic β-cell membrane, which triggers an increase in insulin secretion regardless of glucose levels [14]. Meglitinide analogues stimulate insulin release by inhibiting ATP-sensitive potassium channels on the beta-cell membrane, binding to a receptor different from that of sulfonylureas [15].

Regarding insulin sensitizers, there are two main classes: biguanides (metformin) and thiazolidinediones [16]. Biguanides, such as metformin, stimulate AMP-activated protein kinase (AMPK) which leads to decreased blood glucose concentration by different mechanisms, such as decreased hepatic gluconeogenesis, improved tissue sensitivity to insulin, increased peripheral glucose uptake and decreased intestinal absorption of glucose [17]. Thiazolidinediones, also known as glitazones, activate the γ isoform of peroxisome proliferator-

activated receptor - PPAR-γ -, leading to the alteration of gene transcription involved in glucose metabolism. This alteration reduces insulin resistance in adipose tissue, liver, and muscles [18].

Alpha-glucosidase inhibitors (AGIs) are drugs that delay the absorption of carbohydrates. They bind reversibly to the oligosaccharide binding site of enzymes that do the degradation of complex nonabsorbable carbohydrates, leading to a reduced peak of blood glucose after meals [19].

In 2017, an estimated 462 million individuals worldwide were living with type 2 DM, representing 6.28% of the world population. Diabetes is accountable for more than 1 million deaths per year, being the ninth leading cause of mortality worldwide [20]. Type 2 DM represents 90-95% of all diabetes cases [21].

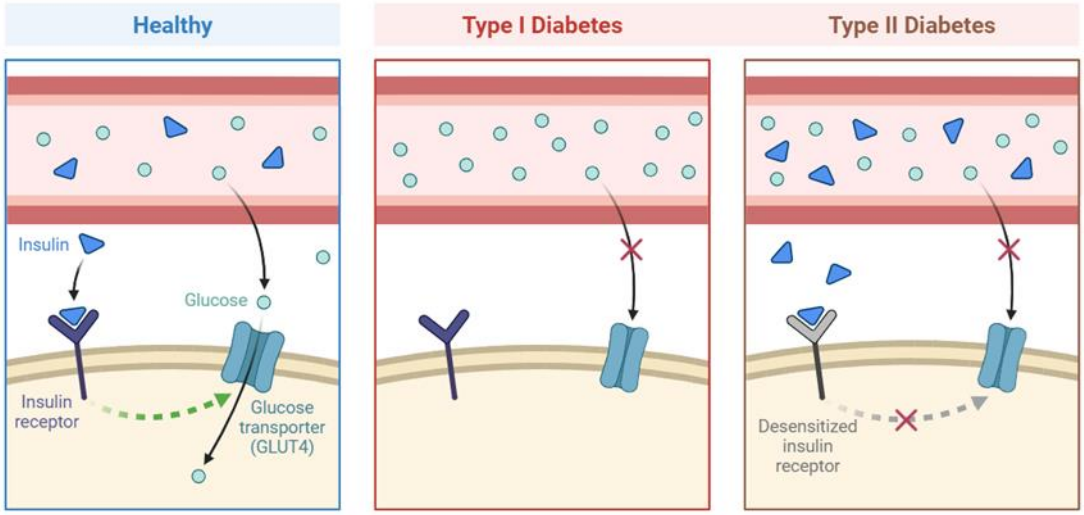

Figure 1 - Scheme illustrating the pathology of type I Diabetes and type II Diabetes, compared to a healthy individual.

1.1.3 MODY (Maturity-onset diabetes of the young)

Maturity-onset diabetes of the young (MODY) is a monogenic type of diabetes with autosomal dominant inheritance, first described by Tattersall and Fajans in 1974. Although there are at least fourteen different known mutations, the four most common types of MODY are related to the gene HNF1-alpha (MODY 3), HNF4-alpha (MODY 1), HNF1-beta (MODY 5) or Glucokinase (MODY 2). HNF1-alpha is responsible for 70% of MODY´s cases. Impairment of HNF-1 alpha leads to diabetes by lowering the amount of insulin produced by the pancreas. HNF4-alpha impairment is less common and usually, those that carry this gene defect were born with 4 or

more kilograms. Both these kinds of MODY are treated with sulphonylureas. HNF1-beta apart from diabetes can also lead to renal cysts, uterine abnormalities, and gout [22], [23].

Glucokinase is a monomeric intracellular enzyme that phosphorylates glucose to glucose-6-phosphate, helping the body recognize blood glucose levels. Impairment of this gene leads to defective enzymes and less control of glucose levels. Normally, patients are asymptomatic, and they do not need treatment. Generally, MODY manifests before 25 years of age and is often misdiagnosed as type 1 or type 2 DM [22], [23].

The Practice Guidelines for MODY defined some criteria for MODY diagnosis: onset of diabetes in a family member before 25 years of age, two consecutive generations of patients with diabetes in the family, absence of beta-cell antibodies, persistent endogenous insulin production in addition to preservation of pancreatic beta-cell function as evidenced by C-peptide levels >200pmol/L in addition to lack of necessity for insulin therapy even years after diagnosis [24]. Nkonge et al also proposed in 2020 a flowchart ([25]) on how to diagnose MODY cases [26]. It is estimated that MODY accounts for 1-5% of all DM cases worldwide [26].

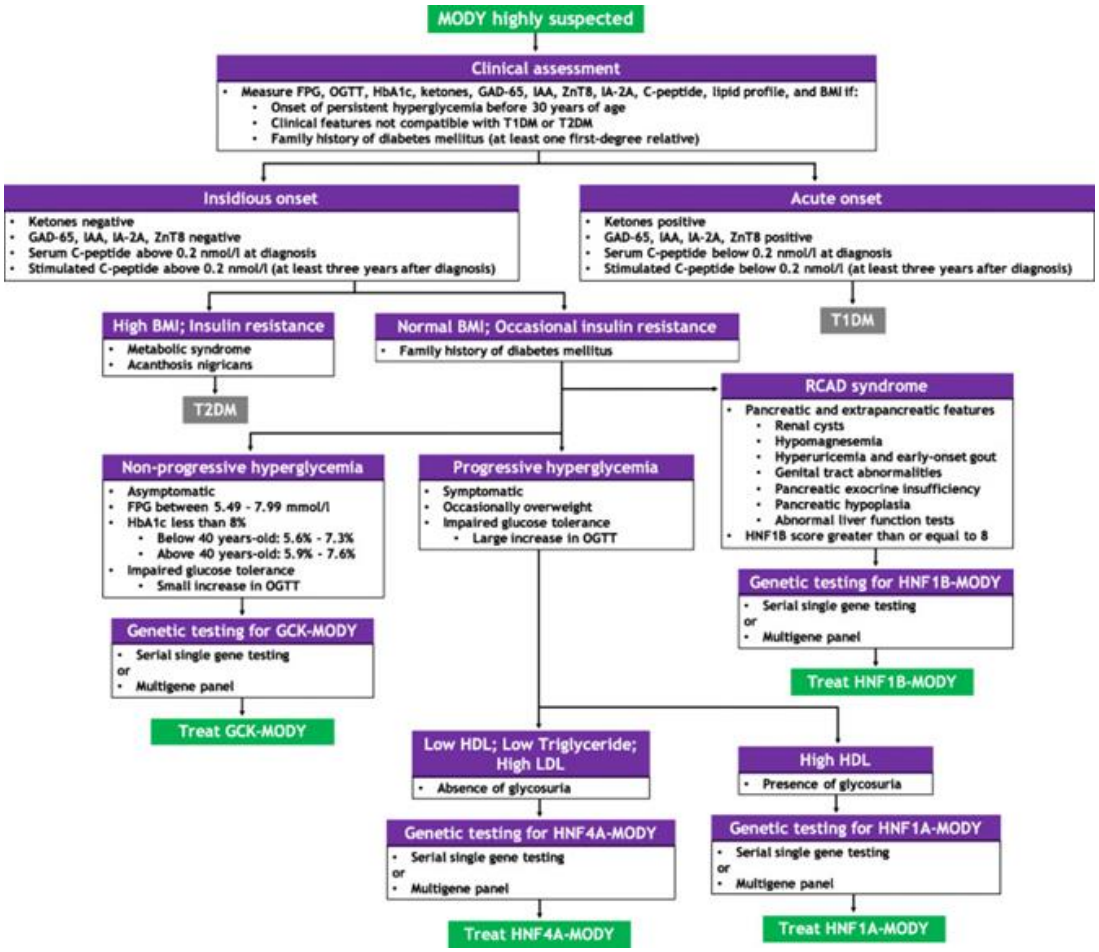

Figure 2 - MODY diagnosis flowchart, sourced from [25].

1.1.4 Gestational diabetes

Gestational diabetes mellitus (GDM) is characterized by any degree of glucose intolerance that begins or is first identified during pregnancy. GDM can be classified into two categories: A1GDM or A2GDM. A1GDM is managed without the need for medication, resorting only to a nutritional-controlled diet. A2GDM patients need medication to achieve adequate blood glucose levels [27]. The gold-standard method to diagnose GDM is the Oral Glucose Tolerance Test (OGTT), where a dose of glucose is orally administered, and blood glucose levels are screened one or two hours after [28], [29].

Several risk factors increase the likelihood of developing GDM, including being overweight or obese, having prediabetes, previous record of GDM, having polycystic ovary syndrome, or having an immediate family member with diabetes [30]. Although GDM typically resolves after delivery, there can be consequences for both the mother and the child. Regarding the mother, GDM is associated with antenatal depression, increased risk of developing T2DM (60%), and permanent alterations in the vasculature, which lead to a higher risk of cardiovascular disease – the number one cause of death worldwide. For the child, GDM can lead to macrosomia at birth, insulin resistance, a higher risk of childhood obesity, and cardiovascular and metabolic diseases [31].

Gestational diabetes affects 14% of pregnancies worldwide, although some authors claim an overdiagnosis of GDM in recent years [32], [33].

1.1.5 Neonatal diabetes

Neonatal diabetes is characterized by the development of persistent hyperglycemia within the first six months of life. Although many genes are associated with neonatal diabetes (Table 1), 80% of cases are caused by a mutation in KCNJ11 or ABCC8 genes, which 2encode the two subunits of the ATP-sensitive potassium channel [34], [35].

In a normal pancreatic beta-cell, when there are increased glucose levels, glucose is transported across the cell membrane by GLUT-2 and metabolized by glucokinase. This process raises ATP production, leading to the closure of potassium channels (K_{ATP}). As a result, the cell membrane depolarizes, prompting calcium to enter through voltage-gated calcium channels and triggering the release of insulin granules via exocytosis.

The KCNJ11 gene encodes the inner subunit (Kir6.2) of the K_{ATP} channel, while the ABCC8 gene encodes the outer subunit (SUR1). Mutations in these genes can cause the K_{ATP} channels to stay open, even when glucose levels are high. This prevents effective depolarization of the cell membrane, thereby hindering the release of insulin from the beta-cell [36].

Diagnosis of neonatal diabetes involves genetic testing, as well as laboratory screening for urine ketones, serum glucose, c-peptide, and insulin levels. Additionally, a pancreatic ultrasound may be conducted to assess the presence or absence of the pancreas. Treatment typically includes the administration of sulfonylurea, since this drug acts on K_{ATP} channels, promoting their closure and allowing insulin to be released [36]. Depending on the duration of the treatment, neonatal diabetes can be subdivided into transient or permanent. Transient neonatal diabetes patients stop treatment between the first weeks and 5 years of age. On the other side, permanent neonatal diabetes patients need lifelong treatment. This condition is very rare, only affecting 1 in every 90,000 live births [37].

Table 1 - Genes responsible for Neonatal Diabetes, sourced from [38].

Gene name	Cytogenetic band	Encodes for
PLAGL1	8q12.1	Zinc finger protein
HYMAI	6q24.2	Non-protein coding transcript
ZFP57	6p22.1	Zinc finger protein
KCNJ11	11p15.1	Integral membrane protein
ABCC8	11p15.1	ATP-binding cassette transporters
PTF1A	10p12.2	Protein of pancreas transcription factor 1 complex
NEUROD1	2q31.3	NeuroD family of basic helix-loop-helix (bHLH) transcription factors
NEUROG3	10q22.1	bHLH transcription factor
RFX6	6q22.1	Regulatory factor X (RFX) family of transcription factors
IER3IP1	18q21.1	Small protein of endoplasmic reticulum (ER)
HNF1B	17q12	Homeodomain-containing superfamily of transcription factors
INS	11p15.5	Insulin
EIF2AK3	2p12.2	Type I membrane protein located in the ER
FOXP3	Xp11.23	Forkhead/winged-helix family of transcriptional regulators
GCK	7p13	Glucokinase
PDX1	13q12.2	Transcriptional activator
GLIS3	9p24.2	Zinc finger protein
PAX6	11p13	Paired box protein Pax-6
WSF1	4p16.1	Transmembrane protein of ER
SLC19A2	1q24.2	Thiamin transporter protein
SLCA2	11q12.3	Cell surface transmembrane protein

1.1.6 Diabetes mellitus secondary to endocrinal pathologies

Several endocrine pathologies can lead to diabetes mellitus, namely acromegaly, Cushing´s syndrome, pheochromocytoma, Graves´ disease, primary aldosteronism, and somatostatinoma [39].

Acromegaly is characterized by an excessive secretion of growth hormone. This disease can be caused by a growth hormone-secreting pituitary adenoma or other causes, like multiple endocrine-neoplasia 1, McCune-Albright syndrome, or medullary thyroid carcinoma [39]. The excess growth hormone stimulates gluconeogenesis, causing hyperglycemia, and also leads to both hepatic and peripheral insulin resistance, with compensatory hyperinsulinemia [40]. A study conducted with acromegaly patients showed that 50% of patients had an altered glycemic status, with 28.5% having diabetes [41]. The first line of treatment for acromegaly patients is transsphenoidal surgical resection of the growth hormone-secreting adenoma. After the excision, most patients improve insulin sensitivity and resistance, with glucose metabolism becoming normal [42].

Cushing´s syndrome occurs when the human body produces an excess of the hormone cortisol, which is produced in the fasciculata area of the adrenal glands [39], [43]. Cortisol, a glucocorticoid, in excess causes beta cell dysfunction, reducing insulin sensitivity and impairing beta cell function. This can occur through genomic action, with the modulation by nuclear glucocorticoid receptors, leading to a decrease in the efficiency of cytoplasmic calcium. This shortage of calcium function leads to an impairment of the exocytotic process of insulin secretory vesicles. Exposure to glucocorticoids also reduces the insulinotropic effects of glucagon-like peptide 1 (GLP-1) [44]. It is estimated that up to half of all patients with Cushing´s syndrome exhibit varying degrees of disrupted glucose metabolism [45]. The gold-standard treatment involves surgical intervention including selective pituitary transsphenoidal adenomectomy, unilateral or bilateral adrenalectomy, or excision of the ectopic ACTH-secreting tumor. After the surgical procedure, glycemic values can become normal, but insulin resistance can persist [39]. A study showed that after surgery, 47% showed improvement in serum glucose levels, and 21% returned to normal limits [46].

Pheochromocytomas are benign and rare tumors of chromaffin cells of the adrenal medulla or of a paraganglion that produce catecholamines (dopamine, epinephrine, and norepinephrine) [47], [48]. Excessive catecholamines suppress insulin secretion from the pancreas primarily through stimulation of α-adrenergic receptors and induce insulin resistance in peripheral tissues via β-adrenergic receptors. In muscle tissue, catecholamines inhibit glucose uptake and utilization. In the liver, elevated catecholamine levels promote glucose production by enhancing glycogenolysis and gluconeogenesis [39]. Surgical intervention is the only permanent treatment available. As with the pathologies mentioned above, after the surgical removal of the tumor,

glucose levels are expected to improve [39]. A study conducted by Beninato et al showed that 90% of patients improved glycemic values, and in 79% of cases the diabetic condition was resolved [49].

Graves´ disease is an autoimmune condition that causes hyperthyroidism, which means the body produces an excess of thyroid hormone [50]. This excess leads to diabetes by affecting insulin secretion and increasing insulin resistance at the peripheral level. An increase in triiodothyronine (T3) and thyroxine (T4) leads to an increase in gluconeogenesis, apoptosis of pancreatic beta cells, increased activity of pancreatic alpha cells, and an increase in inactive insulin precursors [39]. In a study conducted in 2021, following 4593 patients with Grave´s disease, diabetes was diagnosed in 16.3% of them. That study also showed that treatment with radioactive iodine is more likely to lead to diabetes in comparison to treatment with synthetic antithyroid drugs [51]. Thiazolidinediones are contraindicated once they stimulate the differentiation of adipocytes at the orbital level aggravating ophthalmopathy, a symptom of Grave´s disease [39].

Primary aldosteronism (PA) is characterized by the excessive production of the hormone aldosterone and is the most common form of secondary hypertension [52]. Aldosterone is a mineralocorticoid hormone produced in the zona glomerulosa of the adrenal cortex with implications in water and salt regulation in the kidneys [53]. Although the mechanism of the pathophysiology associated with PA and DM is not yet fully comprehended, aldosterone triggers oxidative stress and inflammation, disrupts adipokine expression, thermogenesis, and lipogenesis in adipose tissue, and promotes hepatic steatosis. In the pancreas, increased oxidative stress and inflammation of beta cells, primarily through glucocorticoid receptor activation, impair insulin secretion. It is estimated that one in five patients with PA has DM [2]. Surgical intervention is the best treatment for PA, and a study with 14 patients showed that after surgery, the first and second phases of insulin secretion during the hyperglycaemic clamp, insulinogenic index, and total insulin secretion measured during OGTT were improved [55].

Somatostatinomas are rare neuroendocrine tumors, originating from the delta cells of the pancreas, that release a peptide called somatostatin [56]. This peptide is present in two isoforms, with the shorter isoform operating in the brain, and the longer isoform working in the gastrointestinal tract (GI). Somatostatin produces neuroendocrine inhibitory effects in GI, endocrine, exocrine, pancreatic, and pituitary secretions. It also modifies neurotransmission and modifies memory formation in the central nervous system [56]. Since it also inhibits insulin and glucagon secretion from the pancreatic islet cells, somatostatinoma can lead to both hyperglycemic and hypoglycemic stages. Distal pancreatectomy with splenectomy, proximal pancreatoduodenectomy with preservation of the folds, or the Whipple procedure are the preferred surgical procedures to remove somatostatinomas. Pharmacological treatment of this tumor is associated with hyperglycemia as an adverse effect [39].

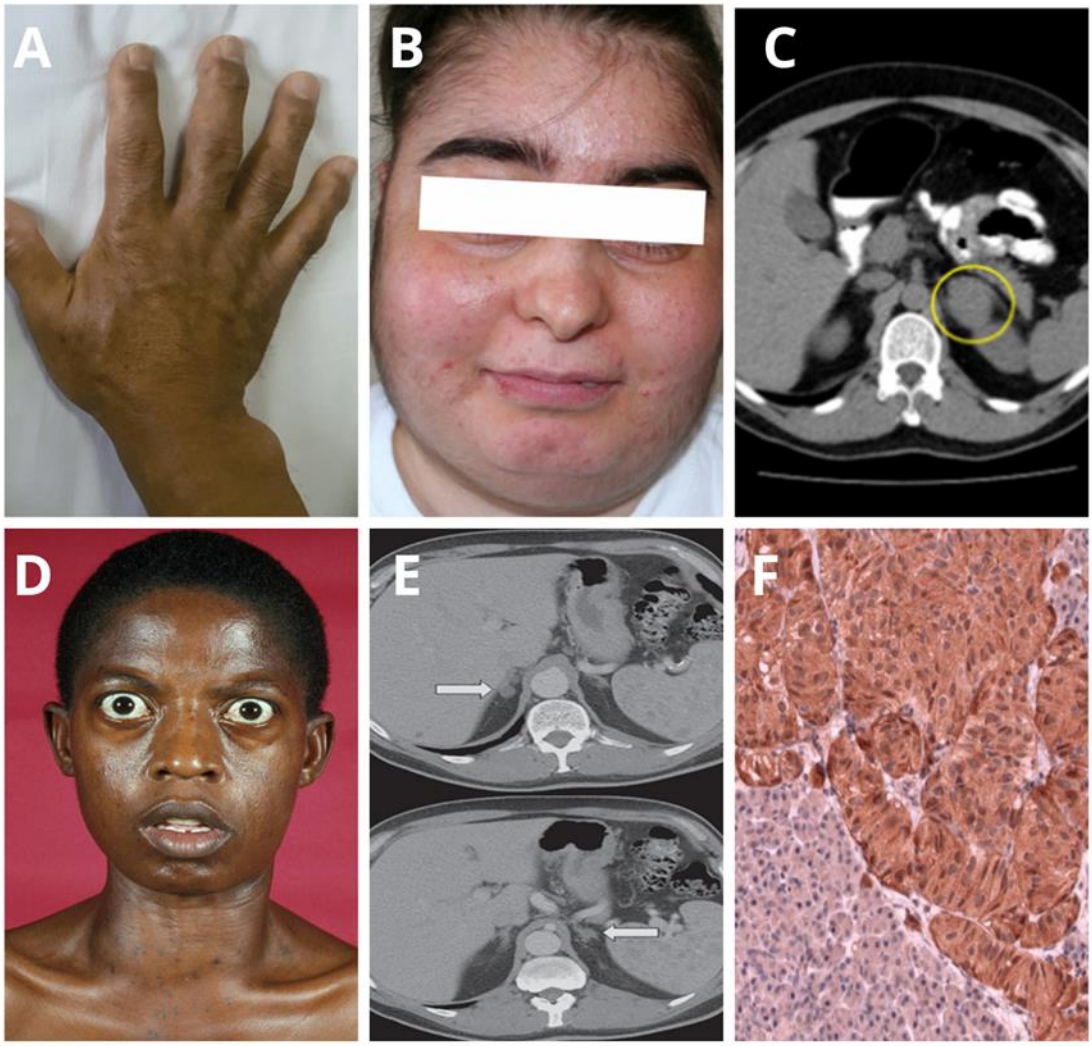

Figure 3 - Illustrating images of endocrine pathologies that lead to diabetes. A) Enlarged hands of an acromegaly patient [187]; B) Round face in a Cushing´s syndrome patient [188]; C) CT scan showing a pheochromocytoma [189]; D) Exophtalmus in a Graves´ disease patient [190]; E) CT scan showing two benign tumors in a primary aldosteronism patient [191]; E) Histological staining of a somatostaninoma [192].

1.2 Diagnosis

There are four criteria for the diagnosis of diabetes in nonpregnant individuals: hemoglobin A1c (HbA1C) over 6.5% or fasting plasma glucose (FPG) over 126 mg/dl or 2 hours plasma glucose (2H-PG) over 200 mg/dl during OGTT or random plasma glucose over 200 mg/dl in an individual with classic symptoms of hyperglycemia or hyperglycemic crisis. For diagnosis of prediabetic individuals: HbA1C between 5.7-6.4% or fasting plasma glucose between 100 and 125 mg/dl or 2 hours plasma glucose between 140-199 mg/dl during OGTT. Normal reference values are considered: HbA1C less than 5.7% or fasting plasma glucose between 70 and 99 mg/dl or 2 hours plasma glucose (2H-PG) between 140-199 mg/dl during OGTT [57], [58].

HbA1C, or glycated hemoglobin, is a test performed to evaluate the level of glucose control. The value of this test represents an average of the blood sugar levels of the past 90 days since that is the average lifespan of red blood cells. If there is an excess of glucose in the bloodstream, this molecule will attach to hemoglobin, and therefore there will be higher HbA1C levels [58]. The fasting plasma glucose (FPG) test is the simplest and fastest way to measure blood glucose levels. In fasting individuals, blood glucose levels are kept constant, since the body only releases just enough glucose from glycogen stores in the liver and skeletal muscles to maintain homeostasis [59]. The 2H-PG test is a timed procedure that allows doctors to evaluate the ability of a patient to process glucose. The patient is given a determined amount of glucose, generally 75 grams, and after 2 hours the glucose levels are measured [60].

Table 2 - Reference values, prediabetes, and diabetes values for diagnosis, sourced from [61]. *HbA1C: glycated hemoglobin; FPG: fasting plasma glucose; 2H-PG: 2 hours – plasma glucose.*

Tests	Reference values	Prediabetes	Diabetes
HbA1C (%)	<5.7	5.7-6.4	≥6.5
FPG (mg/ml)	70-99	100-125	≥126
2h-PG (mg/ml)	<140	140-199	≥200

1.3 Complications

Diabetes is considered a multisystem pathology, once it affects multiple organs and tissues throughout the body [62].

1.3.1 Cardiovascular System

DM, and specifically insulin resistance, are linked to the overexpression of numerous cytokines by adipose tissue, including tumor necrosis factor-α (TNF- α), interleukin (IL) 1, IL-6, leptin, resistin, monocyte chemoattractant protein-1 (MCP-1), plasminogen activator inhibitor-1 (PAI-1), fibrinogen and angiotensin. The overexpression of these cytokines leads to increased inflammation and lipid accumulation, affecting blood vessels, and can lead to the development of endothelial dysfunction, myocardial infarction (MI), and cardiomyopathy (CMP) [62].

Diabetes is also associated with increased amounts of C-reactive protein (CRP), with studies demonstrating that CRP impairs the endothelial production of nitric oxide (NO) and prostacyclin. Both these molecules are essential for vessel compliance. CRP has also been found to enhance the uptake of oxidized low-density lipoprotein (LDL) in the walls of coronary vessels. This uptake contributes to endothelial dysfunction and the development of atherosclerotic plaque [62].

This atheroma formation can lead to peripheral arterial disease (PAD), which involves partial or complete blockage of peripheral blood vessels in the upper and lower limbs. In patients with DM, the most affected blood vessel is the dorsal pedis artery (Figure 4) [63]. Increased levels of IL-1 contribute to the destabilization of atheromatous plaques leading to MI [62].

Vascular disease characterized by abnormal angiogenesis is also a feature of some long-term complications of diabetes [64].

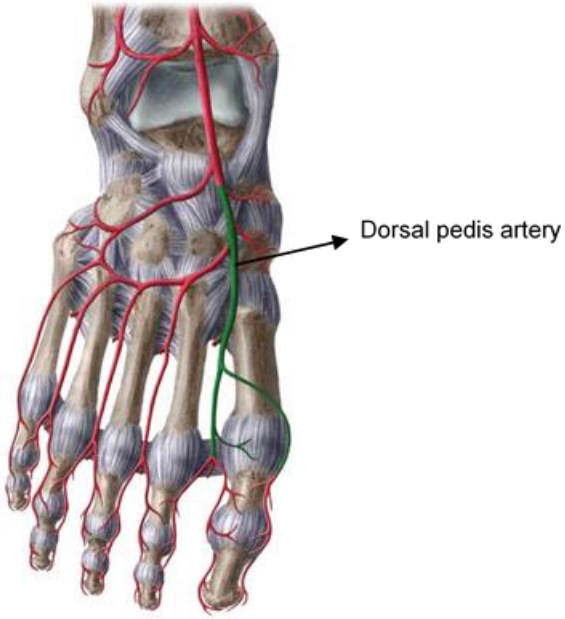

Figure 4 - Anatomy of the blood vessels of the foot, highlighting the dorsal pedis artery in green [193].

1.3.2 Renal system

The prolonged duration of DM associated with uncontrolled hypertension is an important risk factor for the development of diabetic nephropathy [65]. Diabetic nephropathy, also known as diabetic kidney disease (DKD), is a serious complication that affects the ability of the kidneys to remove waste products and excess fluid from the body, by slowly damaging the filtering system of the kidneys [66].

DKD can progress to kidney failure, also known as end-stage kidney disease (ESRD), a terminal condition characterized by a glomerular filtration rate lower than 15 ml/min [64]. Several biochemical pathways, including the protein kinase C pathway, hexosamine pathway, AGE-related pathway, and polyol pathway, contribute to oxidative stress, dysregulated autophagy, activation of intracellular signaling pathways, and epigenetic changes that drive inflammation and fibrosis, ultimately leading to DKD (Figure 5).

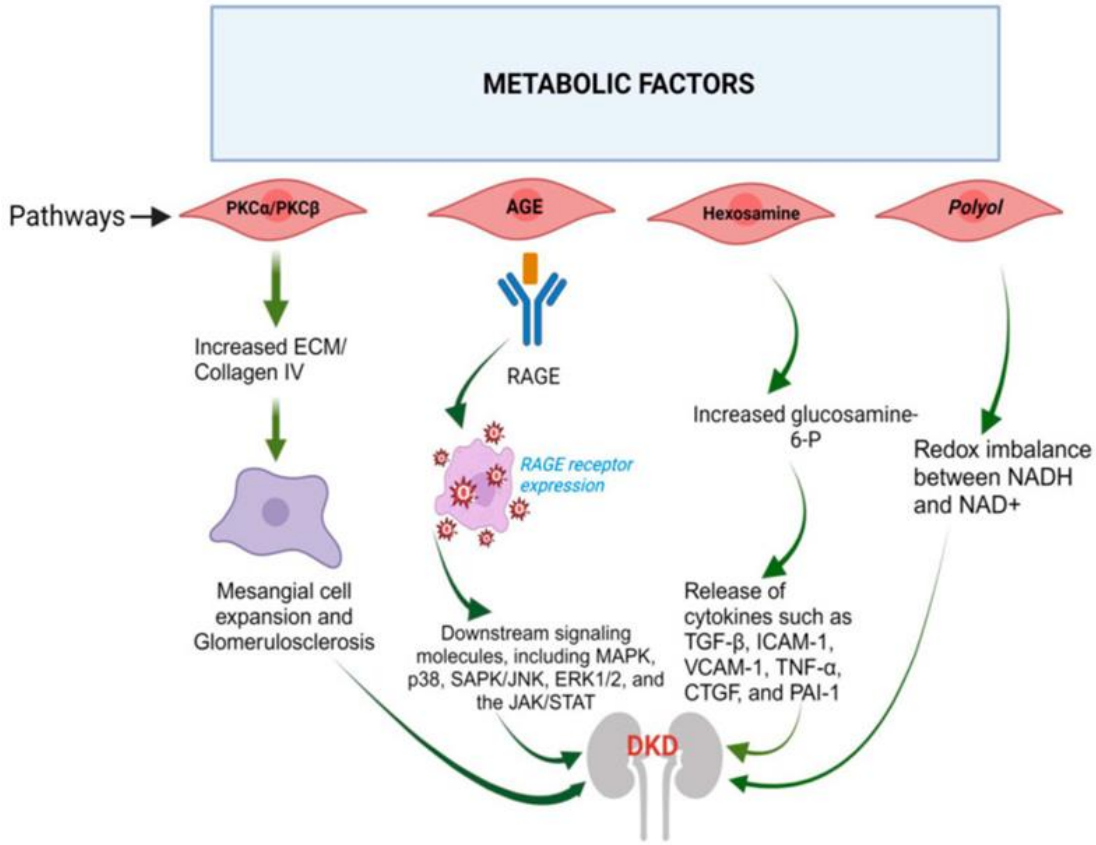

Figure 5 - Implications of diabetes in several pathways ultimately leading to DKD, sourced from [67] PKC: protein kinase; AGE: advanced glycation end products; ECM: extracellular matrix; RAGE: receptor for advanced glycation end products, SAPK/JNK: stress-activated protein kinases/Jun amino-terminal kinases, ERK1/2: extracellular signal-regulated kinase 1/2, JAK/STAT: Janus kinase/signal transducers and activators of transcription, ICAM-1: intercellular adhesion molecule 1, VCAM-1: vascular cell adhesion molecule 1, TNF-α: tumor necrosis factor alpha, CTGF: connective tissue growth factor, PAI-1: plasminogen activator inhibitor 1.

The polyol pathway is particularly important as it activates the enzyme aldose reductase in cells when intracellular glucose levels rise. This activation reduces the concentration of cellular nicotinamide adenine dinucleotide phosphate hydrogen (NADPH), altering the redox ratio, which leads to reduced nitric oxide availability and impaired enzyme function.

The hexosamine pathway, with glutamine:fructose-6-phosphate-amidotransferase (GFAT) as its rate-limiting enzyme, also plays a critical role. High glucose levels lead to the production of transforming growth factor β1 (TGF-β1), an effect mitigated by GFAT inhibition. Although GFAT is typically absent in human glomerular cells, it is expressed in patients with DKD, suggesting a pathophysiological role [65].

Hyperglycemia triggers the production of pro-inflammatory cytokines and chemokines in various kidney cell types, including endothelial cells, mesangial cells, podocytes, and tubular epithelial cells. This process induces inflammation through signaling pathways such as

JAK/STAT, TGF-β, and Notch, ultimately leading to fibrosis. DKD is present in approximately 40% of patients with DM worldwide [65].

1.3.3 Ocular system

Diabetic retinopathy (DR) is a complication of diabetes that causes vision loss and blindness, by affecting blood vessels in the retina [67]. The retina is located at the back of the eye, opposing the lens and pupil (Figure 6).

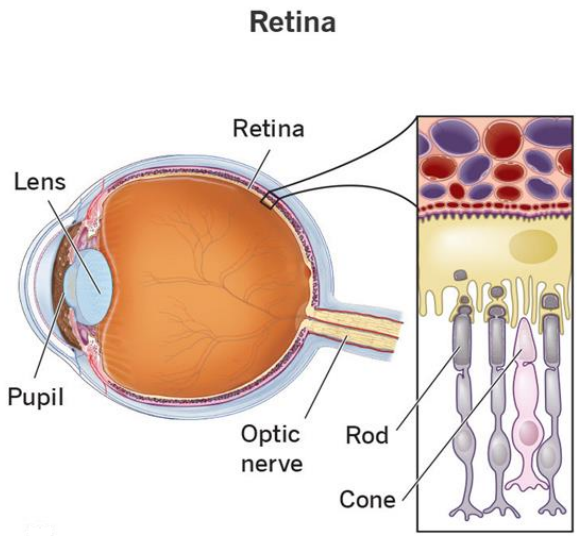

Figure 6 - Retina location and anatomy [194].

DR can be divided into two stages, non-proliferative diabetic retinopathy (NPDR) and proliferative diabetic retinopathy (PDR). In NPDR, there is increased vascular permeability and capillary occlusion. The symptoms include microaneurysms, hemorrhages, and hard exudates. In PDR, which is a more advanced stage, occurs neovascularization, with new abnormal vessels bleeding into the vitreous or occurrence of retinal detachment. This leads to serious vision impairment in patients [68].

DR is a microvascular disease with hyperglycemia manifesting an important role in retinal microvascular damage. The same pathways implied in diabetic nephropathy (polyol pathway, advanced glycation end product accumulation, the protein kinase C (PKC) pathway, and the hexosamine pathway) imply DR.

The first response of blood vessels to high glucose is their dilatation and change in blood flow, a metabolic autoregulation to increase retinal metabolism. In the early stages of DR, pericytes -responsible for providing structural support for capillaries -, are lost, leading to the formation

of microaneurysms. A heavy loss of pericytes and endothelial cells leads to capillary occlusion and ischemia [68].

Retinal ischemia and hypoxia trigger the upregulation of VEGF (Vascular Endothelial Growth Factor) through the activation of hypoxia-inducible factor 1 (HIF-1) [68]. DR is present in 22% of diabetic patients, worldwide [69].

1.3.4 Nervous system

Nerve injury in diabetic neuropathy (DN) can present in several patterns, with distal symmetric polyneuropathy being the most common. In this pattern, both hands and lower limbs are affected. DN primarily affects sensory axons (sensory neuropathy) and autonomic axons (autonomic neuropathy), and to a lesser extent, motor axons (motor neuropathy) [70], [71]. Sensory neuropathy damages nerves responsible for sensations, leading to abnormal sensations or loss of them [72]. Autonomic neuropathy occurs when there is damage to the nerves that control body processes without conscious effort (e.g., digestive system, bladder, sex organs) [73]. Damage to the nerves that control motor functions, such as movement, is known as motor neuropathy [71].

Elevated glucose levels initiate glucose metabolism through the polyol and hexosamine pathways, leading to an increase in reactive oxygen species (ROS) and inflammation, resulting in mitochondrial damage. This cascade contributes to persistent nervous system impairment. High glucose also promotes the glycation of various structural and functional proteins, forming AGEs. These AGEs disrupt protein function and engage with AGE-specific receptors (RAGE), altering gene expression, intracellular signaling, and stimulating the release of pro-inflammatory molecules and free radicals [71].

Concurrently, excessive free fatty acids, processed via β-oxidation due to hyperlipidemia, can harm the peripheral nervous system—especially Schwann cells—by generating ROS and inducing both systemic and local inflammation. This inflammatory response involves macrophage activation and the subsequent production of cytokines and chemokines [71].

Regarding the central nervous system, advanced forms of DN can also have consequences in the neurons of the spinal medulla, such as axonal loss, gliosis, demyelination, and general spinal cord atrophy. Diabetes can also lead to cognitive dysfunction, with cross-sectional studies suggesting a link between DM and an increased risk of dementia [74]. DN is the most common form of neuropathy worldwide, affecting about 50% of all adults with diabetes at some point in their lives [75]. Table 3 presents a compilation of the type of neuropathies, affected axons, symptoms, and pathophysiological mechanisms of neuropathies related to diabetes.

Table 3 - Types of neuropathies, affected axons, symptoms, and pathophysiological mechanisms of neuropathies related to diabetes, sourced from [70], [71], [72], [73], [74] and [75].

Type of neuropathy	Affected axons	Symptoms	Pathophysiological mechanism
Sensory neuropathy	Sensory	Abnormal sensations or loss of sensations	Increased ROS and inflammation from elevated glucose and AGEs disrupt sensory nerve function.
Autonomic neuropathy	Autonomic	Digestive system issues, bladder dysfunction, sex organ dysfunction	Damage to autonomic nerves affecting involuntary processes; influenced by high glucose and inflammatory responses.
Motor neuropathy	Motor	Movement issues	Damage to nerves responsible for movement due to glucose-induced inflammation and oxidative stress.
Central nervous system	Neurons in the spinal medulla	Axonal loss, gliosis, demyelination, spinal cord atrophy, cognitive dysfunction	Diabetes-related changes lead to spinal cord damage and increased risk of cognitive decline.

1.3.5 Immune system

One of the complications of diabetes mellitus (DM) is an impaired and weakened immune system, which occurs through various mechanisms. Studies have shown that individuals with diabetes exhibit reduced cytokine production, with suppression of IL-2, IL-6, and IL-10 when stimulated by CD3 antibodies [70].

IL-6 is crucial for regulating the response to pathogens and for the adaptive immune response, as it induces antibody production and the development of effector T cells development [70]. IL-2 is essential for maintaining regulatory T cells and for the differentiation of CD4+ T cells into specific effector T cell subsets following antigen-mediated activation [71]. IL-10, an anti-inflammatory cytokine, plays a key role in managing infections by regulating the immune response to pathogens and thereby preventing host damage [72].

Elevated glucose levels in diabetes lead to increased glycation, which affects IL-10 secretion by myeloid cells. Hyperglycemia also impairs the activity of macrophages and other leukocytes in pathogen elimination. Additionally, DM results in inhibited leukocyte recruitment due to reduced production of CXCL1, CXCL2, IL-1β, and TNF-α. There are also defects in pathogen recognition due to downregulation of TLR and TIRAP expression. Furthermore, dysfunction of

neutrophils and natural killer cells, along with inhibition of antibodies and complement effectors, can be present in DM patients [70].

Overall, defects in the innate immune response and dysfunctions in the adaptive immune response are significant complications associated with diabetes mellitus [70].

1.3.6 Other systems

DM is a multisystemic disease affecting almost every organ in the human body. Apart from those already mentioned, DM can also affect and have considerable consequences on the reproductive, digestive, and musculoskeletal systems.

Reproductive dysfunction linked to diabetes can result in delayed puberty and menarche, menstrual cycle abnormalities, reduced fertility, adverse pregnancy outcomes, and potentially early menopause [73].

The most common digestive issue in diabetic patients is diabetic gastroparesis, characterized by an abnormal delayed gastric emptying [74]. The use of incretin mimetics to treat DM2 is a risk factor for the development of this complication [75].

Regarding the musculoskeletal system, diabetes increases the risk of complications like cheiroarthropathy, frozen shoulder, Dupuytren's contracture, carpal tunnel syndrome, flexor tenosynovitis, joint disorders, and other related problems [76].

2. Diabetic foot wounds

Diabetic foot ulcers (DFU) are a complication that stems from the pathology of diabetes [77]. With the exponential growth in the number of people affected by diabetes worldwide and the increasing likelihood of necrosis and amputation episodes resulting from diabetic foot wounds, research in this area proves necessary and has a high impact on public health [77], [78].

2.1. Definition and Epidemiology

Diabetic Foot Ulcers (DFU), as outlined by the World Health Organization (WHO), denotes “ulceration of the foot (extending distally from the ankle and encompassing the ankle) associated with neuropathy and varying degrees of ischemia and infection" [79].

The clinical features of diabetic foot are diverse, encompassing phenomena such as changes in skin color, skin temperature, swelling in the foot and heel, leg pain, non-healing open wounds, calluses, dry fissures, and ulcers [80].

There are several risk factors associated with diabetic foot pathology. The non-modifiable factors are the patient's sex - with this condition being more prevalent in men – and age; and the modifiable, prolonged duration of diabetes, pre-existing bone deformities, nephropathy, retinopathy, smoking, or low socioeconomic conditions [81].

Regarding DFU, it is expected that 15 to 25% of diabetics will develop diabetic foot wounds at some point in their lives. It is the most frequent cause of non-traumatic lower limb amputations [81].

Regarding worldwide differences in prevalence, as of 2016, North America had the highest prevalence (13%), followed by Africa (7.2%), Asia (5.5%), Europe (5.1%) and Oceania had the lowest prevalence (3,0%). Regarding countries, Belgium had the highest prevalence (16.6%) and Australia the lowest (1.5%) [82].

2.2. Physiopathology

The pathophysiology of diabetic foot ulcers (DFU) is primarily driven by a triad of factors involving neural, arterial, and immune components [83]. Diabetic peripheral sensorial neuropathy reduces the ability to feel pain and pressure. Therefore, due to a lack of pain perception, the risk of trauma is significantly higher, which may result in people with diabetes not noticing a puncture in the skin that leads to a foot ulcer. The combination of sensory and motor peripheral neuropathies leads to uneven foot pressure distribution and an abnormal gait. Gradually, the compressed skin develops hyperkeratosis. Hyperkeratosis can form a hematoma that eventually breaks due to increased plantar pressure load, leading to an ulcer that is resistant to healing [84]. An important and key factor in DFU is wound healing impairment. Unlike non-diabetic patients, wounds in DM individuals tend to not heal, regenerate, or cicatrize. Normally, wound healing passes through the stages of coagulation, inflammation, proliferation, and remodeling (Figure 7) [85].

In DFU, tissue ischemia, hypoxia, and a high-glucose microenvironment disrupt the normal healing process, leading to delayed or nonhealing wounds and various clinical complications. Peripheral arterial disease (PAD) is characterized by the constriction or obstruction of the blood vessels responsible for transporting blood from the heart to the legs, which leads to tissue ischemia and hypoxia [85]. The macro and microcirculation are essential for healing, once insufficient blood perfusion impairs angiogenesis, collagen deposition, and epithelialization. Severe hypoxia disrupts the cellular mechanisms essential for wound healing, including

angiogenesis and the activation of various growth factors and cytokines – such as VEGF, TGF-β1, and platelet-derived growth factor (PDGF) – which are crucial for stimulating the proliferation and migration of endothelial cells, fibroblasts, and keratinocytes [86].

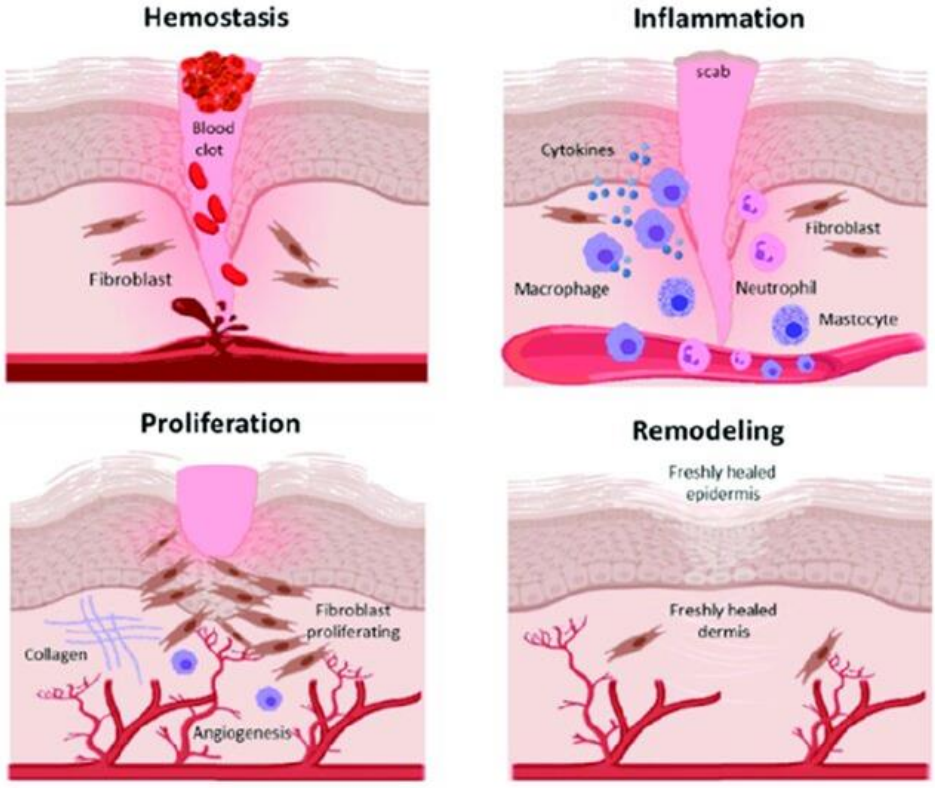

Figure 7 - Four stages of wound healing: hemostasis (coagulation), inflammation, proliferation and remodeling, sourced from [87].

Diabetes also leads to the patient's immune system being weakened and providing a less effective response to infections. This factor proves to be particularly important in the worsening of diabetic foot pathology [88]. In the initial stages of wound healing, neutrophils typically release granular molecules to eliminate pathogens through a process called neutrophil extracellular traps – NETosis (Figure 8) [89]. In a diabetic environment, however, NETosis becomes dysregulated, leading to an excessive inflammatory response, with increased cytokine and superoxide production, ultimately hindering the wound healing process [90]

The Warburg effect, originally characterized in cancer metabolism, has recently been implicated in various physiological processes, including wound healing. This metabolic shift involves cells favoring aerobic glycolysis over oxidative phosphorylation, even in the presence of oxygen, to support rapid cell proliferation and function. In the context of wound healing, the Warburg effect enables critical cellular activities such as fibroblast and keratinocyte proliferation, migration, and extracellular matrix production, all of which are necessary for effective tissue repair [91].

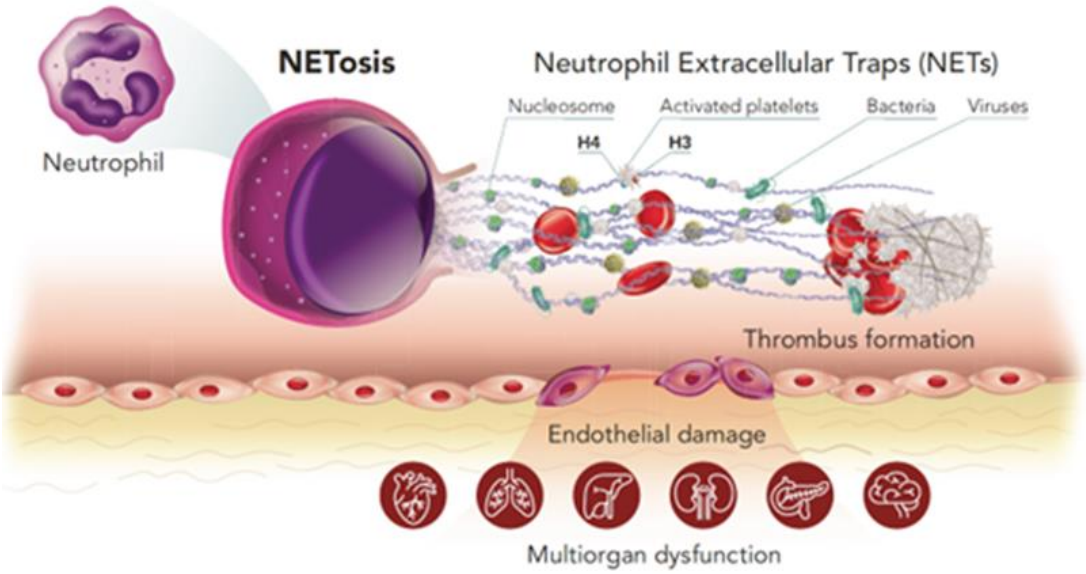

Figure 8 - NETosis: Formation of Neutrophil Extracellular Traps (NETs), sourced from [195].

During the early stages of wound healing, cells within the injured area experience an increased demand for energy and biosynthetic precursors. Aerobic glycolysis, despite being less efficient in ATP production compared to oxidative phosphorylation, provides the rapid energy supply and metabolic intermediates required for the synthesis of macromolecules, including proteins, nucleotides, and lipids. These metabolic products are essential for cell proliferation, immune response activation, and angiogenesis, which collectively promote tissue regeneration and wound closure [91].

2.3. Classification and Staging

There are several classification systems and different severities of diabetic foot pathology, among them the PEDIS (Perfusion, Extent, Depth, Infection, and Sensation), SINBAD (Site, Ischemia, Bacterial Infection, Area, and Depth), and the Meggitt-Wagner classification, which is particularly useful as a predictive system for amputation [92].

The PEDIS classification has 4 grades (0,1,2,3) that increase in severity (Table *4*) [93]. The SINBAD classification focused mostly on the risk of lower limb amputation, having a score grading system divided by categories. The final score ranges between 0 and 6 (0-2 low grade, 3-4 moderate grade, 5-6 high grade) [94]. The Meggitt-Wagner classification has 6 grades regarding clinical signs: Grade 0 – skin intact but bony deformities lead to “foot at risk”; Grade 1 – superficial ulcer; Grade 2 – Deeper, full thickness extension; Grade 3 – deep abscess formation or osteomyelitis; Grade 4 – partial gangrene or forefoot; Grade 5 – extensive gangrene [95].

Table 4 - PEDIS classification, sourced from [*93*]. PAD - Peripheral Arterial Disease; CLI - Critical Limb Ischemia; SIRS - Systemic Inflammatory Response Syndrome.

Grade	Perfusion	Extent	Depth	Infection	Sensation	Score
1	No PAD	Skin intact	Skin intact	None	No loss	0
2	PAD, no CLI	<1cm2	Superficial	Surface	Loss	1
3	CLI	1-3 cm2	Fascia, muscle, tendon	Abscess, fasciitis, septic arthritis		2
4		>3cm2	Bone or joint	SIRS		3

2.4. Complications of diabetic foot

Diabetic foot presents a series of complications, with some having a high degree of severity. The most feared complication is lower limb amputation, but complications such as gangrene, bone deformities - such as Charcot's foot - and osteomyelitis also have significant clinical relevance [96].

Gangrene is a medical condition of ischemic and necrotic tissue, resulting in the death and decay of this tissue. It typically affects a finger or lower limb, being recognized by discolored or blackened tissue and the shedding of the affected tissue layers (Figure 9). The primary types of gangrene include wet gangrene, dry gangrene, and gas gangrene. Diabetic foot patients normally have wet and/or gas gangrene, in which there is the presence of bacteria [97].

Foot deformities can be less harmless as a hammer/claw toe and hallux valgus, or present more harmful forms such as Charcot's foot – a complication described in 1868 by Jean-Martin Charcot, a French pathologist and neurologist [98].

Diabetic foot osteomyelitis is an infection of the bone resulting from a tissue infection that spreads into the bone. Osteomyelitis is usually caused by a bacterial infection. In diabetic patients, reduced blood flow to the foot hinders the delivery of white blood cells, which are essential for fighting infections. As a result, these patients are more susceptible to developing infections

Amputation is only considered as a last resort in treatment when there is severe tissue loss, or the patient has a life-threatening infection [99]. Half of patients who undergo lower limb amputation due to diabetic foot pathology die within the first 5 years post-amputation [100].

Diabetic foot ulcers are the leading cause of non-traumatic lower extremity amputations, responsible for over 80% of all such cases.

Figure 9 - Illustrative figure of gangrenous and healthy tissue in a foot [196].

2.5. Diagnosis and clinical evaluation

It is important to obtain a differential diagnosis of diabetic foot, as other pathologies lead to similar complications. Therefore, it is important to do a clinical history and exams. Clinical history should focus on the history of trauma, puncture wound, change in shoe gear, deformity – acquired or congenital, callus or blister, wound care management, off-loading, local signs of infection, and systemic signs of infection [101].

The physical examination can be subdivided into 4 categories – examination of ulceration; examination of the feet; assessment of the possibility of vascular insufficiency; and assessment of the possibility of peripheral neuropathy. When examining ulceration, it's crucial to determine its location accurately, measure both its size and depth, describe the wound base thoroughly, inspect for signs of probing to the bone, check for any undermining or tunneling, detail any drainage present, and describe the condition of the peri-wound area [102].

When examining the feet, it's essential to inspect both static posture and weight-bearing posture, assess for gross deformities, evaluate ankle range of motion utilizing the Silfverskiöld test, examine range of motion across various joints, assess muscle power, and inspect the skin for signs of dryness, fissures, and isolated calluses. When assessing for PAD, major pulse palpitation should be assessed, and an ankle-brachial test – which compares blood pressure in your ankles and arms – can be performed [102].

When assessing for possible peripheral neuropathy, signs of vibratory and position sense loss should be assessed. The Semmes-Weinstein monofilament test can be performed to measure the response to a touching sensation of the monofilaments [103], [104]. Other tests that can be used are the turning for and vibration perception threshold tests, the pinprick test, or access for ankle reflexes [105].

Imaging techniques to see osteomyelitis risk in diabetic foot ulcers can be done, such as MRI, PET scans, or SPECT scans. Osteomyelitis can also be potentially identified with blood tests, including white blood cell count, C reactive protein, and erythrocyte sedimentation rate. Generally, diagnostic imaging techniques enhance diagnosis and diminish the necessity for unnecessary biopsies, which can be invasive and painful [106].

2.6. Treatment and management of diabetic foot

Currently, there are various therapies and treatments available for diabetic foot wounds. One of the strategies used is off-loading, which consists of reducing or removing weight placed on the foot to facilitate healing or prevent the occurrence of ulcers. Total contact casting (TCC) is still considered the gold standard device, but studies showed that any non-removable knee-high devices can achieve similar results – 87% of reduced peak pressure [107].

Another effective treatment is Negative Pressure Wound Therapy (NPWT), which uses controlled negative pressure to draw out excess fluid, promote the formulation of granulation tissue, and increase the angiogenic process [108]. The wounds are covered with a specialized adhesive dressing that, coupled with an NPWT suction device, can apply sub-atmospheric pressure to the wound [109].

Hyperbaric Oxygen Therapy is also widely used, particularly for treating deep and chronic infections such as necrosis and osteomyelitis. This therapy involves supplying patients with 100% oxygen at supra-atmospheric pressures for a specific duration, promoting healing in affected tissues [110].

Additionally, the use of biomaterials in the form of skin dressings is in vogue. A perfect wound dressing material should absorb wound exudates, facilitate proper gas exchange, and provide protection against microbial infections. Additionally, it should promote the synthesis of biochemical mediators like cytokines and growth factors, which are essential for accelerating wound healing. They can appear in various shapes and forms, such as membranes, hydrogels, foams, sponges, bandages, or nanofibers [111].

3. Animal models

3.1. Importance of Animal Models in Wound Healing Research

In vivo models remain the gold standard approach for studying physiological and pathological processes. They allow for the examination of complex interaction within an entire organism, considering all potential factors that could influence the results. Contrary to *in vitro* or ex vivo models, *in vivo* models account for the full spectrum of biological interactions that occur in a living organism [112].

When studying wound healing, *in vivo* models allow researchers to observe not just the local cellular responses at the wound site, but also how systemic factors such as immune cell recruitment, blood vessel formation and metabolic state contribute to the wound healing process [113].

Similar to humans, mammals have a wound healing process consisting of four consecutive phases: coagulation, inflammation, proliferation and remodeling [114]. Since 1993, at least 20 species have been used in wound model research. Among these, mice, rats ang swine models are the most commonly used and well-established for studying wound healing in biomedical research [115].

3.2. Commonly Used Animal Models for Diabetic Wound Studies

The most used species in diabetic wound studies are rodents (Figure 10), among which streptozotocin (STZ) and db/db models are the most widely used [116].

Figure 10 - Example of rodents used in research: on the left, a C57BL/6 (mice); on the right, a Sprague-Dawley (rat) [202], [203].

STZ leads to pancreatic islet β-cell destruction, being used to produce models of T1DM in rats and mice. Streptozotocin can be administered in a single high dose to induce complete β-cell destruction and diabetes. However, the multiple low-dose approach is often recommended. This method causes partial damage to pancreatic islets while also triggering an immune

response that leads to further β-cell loss (Figure 11). This better mimic the pathogenesis and morphological changes observed in type 1 diabetes mellitus in humans [117] .

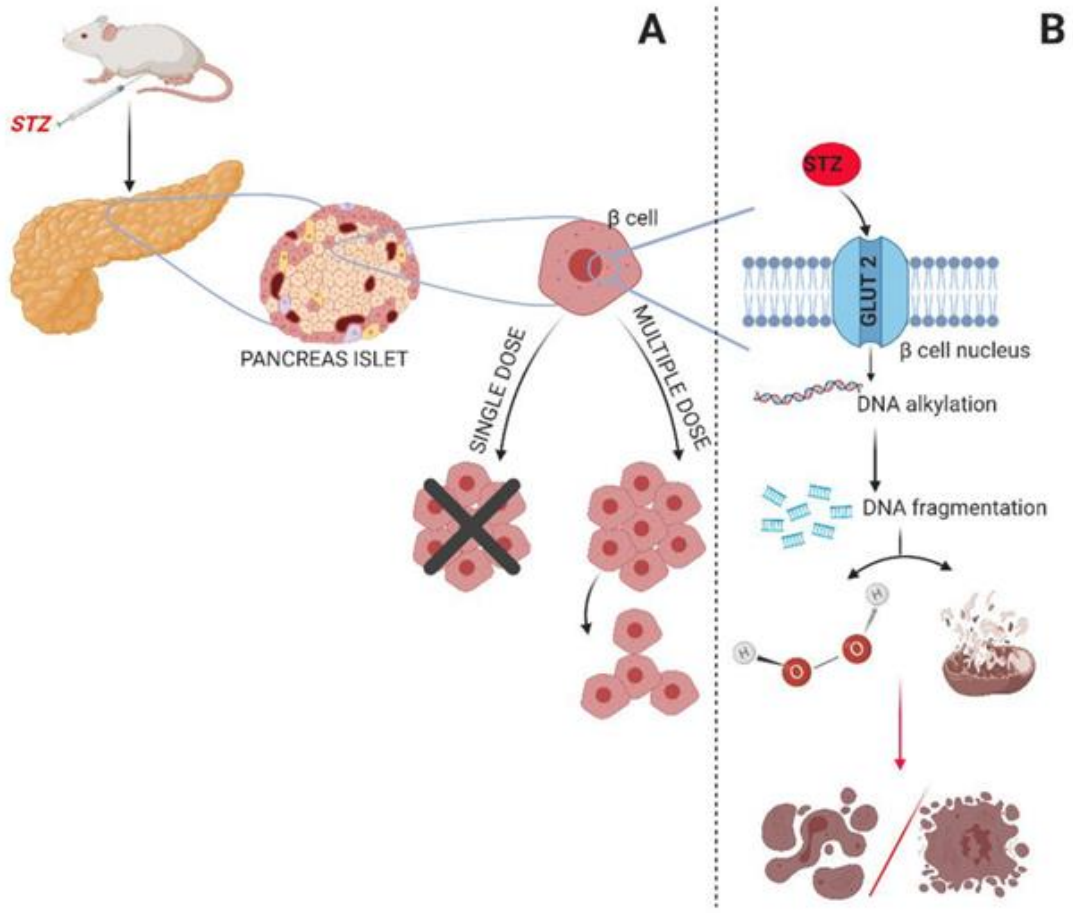

Figure 11 - STZ-Induced Diabetes Model. (A) Mechanism of pancreatic β-cell damage through single or multiple doses of STZ. (B) STZ's action mechanism within the nucleus of β-cells, sourced from [204].

Db/db mice (Figure 12) are genetically engineered to carry a spontaneous mutation in the leptin receptor gene, which leads to obesity and the development of type 2 diabetes mellitus [118]. This mutation renders the leptin receptor nonfunctional, resulting in the mice's inability to regulate food intake and energy balance properly. Consequently, they exhibit significant weight gain, hyperglycemia, insulin resistance, and other hallmark features of T2DM [119].

These mice are particularly valuable as animal models for studying T2DM because they closely mimic many of the metabolic and physiological abnormalities seen in human patients with the disease. One of the key advantages of using db/db mice is their propensity to develop diabetic complications, including neuropathy, which is a common and severe complication of T2DM Neuropathy in these mice can manifest as sensory deficits and impaired wound healing, making them an excellent model for researching diabetic wounds [118].

Figure 12 - Db/db mice [205].

Apart STZ and db/db models, there are more rodent models, such as Akita, alloxan induced, ob/ob or high fat diet induced [116].

After rodents, pigs are the most commonly used animals for research in diabetic wound healing [116]. The most frequently used pig model involves inducing diabetes through the administration of streptozotocin (STZ). Pigs offer the advantage of having anatomy and physiology that closely resemble those of humans, and they provide more surface area for wound creation and study [120].

4. Polycaprolactone membranes

Polycaprolactone (PCL) is a biodegradable polymer with various applications in biomedical research, such as tissue engineering and drug delivery [121]. PCL fibers can be arranged in a manner that replicates the structure of an extracellular matrix. Although PCL was first synthesized in the 1930s, it only became popular in biomedical research in the 1990s due to its applications in tissue regeneration [122].

4.1. Characteristics

Biodegradable materials “are solid polymeric materials and devices which break down due to macromolecular degradation with dispersion *in vivo* but no proof for the elimination from the body” [123]. PCL consists of a chain of a recurring sequence of Ɛ-caprolactone units (Figure 13). The number of these unit repetitions determines the length of the polymer, which determines its time of degradation via ester-bond hydrolysis. This cleavage occurs primarily environmentally through microorganisms, while physiologically, degradation occurs mostly through oxidative and enzymatic catalysis [124]. PCL has a long degradation time, which is essential once it allows the membrane to support tissue regeneration while slowly being absorbed by the body [123].

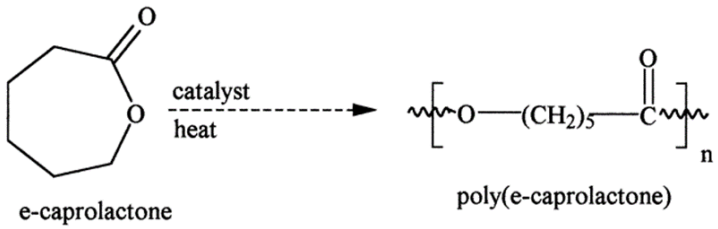

Figure 13 - Synthesis of poly(e-caprolactone), highlighting the recurring sequence of e-caprolactone units [197].

PCL is a semi-crystalline, permeable, biocompatible, hydrophobic polymer with a low melting point of 59º to 64ºC. The melting point ranges between 59 and 64ºC. At room temperature, it is soluble in chloroform, dichloromethane, carbon tetrachloride, benzene, toluene, cyclohexanone, and 2-nitropropane. It can be tailored to a certain application, by changing two major characteristics: molecular weight and degree of crystallinity [125], [126].

4.2. Applications

PCL is of great value in the pharmaceutical and biomedical fields. Polycaprolactone can be used in bone engineering, tissue engineering, and repair, wound healing, drug delivery, or even sutures [126], [127]. In the last decade, PCL has been one of the most widely used biomaterials for bone scaffolds due to its high biocompatibility, low cost, non-carcinogenicity, and slow-degradation rate that makes it useful for use in load-bearing bones, such as ankles, knee, and hips [128], [129].

In the realm of tissue engineering, one recent example of its application and promising research is in the field of corneal regeneration [130]. Regarding wound healing applications, PCL membranes have been successfully applied to treat and regenerate wounds, such as burn wounds [124].

Due to its properties and characteristics, PCL is also an excellent candidate for drug delivery systems. PCL can effectively control the release of a drug for extended periods, as demonstrated by Capronor, a commercial contraceptive made of PCL, which provides sustained release for up to 2 years [131].

Concerning sutures, PCL serves as a prevalent component in various types, including the STRATAFIX™ Spiral PGAPCL Suture and Quill™ Monoderm Suture [132], [133].

4.3. Fabrication process

There are several ways to synthesize PCL biomaterials, such as extrusion molding, compression molding, injection molding, electrospinning, 3D printing, melt spinning, film blowing, or ball mixing. Of all these, 3D printing and electrospinning are the ones preferred by the biomedical and pharmaceutical industries due to the higher quality of the final product [126].

In 3D printing, the fabrication is achieved layer-by-layer. Among the different printing techniques, PCL biomaterials usually resort to fused deposition modeling (FDM) [134].

Electrospinning relies on utilizing an electrostatic force to initiate fiber formation. Initially, high voltage is applied to the tip of a capillary tube containing the polymeric solution, generating a mutual charge repulsion within the solution. As the intensity of the electric field increases, the repulsive forces overcome surface tension, resulting in the formation of a jet. This jet subsequently solidifies into a fiber that is deposited onto a collector. Analytical models have been developed to forecast the eventual fiber diameters, factoring in parameters such as applied current, flow rate, initial jet length, and needle diameter [135].

4.4. Advantages and Disadvantages

Like every biomaterial, PCL presents both advantages and disadvantages. Its advantages include high biocompatibility, significant biodegradability, excellent electrospinning properties, a prolonged biodegradation time, and high material purity. However, there are also disadvantages, such as poor cell adherence due to its hydrophobic surface, the potential toxicity of solvents used, a low melting point limiting its application at higher temperatures, and the complexity and expense of production. Nevertheless, these disadvantages can be overcome using PCL-based biocomposites [136].

5. Bioactive compounds

One of the objectives of this line of research is to functionalize polycaprolactone membranes with bioactive compounds to improve their regenerative potential. For this purpose, we use two bioactive compounds: grape stem extract (GSE) and cannabidiol (CBD) extract.

5.1. Grape stem extract

5.1.1. Introduction

Grape stem extract is one of the many byproducts of the wine production industry. The process of winemaking can be divided into four stages: pruning; harvesting; crushing and pressing; fermentation, and clarification. During the crushing and pressing, the grapes are broken into juice, seeds, pulp, skins, and stems, after which the juice is separated from the solid components. In this stage, grape stems (Figure 14) can be collected [137].

Figure 14 - Grape stem [199].

5.1.2. Chemical composition

Grape stem extract (GSE) is rich in cellulose, hemicellulose, lignin, monosaccharides -xylose and glucose -, essential minerals, and phenolic compounds, with the latter providing the bioactivity of the extract. Various proanthocyanidins, anthocyanidins, flavonols, hydroxycinnamic acids, and stilbenes have been identified in these extracts. The most studied compounds include trans-resveratrol, ε-viniferin, caftaric acid, gallic acid, catechin (one of the most abundant polyphenols), epicatechin, malvidin derivatives, quercetin, and glycosylated derivatives of quercetin at the 3-position [138], [139]. Otherwise, GSE compositions can be influenced by grape variety, size, maturation state, and extraction methods used [139].

5.1.3. Extraction methods

There are several extraction methods used to obtain grape stem extracts, being the focus on the acquisition of the greatest percentage of phenolic compounds. Some of them include using an extraction method using GRAS solvents, pressurized liquid extraction with ethanol: water mixtures, or even ultrasound-assisted extraction combined with a pulsed electric field. Solvent extraction is a widely used method that employs a suitable solvent to extract compounds from plant material. However, this technique has several drawbacks, including lengthy extraction times, high labor demands, and the need for large quantities of solvents, which can be expensive and have negative environmental impacts [139].

5.1.4. Analytical analysis

To gain insight into the exact content of grape stem extract (GSE), several techniques can be performed. Qualitative methods, primarily based on color reactions, can be used to detect the presence of phenolics, flavonoids, and other compounds [140]. Quantitative analysis can also be conducted using the Folin-Ciocalteu method (Figure 15) to determine the Total Phenolic Content (TPC) or the aluminum chloride colorimetric assay to identify the Total Flavonoid Content (TFC) [141], [142]. Chromatographic techniques such as HPLC, GC-MS, and LC-MS allow for the separation, identification, and quantification of individual compounds [143]. Spectroscopic techniques, including Nuclear Magnetic Resonance (NMR) Spectroscopy and Fourier-Transform Infrared (FTIR) Spectroscopy, enable the identification of functional groups and the determination of the molecular structure of these compounds [144].

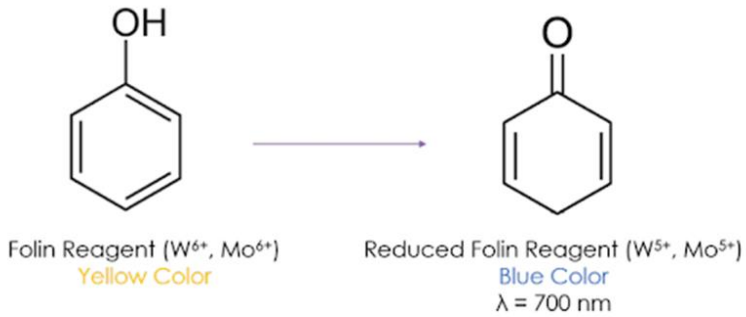

Figure 15 - Principle of Folin-Ciocalteu method to assess Total Phenolic Content [200].

5.1.5. Biological activity

Grape stem extract is utilized in biomedical research due to its significant biological activity. Numerous studies have demonstrated its antimicrobial and antioxidant potential, such as the work by F. J. Vázquez-Armenta et al., who applied grape stem extract in a disinfectant for fresh vegetables [145]. GSE can also have an anti-inflammatory effect due to their phenolic compounds, such as resveratrol and flavonoids [146]. Recent studies show that in parallel to its anti-aging properties, grape stem extract promotes the extension of the life of fibroblasts and stimulates their regeneration [147].

5.1.6. Current applications

As of today, GSE is mainly applied in two major areas: nutraceutical and cosmetic [148]. Regarding the nutraceutical area, grape seed and stem extract supplements are beginning to appear on supermarket shelves [149], [150]. In cosmetics, grape stem extract is a component present in various anti-wrinkle and anti-aging creams [151]. As GSE has been more studied in recent years, shortly, more products will arise and be available for purchase.

5.1.7. Sustainability

One of the biggest advantages of using grape stem extract is that it reutilizes waste from the winery industry, with GSE accounting for 25% of the organic waste from this industry. The usage of GSE could be beneficial not only for the user and the environment but also economically beneficial for the wine enterprises by transforming waste residue into a profitable product they could sell [152].

5.2. Cannabidiol extract

Cannabidiol (CBD) is a phytocannabinoid discovered in 1940 by Roger Adams, extracted from the *Cannabis* plant [153]. CBD has a high affinity to various receptors, such as Type 1 cannabinoid receptor (CB1), Type 2 cannabinoid receptor (CB2), peroxisome proliferator-activated receptor gamma (PPARγ), and more. In opposition to tetrahydrocannabinol (THC), CBD does not have psychoactive effects [154].

5.2.1. Chemical composition and pharmacokinetics

CBD is a non-psychoactive cannabinoid presented in the form of a cyclohexane substituted by a methyl group at position 1, a 2,6-dihydroxy-4-pentylphenyl group at position 3, and a prop-1-en-2-yl group at position 4 (Figure 16) [155]. It is produced by the same metabolic pathway as THC, only differing in the last steps. In the case of THC, the enzyme THCA synthase catalyzes the formation of tetrahydrocannabinolic acid (THCA), the precursor to THC. Conversely, in the synthesis of CBD, the enzyme CBDA synthase catalyzes the production of cannabidiolic acid (CBDA), which is subsequently decarboxylated to form CBD when exposed to heat or light [156].

Regarding the pharmacokinetics of CBD, and more specifically bioavailability, it will vary depending on the administration method. When CBD is administered orally, such as through capsules, edibles, or oils, it undergoes extensive first-pass metabolism in the liver. This results in a relatively low bioavailability in humans, with only about 6% of the ingested dose reaching systemic circulation. If inhaled, the bioavailability can increase up to 45%, with a mean of 31% [157]. Cannabidiol is metabolized in the liver by the cytochrome P450 enzyme system, by enzymes like CYP3A4 and CYP2C19, which leads to the formation of over 40 different metabolites. CBD is eliminated mainly via the feces and some in the urine [158]. The elimination half-life of CBD by chronic users is reported to be between 18 to 32 hours [159].

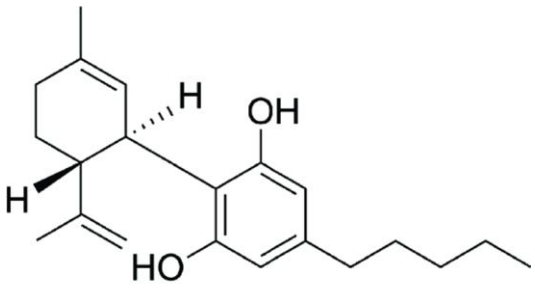

Figure 16 - Molecular structure of cannabidiol [201] .

5.2.2. Extraction methods

Among the extraction methods that can be used, in CBD extraction, supercritical carbon dioxide, and solid-liquid extraction are the gold-standard methods [160].

In supercritical carbon dioxide extraction, CO_2 is subjected to high pressure and temperature, exhibiting properties of a supercritical state (both gas and liquid). Supercritical CO_2 passes through the plant, dissolving the cannabinoids. This method yields high purity and non-toxicity. It´s easy to control the parameters of extraction and it´s an environmentally friendly process

once CO_2 is a natural compound. On the other hand, it is an expensive process due to the high cost of the equipment [161], [162].

Solid-liquid extraction, which involves soaking the plant in a liquid solvent, is a more cost-effective process than the abovementioned one. Although is a more economically viable option, solid-liquid extraction may result in purity concerns, with the need for additional purification, and present more safety risks if the solvent is not properly evaporated [163].

To purify CBD, it is applied a process called winterization, which removes all undesirable fats, waxes, and lipids [164]. In this process, after extraction the CBD oil is mixed with ethanol and subjected to freezing temperatures, between -20 and -80ºC. At these temperatures, unwanted compounds solidify and are easily separated [165].

5.2.3. Biological activity and biomedical applications

Although the application of CBD in medicine remains controversial, CBD is reported to have several biomedical applications. Oral CBD is proven to be an effective antiemetic in adults suffering from chemotherapy-induced nausea and vomiting, due to its interaction with centrally located CB1 receptors and 5-HT3 receptors in the dorsal vagal complex [166], [167].

Regarding chronic pain, CBD offers a clinically significant reduction in pain-related symptoms due to the inhibition of the release of neurotransmitters and neuropeptides from presynaptic nerve endings, reduction of neural inflammation, modulation of postsynaptic neuron excitability, and activation of descending inhibitory pain pathways [167], [168].

Clinical trials have also shown that CBD reduces and prevents some types of seizures, mainly those that occur due to Lennox-Gastaut, Dravet syndrome, and tuberous sclerosis. complex [169]. Despite, the uncertainty of the mechanism of action, it is proposed that CDB antagonizes GPR55 at excitatory synapses [170].

In wound healing, cannabidiol seems to improve cutaneous wound repair through more than one mechanism, via the CB2 receptor the most notable (Figure 17) [171]. This interaction promotes anti-inflammatory effects, modulates immune responses, and may stimulate the proliferation and migration of keratinocytes [172], due to increasing levels of Transforming Growth Factor-beta (TGF-β), promotion of a shift from pro-inflammatory macrophages (M1) to anti-inflammatory ones (M2), and lower levels of reactive oxygen species, Tumor Necrosis Factor-alpha, interleukin-6 (IL-6) and interleukin 1-beta (IL- β), which contribute to wound healing [173]. CBD also promotes the proliferation of keratinocytes by other molecular

mechanisms, such as the upregulation of heme oxygenase 1 (HMOX1) and the BTB and CNC homolog 1 (BACH1) protein [174].

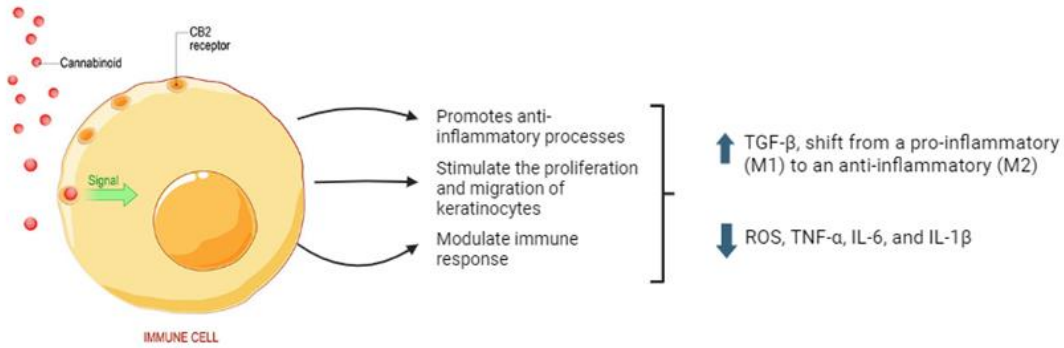

Figure 17 - CBD mechanism of action on CB2 receptor.

5.2.4. Commercialized products

Today, there are two well-known commercialized medical CBD products: Epidiolex® and Sativex®. The first, commercialized by GW Pharma is a drug used to treat patients from 2 years of age with Lennox-Gastaut or Dravet syndrome [175]. The second one, commercialized by the same pharmaceutical group, is used to treat symptoms of adult patients with moderate to severe spasticity due to multiple sclerosis [176].

AIMS

The main goal of this research project is to assess the bioactivity and regenerative potential of functionalized polycaprolactone-based skin dressings for diabetic wound management. For that aim, we will:

- Obtain insight into PCL membrane regenerative potential *in vitro*;
- Search for compounds to functionalize the PCL membrane;
- Do *in vivo* assays with rodents to assess PCL membrane regenerative potential.

MATERIALS AND METHODS

PCL Membranes

Pore size

In this study, we used two types of membranes regarding pore size. A macroporous membrane containing a mesh with pores larger than 50 nanometers and a microporous membrane with pores smaller than 2 nanometers. The differences between pore sizes were achieved during the electrospinning process – the process through which the membranes were made.

Electrospinning process

The PCL membranes used in the present work were made by an electrospinning process. The fabrication process of the PCL membranes was performed at University of Coimbra, according to the methodology described by Taís Faria [177].

Cell lines

In the present work, two cell lines were used. The HDF (Human Dermal Fibroblasts) line was provided by the Biomedicine unit of FMUP and cultured with complete DMEM medium. The HaCat (Human Keratinocyte) line was kindly provided by UFP and cultured with complete DMEM medium. All cells were obtained from ATCC. DMEM medium was supplemented with 10% Fetal Bovine Serum (FBS) and 1% Penicillin-Streptomycin. The cells were maintained in an incubator at 37°C with 5% CO_2.

Cell counting

Hemocytometer

To perform the MTT assay, and wound healing assay, accurate cell counting was essential. This was achieved using a hemocytometer. After preparing a well-mixed cell suspension, 10 µL of the suspension was transferred to an Eppendorf tube. An equal volume of 0.4% Trypan Blue was added to the cell suspension and mixed thoroughly. Subsequently, 10 µL of the stained cell mixture was pipetted into the hemocytometer chamber.

The hemocytometer was then placed under a microscope, and the cells within the designated grid areas were counted using a hand tally counter. The total number of live cells per milliliter was calculated using the formula:

$$"Total\ number\ of\ live\ cells\ per\ mL = \ average\ cell\ count\ per\ square\ x\ dilution\ factor\ x\ 10^4"$$

This calculation provided the total number of viable cells per milliliter of suspension.

Membrane assays

We employed a direct and indirect contact method for each cell assay performed with the PCL membranes. In the direct method, the PCL membranes were in contact with the cell monolayer throughout the assays.

For the indirect contact method, the PCL membranes were embedded in a cell culture medium for 24 hours. Then, that culture media was applied as a treatment throughout the assays.

Cell viability

MTT assay

An MTT assay was used to assess cell viability. Initially, the cell lines were seeded into 96-well plates at a density of 75,000 cells per well. The plates were then incubated for 24 hours at 37ºC in a 5% CO_2 atmosphere. After the first 24 hours, the cells were subjected to various treatments. The plates were returned to the incubation for an additional 24 hours.

On the third day, the MTT assay was performed. In each well, 20% of MTT reagent in PBS dilution was added, followed by incubation in the chamber for 1-2 hours. After that time, the mixture containing MTT was removed, and 100 µL of DMSO was added to the wells. After 5 minutes, the measurement of the absorbance at 570 nm was done using the microplate reader (Varioskan). Then, the data was retrieved and analyzed using GraphPad Prism 8.

Cell motility

Wound healing

To assess cell motility a wound healing assay was performed. Initially, the cell lines were seeded in 6-well plates at a density of 500,000 cells per well. The plates were then incubated for 24 hours at 37ºC in a 5% CO_2 atmosphere. Then, with a 200 µL sterile pipette tip, the confluent monolayer was scratched in a vertical straight movement. After this step, treatments were applied to the cells. The cells were incubated for an additional 24 hours. At different time points (0h and 24h) images were taken of the different wells on the scratch area with a camera and a microscope, in the magnificence of 10x. Images were saved and analyzed later using ImageJ Software and GraphPad Prism 8.

Animal model

In this research project, 18 db/db mice were used, acquired from Charles River Laboratories under project ORBEA_83_2019/2102 approved by the Animal Welfare Committee of the Faculty of Medicine of the University of Porto (Appendix A).

Housing conditions

During the initial phase, the animals were housed in groups in type III cages to allow them to express natural behaviors. After the intervention that caused the wounds, they were individually housed in type II cages to prevent them from removing the biomaterial from their backs. They had *ad libitum* access to food and water, and all animal welfare conditions were monitored daily by the researcher and the Animal Resources Core Facility team at FMUP (Figure 19).

Figure 18 - Animal number 1 being monitored and eating corn.

Skin Wound Healing Model

Under volatile anesthesia with isoflurane, two 3 mm excisional wounds were made on the dorsal region of each animal. The respective biomaterial was then applied to the wound site according to the experimental group (Figures 20 and 21). To ensure well-being during the post-surgery period (first 24 hours) each animal received 0.05 mg/kg of buprenorphine. The biomaterials were replaced whenever necessary, meaning each time an animal removed it. After 21 days, all rodents were euthanized to collect skin and blood samples. For each animal, one of the skin samples was placed in a histological cassette for fixation in 10% formalin solution for 24h, followed by conventional paraffin embedding processing. The other skin sample was snap frozen in liquid nitrogen and then stored at -80ªC to preserve the tissue for further analysis.

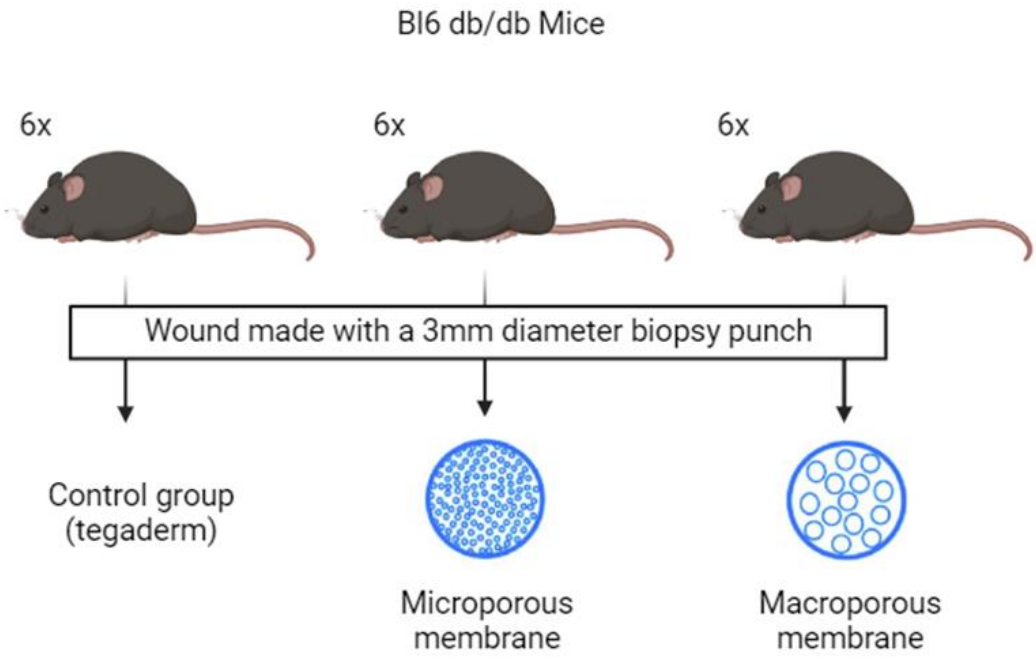

Figure 19 - Db/db mice wound healing model with the 3 experimental groups.

Figure 20 - Moment of application of the membranes to each experimental group.

RNA extraction

RNA extraction from skin rodent samples

To obtain RNA from skin rodent samples, a manual extraction with the aid of Precellys® Evolution Touch Homogenizer was performed. First, the skin samples were homogenized and lysed using the Precellys® Evolution Touch Homogenizer. The following protocol was used:

- Add 3 scoops of new beads.
- Add 500 µl of NZYol.
- Precellys® Evolution Touch Homogenizer parameters:
    - RPM: 4500
    - Time of cycle: 30 seconds
    - Number of cycles: 5

Between homogenization cycles, samples were incubated in ice for 5 minutes to prevent RNA degradation. After that, we added 100 µL of chloroform under a fume hood and incubated for 10 minutes at room temperature. Then, the samples were centrifuged at 13,000 rpm, 4°C, for 15 minutes. After centrifugation, 150 µL of the resulting aqueous phase, where the RNA was located, was pipetted into new Eppendorf tubes. Subsequently, 500 µL of isopropanol was added, and the tubes were gently mixed by inverting them. The samples were then incubated on ice for 10 minutes. Following this, they were centrifuged again at 13,000 rpm, 4°C, for 10 minutes, and the supernatant was discarded.

Next, the pellet was washed with 300 µL of 70% ethanol by adding 150 µL twice and performing an up-and-down motion to ensure thorough washing. The samples were centrifuged once more

at 13,000 rpm, 4°C, for 10 minutes. Afterward, the supernatant was discarded, paying close attention to the pellet. The pellet was then allowed to air dry by leaving the tube open for 5 minutes, until it became translucent. Finally, the pellet was resuspended in 50 µL of milli-Q H_2O.

RNA quality evaluation

To assess the purity of the extracted RNA, we used Thermo Scientific™ NanoDrop™ One/One^C Microvolume UV-Vis Spectrophotometer. First, 2 µl of the elution water used in the RNA extraction was used to perform the blank measurement. Then, 2 µl of the sample was loaded into the reader. The ng/µL concentration, A260/A280 and A260/230 absorbance ratios were recorded for further interpretation.

Reverse Transcriptase Polymerase Chain Reaction (RT-pcr)

Complementary DNA (cDNA) synthesis

To transform the extracted RNA into cDNA, we applied the following program in the thermocycler:

Table 5 - Parameter used in cDNA synthesis.

	CYCLE TIPE			
PARAMETERS	**Primer Annealing**	**Reverse Transcription**	**Enzyme Inactivation**	**Hold**
DURATION (MIN)	5	30	5	∞
TEMPERATURE (ºC)	22	42	85	4

Primers used

Table 6 - List of primers used and respective sequence, both forward and reverse.

PRIMER		SEQUENCE
TGF-B2	Forward	ATGCCCATATCTATGGAGTTC
	Reverse	TAGAGAATGGTCAGTGGTTC
VEGFR2	Forward	CGAGACCATTGAAGTGACTTGCC
	Reverse	TTCCTCACCCTGCGGATAGTCA

Thermocycler

In the thermocycler, the following program was used:

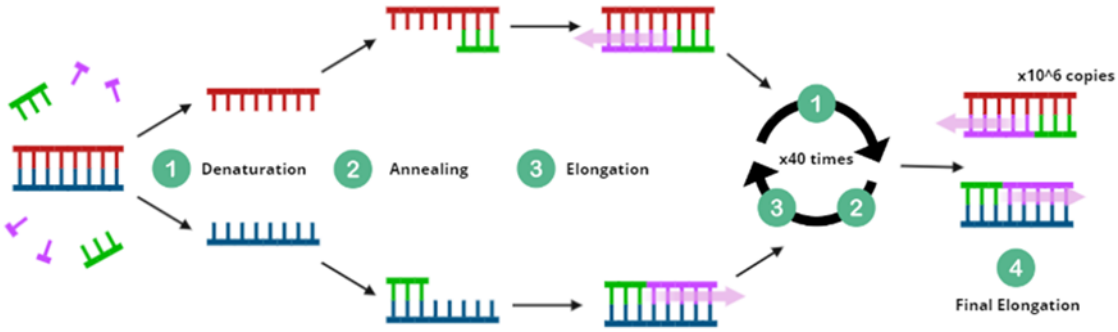

Figure 21 - Schematic program used in the thermocycler.

With the following parameters:

Table 7 - Parameters used in RT-PCR

	CYCLE TIPE			
PARAMETERS	**Denaturation**	**Annealing**	**Elongation**	**Final Elongation**
DURATION (S)	30	60	120	300
TEMPERATURE (°C)	94	55	72	72

Histology

Hematoxylin-Eosin

Hematoxylin and eosin staining was performed. First, the paraffin was removed using xylene. The slide was then passed through several changes of alcohol (ethanol 100%, then 70% and finally 50%) to remove the xylene, thoroughly rinsed with water, and hydrated. Next, the slide was stained with Harris hematoxylin as the nuclear stain and mordant. After rinsing with tap water, the slide was treated with a weakly alkaline solution. Excess background stain was removed using a weak acid alcohol (differentiation), followed by another rinse with tap water. Eosin counterstain was then applied. The slide was passed through several changes of alcohol to remove all traces of water and finally rinsed in multiple baths of xylene. Lastly, the slides were cover slipped with a resinous mounting medium.

Masson´s Trichrome

Masson's Trichrome stain was also performed. As with the previous staining procedure, the slide was passed through the same water, alcohol, and tap water rinsing steps. The first stain applied was Weigert's iron hematoxylin. Next, Biebrich Scarlet-Acid Fuchsin solution was used. The application of phosphomolybdic acid followed this. Finally, a solution containing light green SF yellowish was applied. In the end, the slides were cover slipped with a resinous mounting medium.

Verhoeff-Van Gieson

To perform the Verhoeff-Van Gieson staining (VVG), the slides were first deparaffinized and hydrated to distilled water. The slides were then stained in Verhoeff's solution for 1 hour, ensuring that the tissue turned completely black. After staining, the slides were rinsed in tap water with 2-3 changes to remove excess stain. Differentiation was carried out in 2% ferric chloride for 1-2 minutes. Differentiation was stopped with several changes of tap water, and the staining was checked microscopically to confirm that the elastic fibers were black, and the background was gray. It was advisable to slightly under-differentiate, as the subsequent Van Gieson's counterstain could extract some of the elastic stain. Following this, the slides were washed in tap water and treated with 5% sodium thiosulfate for 1 minute, with the solution discarded afterward. The slides were then washed in running tap water for 5 minutes. Counterstaining was done in Van Gieson's solution for 3-5 minutes. The slides were dehydrated quickly through 95% alcohol, followed by two changes of 100% alcohol. The slides were cleared

in two changes of xylene, each for 3 minutes. Finally, the slides were cover slipped with a resinous mounting medium.

Statistical Analysis

For statistical and graphical analysis, we used GraphPad Prism 8. To compare differences between groups, the test performed was an ordinary one-way ANOVA followed by Tukey's multiple comparisons test with a 95% confidence interval. The results obtained are presented as mean ± standard deviation (SD) and expressed as the average value for each group. In the graph made with ANOVA analysis, (*) represents a result with $p<0.05$, (**) a result with $p<0.01$, (***) a result with $p<0.001$ and (****) a result with $p<0.0001$.

RESULTS

PCL membranes

MTT assay

For the cell viability assays, we employed the MTT assay with the PCL membranes in direct contact with the monolayer and the same assay with just the medium after contact with PCL for 24 hours. The results are shown in Figures 22, 23, 24 and 25.

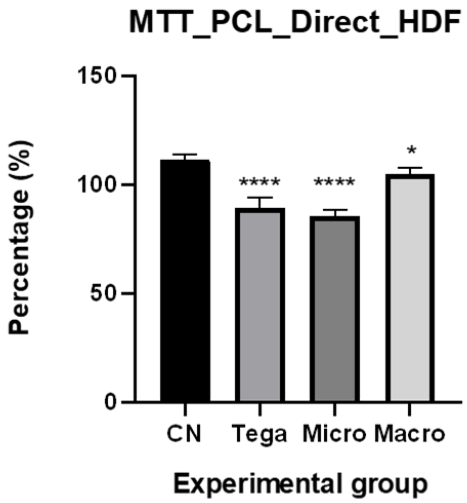

*Figure 22 - MTT direct assay of PCL membranes in HDF cell line (n=2). CN: Control group; Tega: Tegaderm™; Micro: Microporous; Macro: Macroporous. * p<0.05; ** p<0.01; *** p<0.001; **** p<0.0001.*

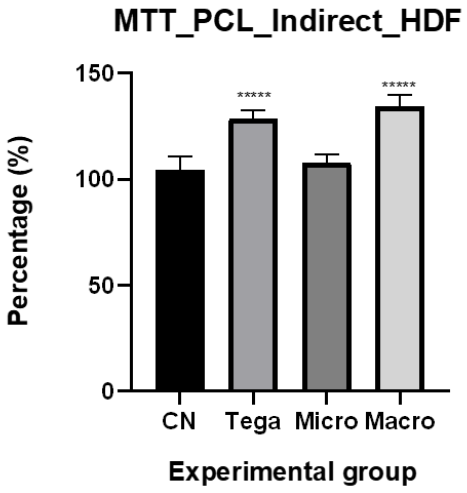

*Figure 23 - MTT indirect contact assay of PCL membranes in HDF cell line (n=2). CN: Control group; Tega: Tegaderm™; Micro: Microporous; Macro: Macroporous. * p<0.05; ** p<0.01; *** p<0.001; **** p<0.0001.*

By analyzing the MTT direct method (Figure 22), there is a significant decrease (****) in the Tegaderm™ and in the microporous membrane experimental group. In the macroporous group, the decrease was less significant (*) than in the other two groups.

Regarding the MTT indirect contact method performed in HDF (Figure 23), the results show a significant increase (****) in viability in the Tegaderm™ and macroporous group. The microporous group does not show a significant difference from the control.

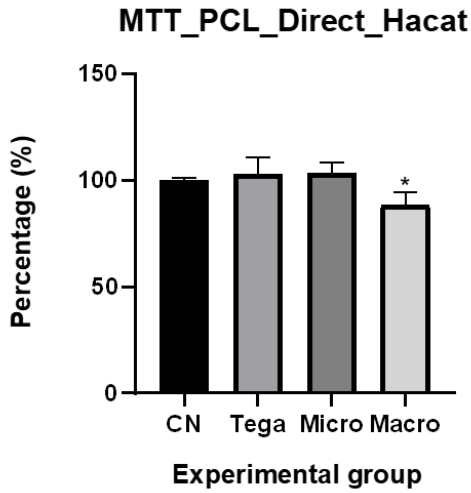

*Figure 24 - MTT direct assay of PCL membranes in HaCat cell line (n=2). CN: Control group; Tega: Tegaderm™; Micro: Microporous; Macro: Macroporous. * p<0.05; ** p<0.01; *** p<0.001; **** p<0.0001.*

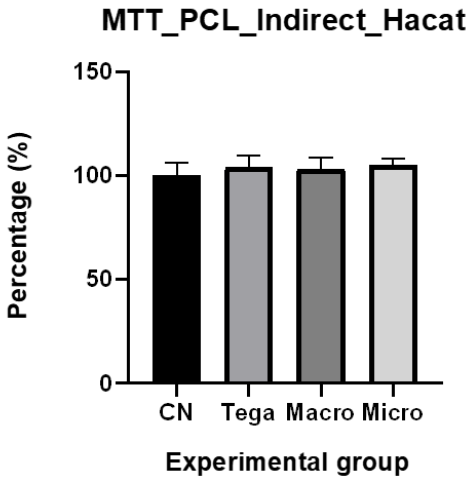

*Figure 25 - MTT indirect contact assay of PCL membranes in HaCat cell line (n=2). CN: Control group; Tega: Tegaderm™; Micro: Microporous; Macro: Macroporous. * p<0.05; ** p<0.01; *** p<0.001; **** p<0.0001.*

When using HaCat, we can see a significant decrease in viability in the macroporous group, with the Tegaderm™ and microporous group not showing significant differences (Figure 24). But, similar to the HDF, this result can be explained by the damage of the membrane to the monolayer.

On the indirect contact method using HaCat cells, there are no significant differences in viability between experimental groups.

Wound Healing

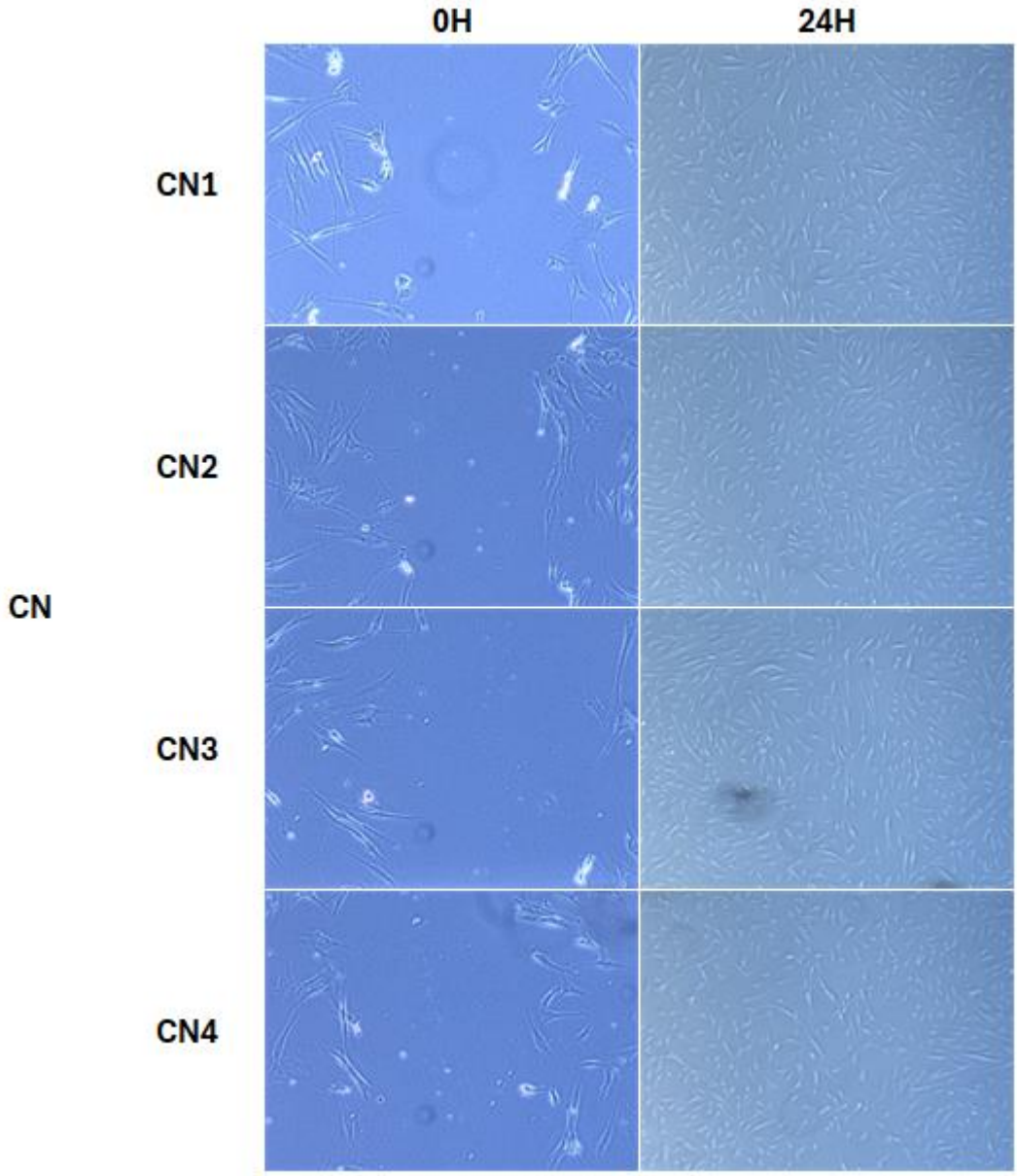

Figure 26 - Wound Healing assay in HDF cells: control group (n=1).

After 24 hours, the gaps appear to be completely closed in all control samples (CN1–CN4).

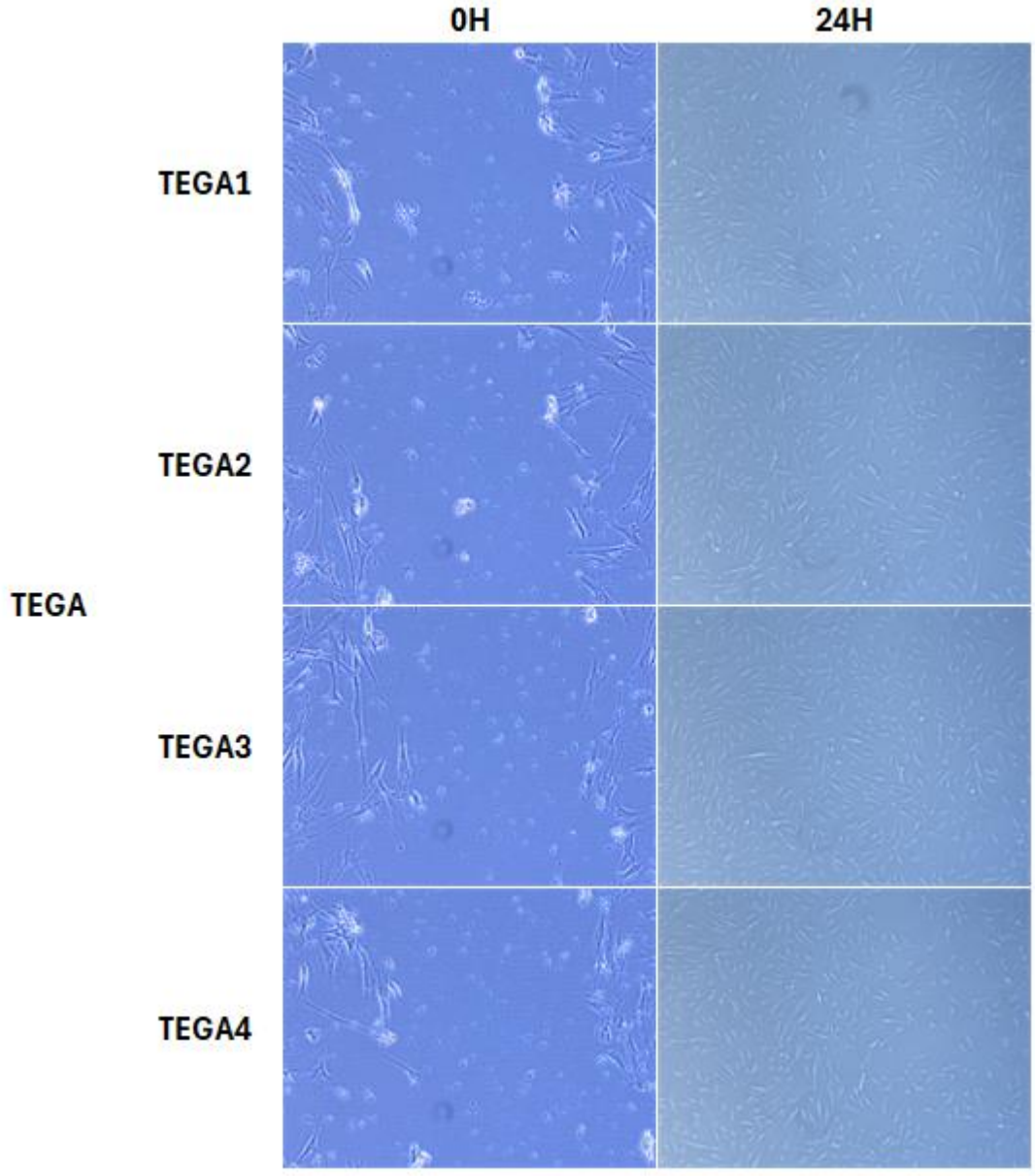

Figure 27 - Wound Healing assay in HDF cells: Tegaderm™ group (n=1).

After 24 hours, the gaps appear to be completely closed in all Tegaderm™ samples (TEGA 1–TEGA 4).

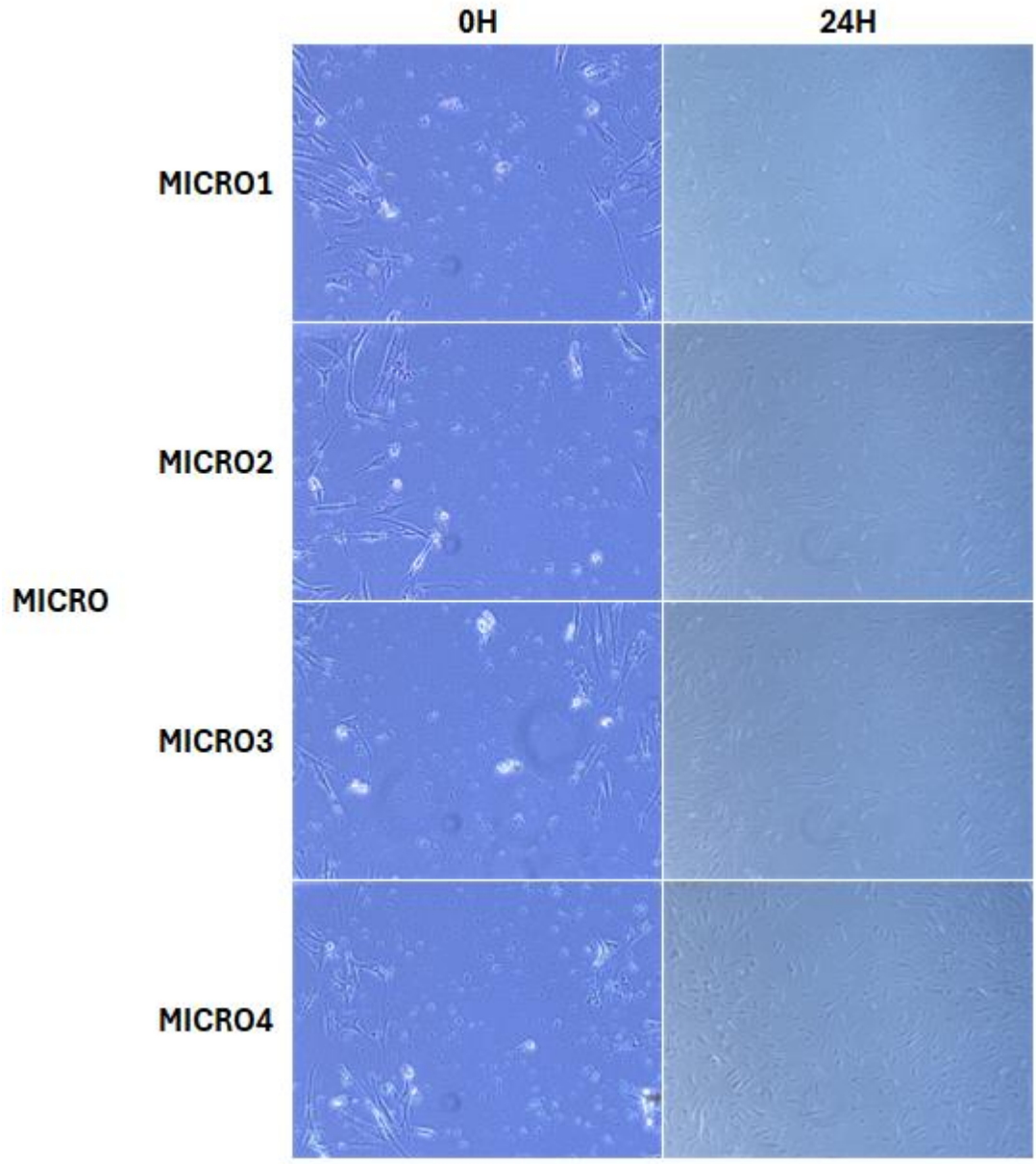

Figure 28 - Wound Healing assay in HDF cells: microporous group (n=1).

After 24 hours, the gaps appear to be completely closed in all microporous samples (MICRO 1–MICRO 4).

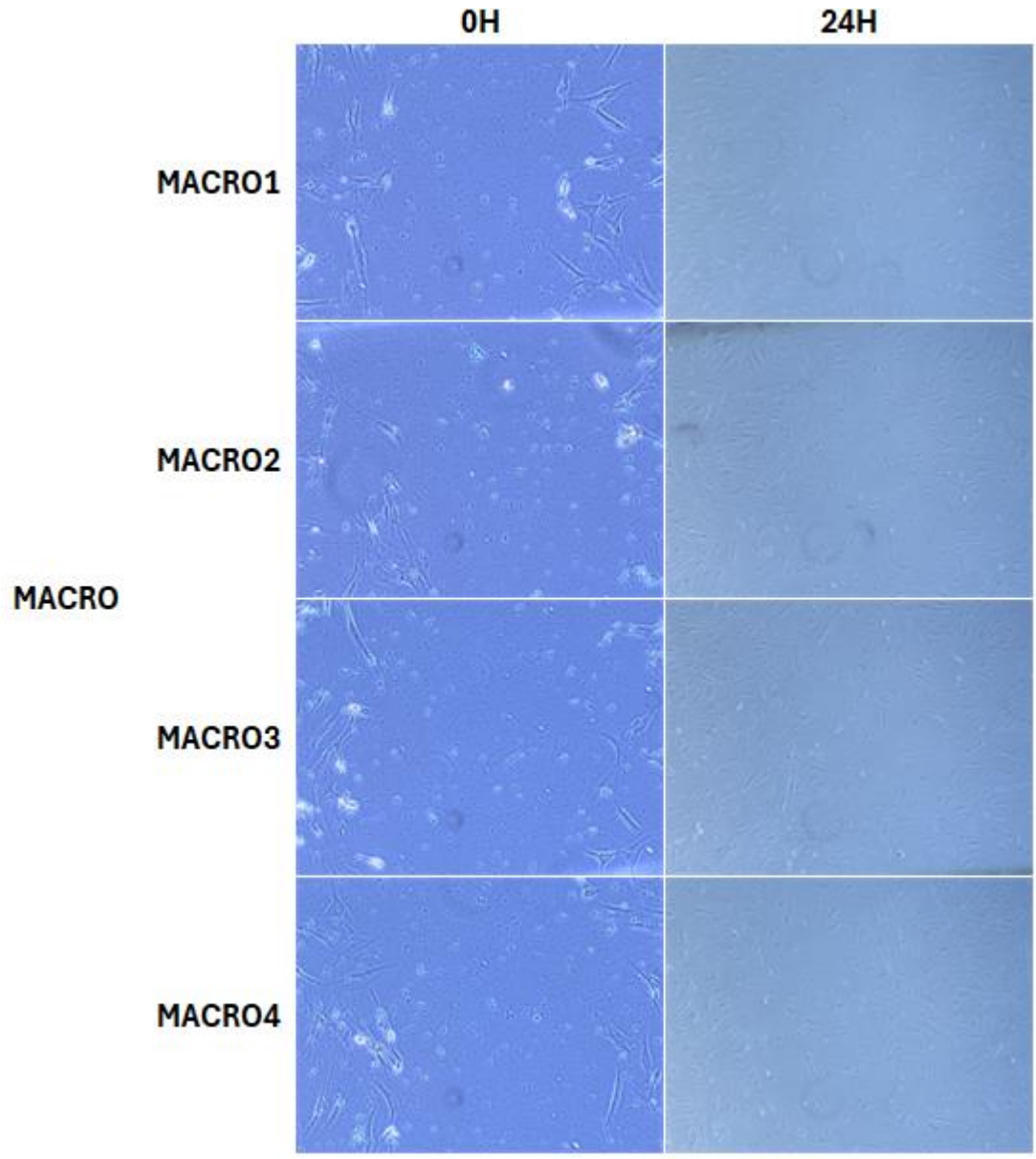

Figure 29 - Wound Healing assay in HDF cells: macroporous group (n=1).

After 24 hours, the gaps appear to be completely closed in all macroporous samples (MACRO 1–MACRO 4).

Table 8 – Percentage of closure of the wound healing assay of the various experimental groups (n=1).

	Experimental group							
	Control				Tegaderm™			
	CN1	CN2	CN3	CN4	TEGA1	TEGA2	TEGA3	TEGA4
Percentage (%) of wound closure	100%	100%	100%	100%	100%	100%	100%	100%
Mean percentage (%)	100%				100%			
	Experimental group							
	Macroporous				Microporous			
	MACRO1	MACRO2	MACRO3	MACRO4	MICRO1	MICRO2	MICRO3	MICRO4
Percentage (%) of wound closure	100%	100%	100%	100%	100%	100%	100%	100%
Mean percentage (%)	100%				100%			

All four replicates from the control group (CN1-CN4) showed 100% wound closure. The mean percentage for this group was 100%.

Similarly, all replicates from the Tegaderm™ group (TEGA1-TEGA1) showed 100% wound closure. The mean for this group is also 100%.

From the macroporous group (MACRO1-MACRO4), all four replicates showed 100% wound closure. The mean being also 100%.

Lastly, from the microporous group (MICRO1-MICRO4) there were 100% wound closure in all replicates. Therefore, the mean was also 100%.

Across all experimental groups (Control, Tegaderm™, Macroporous, and Microporous), 100% wound closure was achieved in all replicates. This indicates that no difference in wound healing ability was observed between the groups based on this particular metric. Every group, including the control, Tegaderm™-treated, and the groups with macroporous and microporous materials, was able to fully close the wound within the experimental period.

Macroscopic evaluation

Figure 30 shows the macroscopic images of the wounds after 21 days of the treatment protocol. The photo of the Tegaderm™ group relates to animal 1, from the microporous group to animal 9 and from the macroporous group from animal 15. The photos of these animals were selected to ensure consistency with those chosen for representing the histological evaluation within this project.

Figure 30 - Macroscopic photos of the wounds after 21 days of regeneration.

Histology

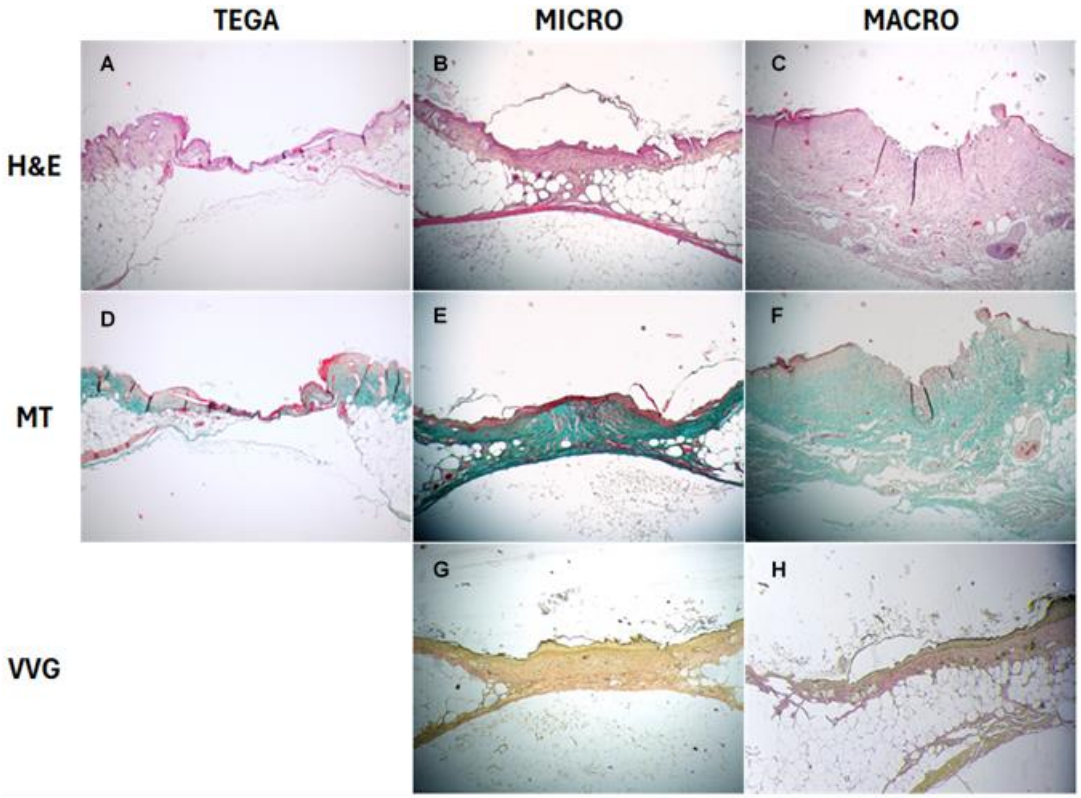

Figure 31 - Histological staining of skin wounds in db/db mice. A: H&E staining of animal 1 (TEGA group). Magnification 4x. B: H&E staining of animal 9 (MICRO group). Magnification 4x. C: H&E staining of animal 15 (MACRO group). Magnification 4x. D: MT staining of animal 1 (TEGA group). Magnification 4x. E: MT staining of animal 9 (MICRO group). Magnification 4x. F: MT staining of animal 15 (MACRO group). Magnification 4x. G: VVG staining of animal 9 (MICRO group). H: VVG staining of animal 15 (MACRO group). H&E: Hematoxylin and Eosin; MT: Masson's Trichrome; VVG: Verhoeff-Van Gieson; TEGA: Tegaderm™; MICRO: Microporous; MACRO: Macroporous.

The previous figure highlights the most representative wound skin histology from each experimental group across the three staining methods used. All images were captured using a 4x magnification objective. Please note that the Verhoeff-Van Gieson staining could not be performed for animal 1 due to complications with the paraffin block.

RNA expression

To assess alteration in molecular pathways related with metabolism and angiogenesis, RT-PCR was performed. Prior to the RT-PCR, RNA was extracted from the skin samples using the methodology described in Material and Methods section. For cost-benefit reasons, only the three samples with the best A260/280 ratio from each experimental group were selected for analysis. Specifically, samples 1, 5, and 6 were chosen from the Tegaderm™ group; samples 8, 9, and 10 from the microporous group; and samples 13, 14, and 18 from the macroporous group.

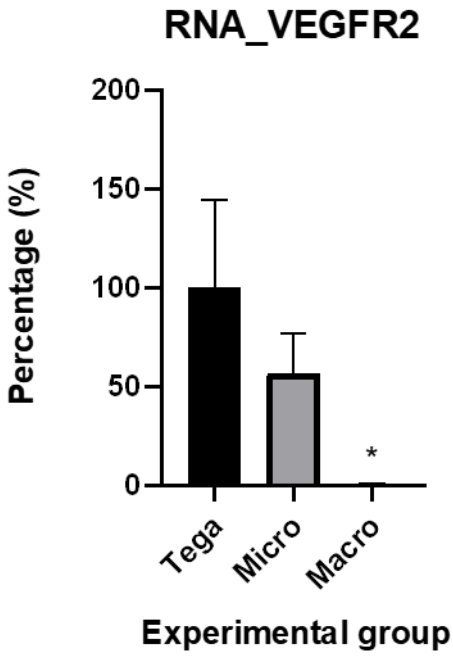

*Figure 32 - RNA expression of VEGFR2. Tega: Tegaderm™; Micro: microporous; Macro: macroporous. * p<0.05; ** p<0.01; *** p<0.001; **** p<0.0001.*

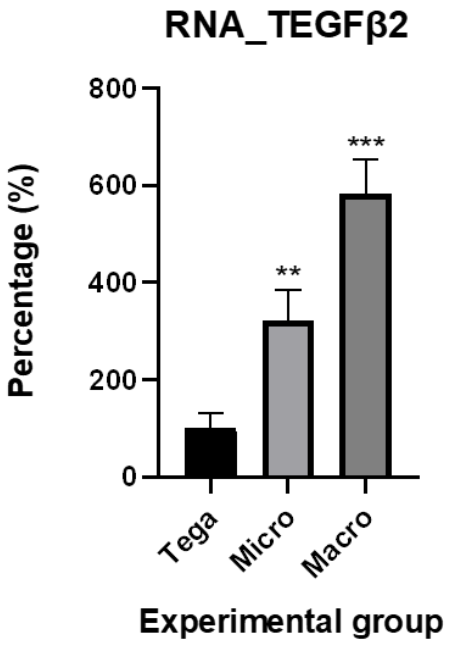

*Figure 33 - RNA expression of TGF-B2. Tega: Tegaderm™; Micro: microporous; Macro: macroporous. * p<0.05; ** p<0.01; *** p<0.001; **** p<0.0001.*

In Figure 32, compared to the control group (Tegaderm™), micro has a lower expression of VEGFR2 but not statistically significant. Macro has almost no expression of VEGFR2.

In Figure 33, Tegaderm™ (group control) shows the lesser expression of TEGFB2. Macro shows a statistically significant increase (**) in TEGFB2 (around 350%), with the macro group showing the highest expression of all the groups – around 600% when compared to the control group.

Biocompounds

MTT assay

In order to assess cell viability of the bioactive compounds, we employed the MTT assay. The results are shown in Figures 34, 35 36 and 37.

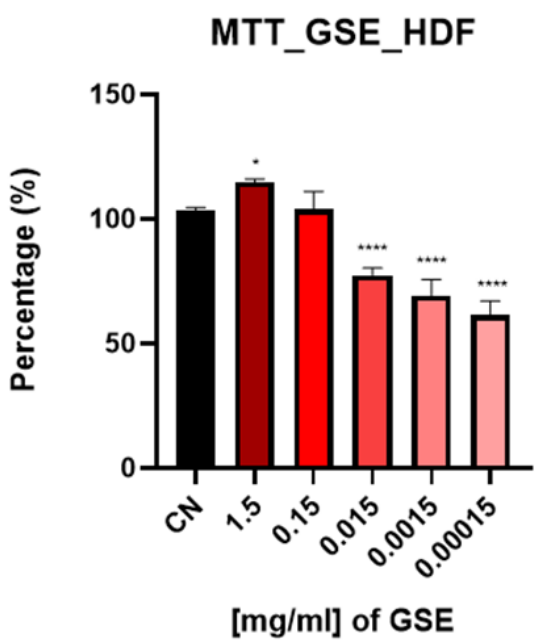

*Figure 34 - MTT assay of GSE in HDF cell line (n=2). * p<0.05; ** p<0.01; *** p<0.001; **** p<0.0001.*

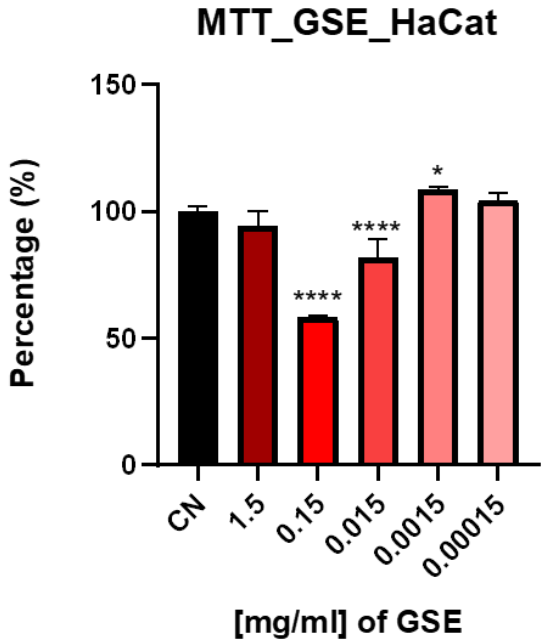

*Figure 35 - MTT assay of GSE in HaCat cell line (n=2). * p<0.05; ** p<0.01; *** p<0.001; **** p<0.0001.*

In this assay (Figure 34), a dose-response effect is evident, with the 1.5 mg/mL concentration of GSE showing the most pronounced proliferative effect on HDF cells. However, as the GSE concentration decreased (from 0.15 mg/mL to 0.00015 mg/mL), a notable decline in cell viability was observed. At 0.0015 mg/mL and lower, the cell viability dropped significantly, with the lowest concentrations (0.00015 mg/mL) resulting in almost a 50% reduction in viability.

On the assay using HaCat (Figure 35), we can see that higher concentrations of GSE (0.15 mg/mL and 0.015 mg/mL) significantly reduce the viability of HaCaT cells, with a statistical significance. At lower concentrations, the viability starts to increase, with 0.0015 mg/ml representing a significant increase when compared to the control.

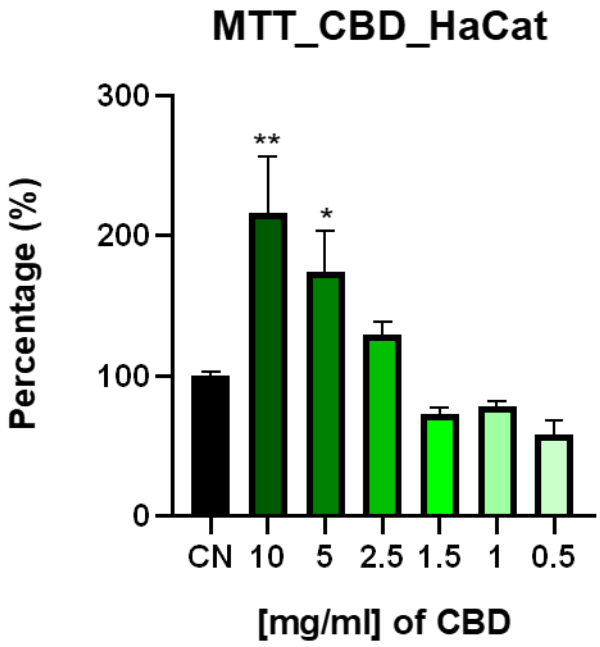

*Figure 36 - MTT assay of CBD in HaCat cell line (n=1). * p<0.05; ** p<0.01; *** p<0.001; **** p<0.0001.*

When using cannabidiol as a treatment in HaCat cells (Figure 36), there is a notable dose-response effect. The highest CBD concentration (10 mg/ml) significantly increased (**) cell viability to around 250%. The 5 mg/ml concentration also increased (*) cell viability to around 200%. At lower concentrations (2.5 mg/ml to 0.5 mg/ml), there is a decreasing trend in cell viability as the concentration of CBD decreases., but with no statistically significant indication.

DISCUSSION

In this study, we aimed to evaluate the bioactivity and regenerative potential of functionalized polycaprolactone-based skin dressings for diabetic wound management. Throughout the research project, we utilized one control group and three experimental groups: Tegaderm™, macroporous (macro), and microporous (micro). The Tegaderm™ group was included as it represents the most commonly used wound dressing, allowing us to compare the results of the PCL membranes against the leading dressing available on the market.

In the first part of our research project, we assessed two types of polycaprolactone-based skin dressings—macroporous and microporous—*in vitro*. To achieve this, we conducted cell viability and wound healing assays using different cell types.

Given that the aim is to use these membranes for diabetic foot wounds, the cells selected for the *in vitro* assays were representative of the various layers of the skin. For this purpose, we used HDF (fibroblasts) and HaCat (keratinocytes). Although it was not possible due to a lack of available cell line, we intended to use HMEC (epithelial cells) as well.

PCL Membranes

MTT

The results of the MTT assays (Figures 22, 23, 24 and 25) generally indicated that neither the macroporous nor the microporous membranes adversely affected the viability of skin cells. In the MTT_PCL_Direct_HDF assay (Figure 22), although a significant decrease is observed in the experimental groups, this is attributed to challenges associated with working with the membrane placed over the cell layers. When the biomaterial is removed, a substantial number of cells are inadvertently damaged or destroyed in the process.

In the MTT_PCL_Indirect_HDF (Figure 23), there is an increase in viability in the Tegaderm™ and macroporous group. In the absence of the physical PCL membrane, it is important to focus on how the PCL membrane may have influenced the culture medium during the incubation period. The observed increase in cell regeneration can be attributed to compounds that leached from the PCL membrane into the culture medium during the 24-hour incubation period. Even though the PCL membrane itself was no longer physically present during the treatment phase, these soluble factors could have promoted cellular regeneration. These substances may include degradation products of the PCL. Increasing the number of repetitions of this assay to prove this result, and further PCL degradation assays can give insight into the mechanism of action behind this increase in viability.

Thus, we can infer that the PCL membranes are non-toxic to skin cells. As anticipated, given the absence of bioactive compounds, these membranes appear safe for use in animal models and potential clinical applications.

Wound Healing

To assess cell migration, we conducted a Wound Healing assay. Similar to the MTT assay, we aimed to utilize both direct and indirect contact methods. However, the challenges posed by the membranes were even more significant in this assay. Each time we removed the PCL membrane to capture images under the microscope, it disrupted the cell monolayer and altered the results, ultimately making it impossible to proceed with the assay.

For that reason, only the indirect contact method was performed. On Figures 26, 27, 28 and 29 we can see the photos at the beginning of the assay and after 24 hours. In Table 8, we can see the analysis of the results after assessing the percentage of wound closure using ImageJ. Looking at the results, we can see that after 24hours, there were no differences in the percentage of wound closure between experimental groups. To perform this assay in order to note more differences, an increase in time points is necessary.

However, although it was not the primary objective of the assay, differences in cell organization between the macroporous and microporous groups were noted. The results of this assay, indicate that at 24h the membranes do not affect the percentage of cell migration *in vitro*, corroborating the previous results that indicate the non-toxicity of them. Thus, they might affect the way cells migrate and organize.

The realization of more assays, including the usage of the membranes directly over the cell monolayer, will provide further insight into the behavior of cell migration *in vitro*. To overcome the problem posed by the membrane when realizing the direct method, alternatives to address this challenge can be used. Coating the PCL membrane with a cell-repellent coating, decrease membrane attachment time, optimizing the removal techniques or used a commercially available physical barrier that allows interaction without direct contact, like using a transwell insert, are the most effective.

Apart from this problem, we also want to standardize the wound healing assay, once the scratch with the micropipette tip is not always the same width. To achieve this, we designed a 3D piece (Appendix C). Other alternatives include using commercially available inserts, but this option comes with more expensive costs to the project.

In vivo

After completing the *in vitro* assays, our next objective was to evaluate the bioactivity and regenerative potential of the PCL membranes *in vivo*. To achieve this, we used the skin wound healing model detailed in the Materials and Methods section.

We selected the db/db mice as our animal model because they most effectively replicate the pathology of T2DM and the associated impairment in wound healing [118]. We used a total of 18 animals, with 3 experimental groups, to ensure a representative sample size of 6 animals per group. Throughout the results, animal number 16 (assigned to the macroporous group) is not included, as it died before the protocol was completed. All animals were handled for one week prior to the start of the protocol to minimize stress and anxiety, promoting their well-being and improving the quality of the experimental results.

Macroscopic evaluation

In Figure 30, a macroscopic assessment of wound healing is provided for a representative animal from each experimental group. A comparison of the animals reveals that those treated with PCL membranes exhibit superior wound closure in terms of diameter. Notably, among the PCL-treated groups, the wounds in the macroporous group display more pronounced signs of scarring, whereas those in the microporous group show signs of enhanced regeneration.

Histology

After collecting the skin samples, we conducted three histological assays to evaluate the effects of the PCL membranes on tissue architecture and cellular composition.

The first assay involved Hematoxylin & Eosin (H&E) staining. H&E allows us to identify cellular components, assess tissue architecture, examine inflammatory response, evaluate re-epithelialization and detect necrosis and tissue damage [178]. In the second histological assay, we did a Masson's Trichrome stain. This stain allows us to assess collagen deposition, differentiation of tissue types, assessment of fibrosis, visualization of granulation tissue and to distinguish between healthy and damaged tissue [179]. Lastly, we did a Verhoeff-Van Gieson stain (VVG), due to the result obtained with the Masson's Trichrome stain – visualization of possible neo-vascularization. VVG stain is a specialized technique primarily used to visualize elastic fibers in tissue samples. Elastic fibers are present in blood vessels, so a positive result would further indicate the presence of them in the samples [180].

After analyzing Figure 31, regarding H&E we can see that the microporous membrane (B), shows the epidermis relatively regenerated with already a noticeable layer of keratinocytes at the surface, indicating that the wound is in the re-epithelialization phase. On the other hand,

the macroporous membrane (C), shows a surface disrupted and irregular representing a wound in the early stages of healing.

Regarding MT, the microporous membrane (E) shows some green bands under the wound surface indicating some collagen deposition. We can also see again the overlying epidermis well-formed with a layer of keratinized cells. This proves the fact that this wound is already in the remodeling phase. In the macroporous membrane (F), we see widespread collagen not as organized as in the microporous membrane image. We can also see that the epidermis is not yet formed, proving that comparing to the microporous membrane wound, this one is less mature, and in an earlier phase of wound healing.

When it comes to VVG stain, the microporous membrane appears to have more elastic fibers highlighted compared to the macroporous membrane. These findings are indicative of a more angiogenic process, which is a crucial factor that is often impaired in diabetic wound healing.

RT-PCR

To access pathways related to metabolism we proposed to used primers for pyruvate kinase (PK) and lactate dehydrogenase (LDH). PK is involved in glycolysis, converting phosphoenolpyruvate to pyruvate [181]. Higher expression of PK can indicate enhanced cellular metabolism, a sign of active tissue regeneration, as cells require energy to proliferate and repair tissue [182]. LDH converts pyruvate to lactate during anaerobic glycolysis [183]. Elevated LDH levels might indicate hypoxic conditions in the wound, often seen in initial stages of wound healing or poor oxygenation.

For seeking information about angiogenesis, we seek to used primers for transforming growth factor beta 1 (TGF-β1) and vascular endothelial growth factor receptor 2 (VEGFR2). TGF-β1 induces angiogenesis *in vivo* through an indirect mechanism. TGF-β1 helps recruit immune cells, stimulates fibroblast proliferation, and promotes collagen deposition. However, excessive or prolonged expression can lead to fibrosis or scarring [184]. VEGFR2 is the primary receptor for VEGF (Vascular Endothelial Growth Factor), which is critical for angiogenesis—the formation of new blood vessels. VEGFR2 promotes endothelial cell proliferation, migration, and survival during blood vessel formation. Increased VEGFR2 expression suggests active angiogenesis, meaning the tissue is promoting new blood vessel formation, which is essential for delivering oxygen and nutrients to regenerating tissues [185].

Unfortunately, primers for PK, LDH, and TGF-β1 were not available. While they have been ordered, they will not arrive in time for the current analysis. As a result, we will proceed with the analysis of VEGFR2 and include TGF-β2.

Although TGF-β1 and TGF-β2 belong to the same family and exhibit overlapping functions, they are not identical. TGF-β1 plays a direct role in wound healing, whereas TGF-β2 is more associated with tissue maintenance and inflammation. Although not as prominent as TGF-β1, TGF-β2 also plays a role in fibrosis and scar formation. While the inclusion of TGF-β2 may offer additional insights, it is important to note that it is not a direct substitute for TGF-β1. Therefore, an analysis of TGF-β1 remains necessary for a comprehensive understanding.

In Figure 32, we can infer that the Tegaderm™ group showed the highest expression of VEGFR2, which express that this skin dressing may promote the stronger angiogenic response. Nonetheless, it is important to note that the wound in contact with the microporous membrane appears to be in the advanced stages of healing, which may affect the expression of these markers, as their expression varies throughout the four stages of wound healing. The microporous membrane, still shows moderate levels of VEGFR2 expression with the macro membrane showing a statistically significant reduction compared to the other groups. These results align with those found in the VVG staining, showing an increase in the angiogenic process. A reduction in VEGFR2 expression, particularly in the macro group, could imply impaired blood vessel formation, which may negatively affect wound healing. The microporous membrane might offer a balance between promoting and controlling the angiogenic response. Further angiogenic parameters evaluation is needed in order to draw results.

Analyzing Figure 33, we see that the Tegaderm™ group shows the baseline level of TGF-β2 expression, serving as control. The microporous membrane leads to a significant increase in TGF-β2 expression. This suggests that this membrane may enhance TGF-β2–mediated processes, such as tissue remodeling and immune modulation, during wound healing. The macroporous membrane showed the highest and most significant increase in TGF-β2 expression. Therefore, elevated TGF-β2 levels may indicate that this membrane promotes an excessive remodeling response, which could lead to fibrosis or scarring in the wound, potentially affecting overall healing quality (Figure 37). The moderate increase in TGF-β2 expression in the microporous membrane might indicate a balanced response, promoting healing without excessive fibrosis.

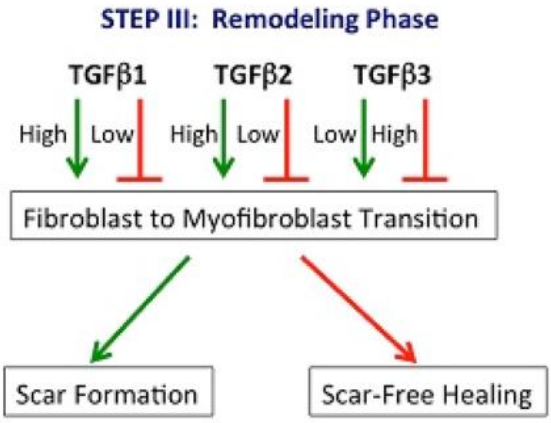

Figure 37 - Scheme highlighting the role of TGF-β2 in scar formation, sourced from [186]

Microporous vs Macroporous

After evaluating the wound healing process through macroscopic examination, histological analysis, and RNA expression of key markers, we can confidently conclude which PCL membrane is the most suitable scaffold for incorporating bioactive compounds.

The microporous membrane appears to offer the best potential for promoting wound healing. Although the macroporous membrane also shows signs of healing, multiple analyses revealed that it is associated with increased scar formation rather than regenerative healing. Histological staining, in particular, indicates that wounds in contact with the macroporous membrane are in a less advanced stage of healing. However, further repetition of these assays, analyzing the RNA expression of the markers described above, will always improve the confidence in our conclusions.

The superior performance of the microporous PCL membrane in promoting wound healing compared to the macroporous membrane can be attributed to several factors. The smaller pores of the microporous membrane more closely mimic the natural extracellular matrix, enhancing cell adhesion and proliferation. Additionally, the microporous structure may allow for a controlled release of growth factors, further supporting tissue repair. The limited pore size also restricts the infiltration of inflammatory cells and the entry of pathogens, creating a more favorable environment for wound healing. Furthermore, the microporous membrane provides better structural support, reducing the risk of collapse or deformation during the healing process.

Bioactive compounds

MTT

After all the *in vitro* and *in vivo* tests were performed on the PCL membranes, we advanced to test biocompounds that could functionalize the membrane, in order to increase its regenerative potential.

To accomplish that, we tested two biocompounds: grape stem extract (GSE) and cannabidiol (CBD).

The grape stem extract was provided by UTAD – Universidade de Trás-os-Montes e Alto Douro. This extract has already been tested in various biomedical applications. Although it is known that GSE contains phenolic compounds, its exact composition must be characterized after each harvest. The composition of GSE can vary based on environmental factors such as weather, season, harvest timing, sunlight exposure, and more. The goal is to develop a model that directly correlates these environmental factors with the GSE composition. If successful, this model could eliminate the need for repeated characterization, allowing us to infer the composition with a high degree of confidence.

In order to assess if the GSE was a good candidate for being incorporated in the PCL membranes, we started by doing a MTT assay in the same cell types used to test the PCL membrane.

Analyzing the results, a dose-response effect is evident (Figure 34), with the 1.5 mg/mL concentration of GSE showing the most pronounced proliferative effect on HDF cells. This suggests that at this concentration, GSE may act as an antioxidant, protecting the cells from oxidative stress and promoting metabolic activity, which is beneficial for fibroblast proliferation and wound healing. However, as the GSE concentration decreased (from 0.15 mg/mL to 0.00015 mg/mL), a notable decline in cell viability was observed. At 0.0015 mg/mL and lower, the cell viability dropped significantly, with the lowest concentrations (0.00015 mg/mL) resulting in almost a 50% reduction in viability. This suggests that at lower concentrations, GSE may exert pro-oxidant effects, leading to increased oxidative stress, cellular damage, or triggering of apoptotic pathways. The decline in viability at these concentrations indicates a potential cytotoxic effect of GSE at suboptimal doses in fibroblasts.

However, HaCat cells responded differently to GSE concentrations compared to HDF cells (Figure 35). The highest concentration of GSE (1.5 mg/mL), which was beneficial for HDF cells, did not significantly promote proliferation in HaCat cells, as the viability remained similar to that of the control. This suggests that keratinocytes may not benefit from high doses of GSE in the same way fibroblasts do.

Interestingly, at 0.15 mg/mL, a significant reduction in cell viability was observed, indicating that this concentration is cytotoxic to HaCat cells. This contrasts with the moderate decline in viability seen in HDF cells at the same concentration. This differential response highlights that keratinocytes are more sensitive to GSE at mid-range concentrations compared to fibroblasts.

Conversely, at the much lower concentration of 0.0015 mg/mL, GSE exhibited a proliferative effect on HaCat cells, with cell viability significantly increasing. This suggests that keratinocytes respond better to low doses of GSE, where the extract may stimulate pathways associated with cell proliferation and differentiation, crucial for epidermal repair. At the lowest concentration (0.00015 mg/mL), cell viability returned to levels comparable to the control, indicating that these concentrations are neither particularly beneficial nor harmful to HaCat cells.

The results from both cell lines reveal distinct dose-dependent responses to GSE. In HDF cells, higher concentrations (1.5 mg/mL) were more effective in promoting cell proliferation, while lower concentrations resulted in cytotoxicity. In contrast, HaCat cells displayed the opposite trend, with low concentrations (0.0015 mg/mL) having the most pronounced positive effect on cell viability, while higher concentrations (0.15 mg/mL) led to toxicity.

This difference may be attributed to the distinct roles that fibroblasts and keratinocytes play in tissue repair and their differential sensitivity to polyphenols and antioxidants found in GSE. Fibroblasts, which are primarily responsible for matrix deposition and tissue remodeling, may require higher concentrations of antioxidants to counteract oxidative stress during wound healing. On the other hand, keratinocytes, which are involved in re-epithelialization, might be more responsive to lower doses of GSE, where the balance between oxidative stress and proliferation is more tightly regulated. These findings suggest that the optimal concentration of GSE for wound healing applications may vary depending on the target cell type.

The cannabidiol (CBD) was isolated from a *Cannabis sativa* distillate provided by FarmCeutica Wellness (Richmond, Canada). The purified CBD sample, with a purity greater than 99.5%, was obtained using Centrifuge Partition Chromatography (CPC) technology, employing an rCPC device from RotaChrom (Purified Solutions, Budapest, Hungary). CBD has gained significant attention due to its anti-inflammatory, antioxidant, and analgesic properties, making it a promising candidate for promoting wound healing. Inflammation is a critical phase in the wound healing process, and excessive or prolonged inflammation can impair tissue regeneration. CBD's ability to modulate inflammatory responses may contribute to a more controlled healing environment, promoting faster and more effective tissue repair [187]. Additionally, CBD has been shown to influence cell proliferation and migration, both of which are key processes in wound closure.

Similar to the GSE, we started by performing a MTT assay using the CBD treatment. The results shown in Figure 36, suggests that CBD has a concentration-dependent positive effect on HaCat

viability. The highest concentration used (10 mg/ml) increased significantly cell viability by about 250%. The following concentration (5 mg/ml) also increased cell viability by about 180%. The concentration of 2.5 mg/ml reported an increased in cell viability, although not statistically significant. Lower concentrations (1.5 mg/ml, 1 mg/ml and 0.5 mg/ml) show a viability close to the control group.

Therefore, we can infer that CBD concentrations from 2.5 mg/ml to 10 mg/ml showed an increase in viability in keratinocyte cells. CBD is known to promote TGF-β production, which plays a role in re-epithelialization, where keratinocytes, like HaCat cells, migrate and proliferate to close the wound. However, while increased cell viability and proliferation are beneficial for wound healing, excessive proliferation can pose risks. Over-stimulation of cellular growth, if uncontrolled, can lead to the formation of defective cells or contribute to tumorigenesis, particularly in epithelial tissues, where rapid proliferation might lead to mutations or abnormal growth patterns. With this in mind, we select 5 mg/ml as the optimal concentration of CBD for promoting wound healing in the HaCaT cell line. This dosage balances enhanced keratinocyte proliferation without risking potential adverse effects from excessive cellular activity.

This MTT assay was conducted only once and exclusively on HaCaT cells, due to unforeseen challenges with the conditioning of the CBD. During the course of the study, a malfunction in the refrigeration system of the biocompounds storage room led to the deterioration of the CBD samples. The degradation of CBD was evidenced by a noticeable change in color, which compromised the compound's integrity. As a result, subsequent MTT assays yielded defective and inconsistent results.

This limitation prevented further replication of the experiment, thus affecting the ability to draw more robust, reproducible conclusions regarding the effects of CBD on keratinocyte viability and wound healing. The degradation of CBD highlights the sensitivity of cannabinoid compounds to storage conditions and emphasizes the importance of proper handling for future studies.

Grape stem extract vs Cannabidiol

Based on the *in vitro* study of the two bioactive compounds, it is not possible to reach a final conclusion on what is the best compound to incorporate in the PCL membrane. While some results point in a promising direction, its required further investigation with more assays needed to draw a definitive conclusion.

Although GSE demonstrated an increase in cell viability, its optimal concentration seems to vary across different skin cell types. Moreover, GSE poses challenges for biomedical

applications, particularly in skin dressings, due to the inconsistent concentration of bioactive molecules, which fluctuates depending on environmental conditions, as previously noted.

Regarding CBD, the results from the MTT assay performed in conjunction with the literature, suggest that this bioactive compound shows promising indicators for incorporation into the PCL membrane. However, to confirm this conclusion, it is crucial to repeat the assays and extend the studies to various skin cell lines. This will ensure the reliability and consistency of CBD's effects across different skin types and conditions. Further studies will provide the definitive evidence needed to fully validate CBD as the best bioactive compound for incorporation into PCL membranes, especially for applications in skin dressings.

Nonetheless, GSE has already shown some results as an antimicrobial strategy [188]. Therefore, the combination of the two compounds in the same membrane, with different roles (GSE – antimicrobial activity; CBD – regeneration), warrants further investigation.

CONCLUSIONS

The final goal of this project is to test the bioactivity and regenerative potential of functionalized polycaprolactone-based skin dressings in a diabetic animal model, in order to later progress to clinical application in human patients suffering from diabetic foot ulcers. The work described in the scope of this master thesis represents the initial phase of the project.

With the work made in this research, we were able to clarify that the microporous membrane is the best membrane to incorporate the bioactive compounds, once it presents the most promising results – faster wound healing and more regeneration. There is limited information available on the comparison of PCL membrane sizes for wound healing applications. Therefore, this study is a pioneering effort, with this goal being of significant importance.

Although we were unable to definitively select one bioactive agent, our preliminary results provide valuable insights. Grape stem extract (GSE) was found to present several challenges, which, when weighed against its therapeutic effects, suggest it may not be the most viable option. In contrast, cannabidiol (CBD) emerged as a promising candidate for incorporation into the membranes, though further research is necessary to confirm and substantiate these findings. In the literature regarding CBD and wound healing, there are good indicators. A study showed that a CBD formulation lowered the levels of prominent pro-inflammatory factors, such as IL-6 and MCP-1, while boosting the level of the anti-inflammatory factor TGF-β in cells stimulated with lipopolysaccharide. Additionally, this formulation accelerated the closure of the scratch wound gap.

Additionally, we successfully validated the db/db mice model as a reliable preclinical system for studying diabetic wound healing. As evidenced in the literature, this model represents an excellent and reliable approach for evaluating impaired wound healing [189].

Overall, this study contributes significantly to the field of clinical medicine by laying the groundwork for the development of a new functionalized biomaterial. Such innovations hold the potential to offer a groundbreaking treatment for diabetic foot ulcers, a condition that affects millions of people worldwide, and opens up new avenues for future research and clinical application.

FUTURE PERSPECTIVES

Since this master's thesis represents the initial phase of a complex project, even though it successfully addresses some of the objectives, there remain several future perspectives to explore.

In the first phase, it is essential to conduct more in-depth studies on the effects of CBD on wound healing to determine if it is the optimal compound for membrane incorporation. Specifically, it will be necessary to repeat the MTT assays, as well as perform BrdU and wound healing assays on various skin cell types. Additionally, the expression of metabolism and angiogenesis markers should be evaluated. Further investigation regarding the combination of the two compounds should also be conducted.

Regarding the membrane, to address the gaps identified in this study, direct wound healing assays should be repeated using the solutions proposed in the discussion. For RNA expression, markers such as PK, LDH, and TGF-β1 should be assessed to complement the data already obtained for VEGFR2 and TGF-β2. Furthermore, these last markers could also be repeated to increase the sample size and mitigate the high variability observed in the RNA expression assays presented in this thesis.

Once the optimal PCL membrane and the chosen bioactive compound have been identified, the next step is to functionalize the PCL membrane by incorporating the bioactive compound. This fabrication process will require additional research to determine the most effective combination. Subsequently, the functionalized membrane will be tested *in vivo* using the db/db animal model, as approved by our research group, to evaluate its potential for enhancing regeneration.

If the results in mice are promising, another animal model should be employed to further validate the findings. For this, I propose developing a swine model for wound healing, as it offers several advantages, including the ability to generate a larger number of wounds per animal. This approach would also support the 3Rs principle of ethical animal experimentation—specifically, the reduction of animal use. By incorporating a swine model, the functionalized PCL membranes can be validated across two distinct animal models, strengthening the case for advancing to clinical trials.

The ultimate goal is to test the functionalized membrane in clinical trials and, ideally, obtain approval from the EMA, FDA, and NMPA to bring the product to market. This innovation has the potential to significantly improve the quality of life for millions of people suffering from diabetic foot ulcers while also reducing the incidence of amputations associated with this condition. Beyond the health benefits, this product could have a substantial economic impact.

The treatment of diabetic foot ulcers and related complications, including amputations, imposes a significant financial burden on healthcare systems worldwide [190]. A more effective treatment, such as the proposed functionalized membrane, could greatly reduce these costs by enhancing healing rates and minimizing the need for invasive surgeries and hospitalizations.

Appendices

List of appendices

- Appendix A - Animal Welfare Committee of the Faculty of Medicine of the University of Porto approval

- Appendix B – Project “6-well insert plate”

- Appendix C – Award “Bragança Parreira” from SPD 2023

- Appendix D – SPD 2023 Poster Certificate

Appendix A - Animal Welfare Committee of the Faculty of Medicine of the University of Porto approval

U.PORTO

FMUP FACULDADE DE MEDICINA
UNIVERSIDADE DO PORTO

PARECER ORGÃO RESPONSÁVEL PELO BEM-ESTAR ANIMAL DA FACULDADE DE MEDICINA DA UNIVERSIDADE DO PORTO

EX^MO SENHOR

DIRECTOR DA DIRECÇÃO GERAL DE ALIMENTAÇÃO E VETERINÁRIA
Largo da Academia Nacional de Belas Artes, 2

1249-105 Lisboa

Assunto: Pedido de creditação ao abrigo do artigo 43 do Decreto-Lei nº113/2013 de 7 de Agosto para o projeto de experimentação animal da Investigadora Raquel Soares Lino.

Nossa Referência: ORBEA_83_2019/2102

Ao abrigo do ponto 2 do **artigo 43º do Decreto-Lei nº 113/2013** de 7 de Agosto vimos por este meio solicitar a Vossa Excelência o licenciamento do projeto de experimentação animal intitulado *"Avaliar o potencial terapêutico de novas formulações na regeneração de feridas em animais diabéticos utilizando biomateriais como veículos de moléculas bioativas"* da responsabilidade da Investigadora **Raquel Soares Lino.**

Informamos que o projeto foi revisto, corrigido e aprovado pelo ORBEA da Faculdade de Medicina da Universidade do Porto.

Porto, 21 de Fevereiro de 2019

BIOTÉRIO
CIM – FMUP • Piso 01
R. Plácido Costa • 4200-450 PORTO
Telefone: +351 220 426 860
bioterio@med.up.pt

Adriana da Cruz Francisco

Adriana da Cruz Francisco

Mestre em Enfermagem-Veterinária

Responsável pelo Bem-Estar Animal do Orgão Responsável pelo Bem-Estar Animal da Faculdade de Medicina da Universidade do Porto

Appendix B – Project “6-well plate insert”

In the scope of the research project:
Bioactivity and regenerative potential of functionalized polycaprolactone-based skin dressings for diabetic wounds management

Project “6-well plate insert”

Description

- *The goal is to create a 6-well plate insert that allows us to standardize the wound healing assay*

Dimensions

- *The 6-well plate has a diameter of about 55 milimeters. We want the wound area to be about 1.5 milimeters wide.*

Solution

- *Using SolidWorks, draw a 3D piece that meets the requirements mentioned above*

Fabrication

- *The first prototype (version 0.0.01) was made of PETG. It was fabricated by Creality Ender 5*

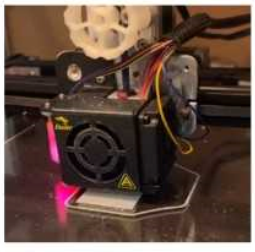

Sterilization

- *For sterilization, the 3D piece was subjected first to UV sterilization and then hydrogen peroxide sterilization.*

1/2

In the scope of the research project:
Bioactivity and regenerative potential of functionalized polycaprolactone-based skin dressings for diabetic wounds management

Project “6-well plate insert”

Prototype

In the following photos, we can see prototype version 0.0.01

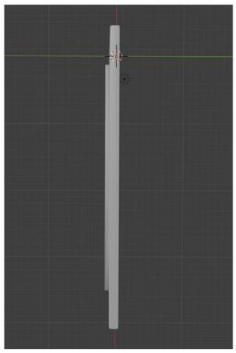

Aerial view

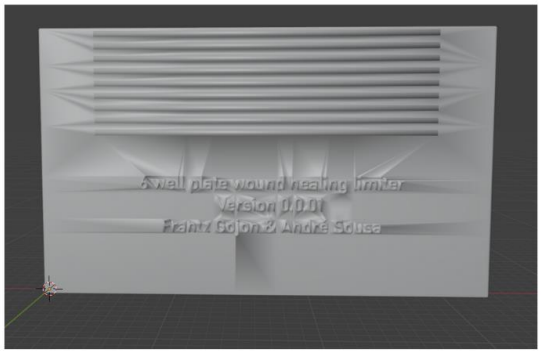

Left side view

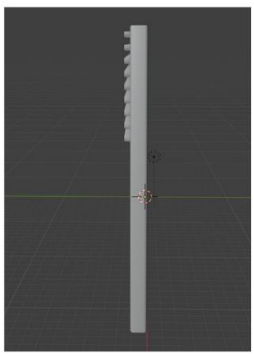

Frontal view

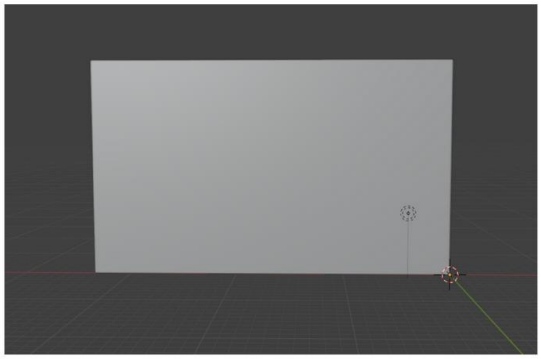

Right side view

Appendix C – Award “Bragança Parreira” from SPD 2023

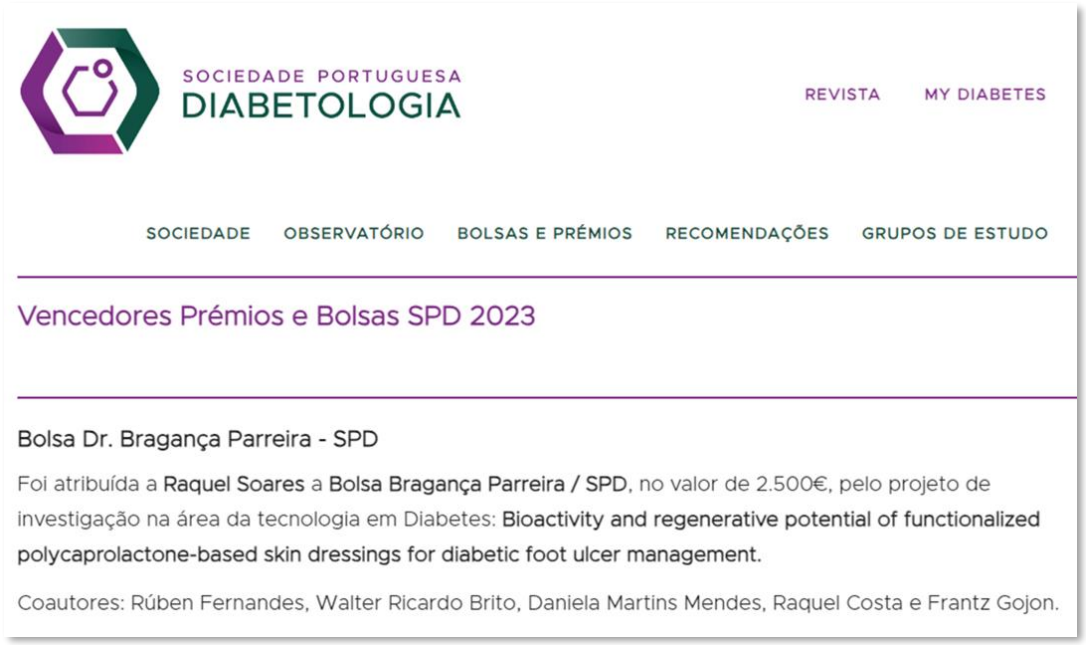

SOCIEDADE PORTUGUESA DIABETOLOGIA

REVISTA MY DIABETES

SOCIEDADE OBSERVATÓRIO BOLSAS E PRÉMIOS RECOMENDAÇÕES GRUPOS DE ESTUDO

Vencedores Prémios e Bolsas SPD 2023

Bolsa Dr. Bragança Parreira - SPD

Foi atribuída a **Raquel Soares** a **Bolsa Bragança Parreira / SPD**, no valor de 2.500€, pelo projeto de investigação na área da tecnologia em Diabetes: **Bioactivity and regenerative potential of functionalized polycaprolactone-based skin dressings for diabetic foot ulcer management.**

Coautores: Rúben Fernandes, Walter Ricardo Brito, Daniela Martins Mendes, Raquel Costa e Frantz Gojon.

Appendix D – SPD 2023 Poster Certificate

REFERENCES

[1] A. Sapra and P. Bhandari, *Diabetes*. 2024. [Online]. Available: http://www.ncbi.nlm.nih.gov/pubmed/30644346

[2] S. Ghosh and A. Collier, “Diagnosis, classification, epidemiology and biochemistry,” *Churchill’s Pocketbook of Diabetes*, pp. 1–49, 2012, doi: 10.1016/B978-0-443-10081-9.00008-7.

[3] J. Lucier and S. C. Dulebohn, *Type 1 Diabetes*. 2024. [Online]. Available: http://www.ncbi.nlm.nih.gov/pubmed/32333879

[4] A. M. Giwa *et al.*, “Current understandings of the pathogenesis of type 1 diabetes: Genetics to environment,” *World J Diabetes*, vol. 11, no. 1, p. 13, Jan. 2020, doi: 10.4239/WJD.V11.I1.13.

[5] “Type 1 diabetes estimates in children and adults | IDF Diabetes Atlas.” Accessed: Jul. 08, 2024. [Online]. Available: https://diabetesatlas.org/atlas/t1d-index-2022/

[6] L. E. Wagenknecht *et al.*, “Trends in incidence of youth-onset type 1 and type 2 diabetes in the USA, 2002–18: results from the population-based SEARCH for Diabetes in Youth study,” *Lancet Diabetes Endocrinol*, vol. 11, no. 4, pp. 242–250, Apr. 2023, doi: 10.1016/S2213-8587(23)00025-6.

[7] G. D. Ogle, F. Wang, G. A. Gregory, and J. Maniam, “Acknowledgements Type 1 diabetes numbers in children and adults”, Accessed: Jul. 08, 2024. [Online]. Available: www.diabetesatlas.org

[8] U. Galicia-Garcia *et al.*, “Pathophysiology of Type 2 Diabetes Mellitus,” *Int J Mol Sci*, vol. 21, no. 17, pp. 1–34, Sep. 2020, doi: 10.3390/IJMS21176275.

[9] “Type 2 diabetes - Symptoms and causes - Mayo Clinic.” Accessed: Jul. 08, 2024. [Online]. Available: https://www.mayoclinic.org/diseases-conditions/type-2-diabetes/symptoms-causes/syc-20351193

[10] R. Weinberg Sibony, O. Segev, S. Dor, and I. Raz, “Drug Therapies for Diabetes.,” *Int J Mol Sci*, vol. 24, no. 24, Dec. 2023, doi: 10.3390/ijms242417147.

[11] D. Spruijt-Metz, G. A. O’Reilly, L. Cook, K. A. Page, and C. Quinn, “Behavioral contributions to the pathogenesis of type 2 diabetes.,” *Curr Diab Rep*, vol. 14, no. 4, p. 475, Apr. 2014, doi: 10.1007/s11892-014-0475-3.

[12] E. L. Chan and M. J. Abrahamson, “Pharmacological management of type 2 diabetes mellitus: Rationale for rational use of insulin,” *Mayo Clin Proc*, vol. 78, no. 4, pp. 459–467, Apr. 2003, doi: 10.4065/78.4.459.

[13] B. Hemmingsen, D. P. Sonne, M. I. Metzendorf, and B. Richter, “Insulin secretagogues for prevention or delay of type 2 diabetes mellitus and its associated complications in persons at increased risk for the development of type 2 diabetes mellitus,” *Cochrane Database Syst Rev*, vol. 2016, no. 10, Apr. 2016, doi: 10.1002/14651858.CD012151.PUB2.

[14] X. Li and Z. Q. Liu, “Pharmacogenetic Factors That Affect Drug Metabolism and Efficacy in Type 2 Diabetes Mellitus,” in *Drug Metabolism in Diseases*, Elsevier, 2017, pp. 157–179. doi: 10.1016/B978-0-12-802949-7.00007-9.

[15] R. Landgraf, “Meglitinide Analogues in the Treatment of Type 2 Diabetes Mellitus,” *Drugs Aging*, vol. 17, no. 5, pp. 411–425, Nov. 2000, doi: 10.2165/00002512-200017050-00007.

[16] R. D. Ferguson, E. J. Gallagher, E. J. Scheinman, R. Damouni, and D. LeRoith, “The Epidemiology and Molecular Mechanisms Linking Obesity, Diabetes, and Cancer,” 2013, pp. 51–98. doi: 10.1016/B978-0-12-416673-8.00010-1.

[17] C. Day and C. J. Bailey, “Biguanides,” *xPharm: The Comprehensive Pharmacology Reference*, pp. 1–3, 2007, doi: 10.1016/B978-008055232-3.61041-4.

[18] C. Palleria *et al.*, “Potential effects of current drug therapies on cognitive impairment in patients with type 2 diabetes,” *Front Neuroendocrinol*, vol. 42, pp. 76–92, Jul. 2016, doi: 10.1016/J.YFRNE.2016.07.002.

[19] A. J. Krentz and A. J. Sinclair, “The Evolution of Glucose-Lowering Drugs for Type 2 Diabetes,” *Nutritional and Therapeutic Interventions for Diabetes and Metabolic Syndrome*, pp. 459–474, Jan. 2012, doi: 10.1016/B978-0-12-385083-6.00036-X.

[20] M. A. B. Khan, M. J. Hashim, J. K. King, R. D. Govender, H. Mustafa, and J. Al Kaabi, “Epidemiology of Type 2 Diabetes - Global Burden of Disease and Forecasted Trends,” *J Epidemiol Glob Health*, vol. 10, no. 1, pp. 107–111, Mar. 2020, doi: 10.2991/JEGH.K.191028.001.

[21] A. B. Olokoba, O. A. Obateru, and L. B. Olokoba, “Type 2 Diabetes Mellitus: A Review of Current Trends,” *Oman Med J*, vol. 27, no. 4, p. 269, 2012, doi: 10.5001/OMJ.2012.68.

[22] L. S. Hoffman, T. J. Fox, C. Anastasopoulou, and I. Jialal, “Maturity Onset Diabetes in the Young,” *StatPearls*, Aug. 2023, Accessed: Jul. 08, 2024. [Online]. Available: https://www.ncbi.nlm.nih.gov/books/NBK532900/

[23] “Maturity onset diabetes of the young (MODY) | Diabetes UK.” Accessed: Jul. 08, 2024. [Online]. Available: https://www.diabetes.org.uk/diabetes-the-basics/other-types-of-diabetes/mody

[24] S. Ellard, C. Bellanné-Chantelot, A. T. Hattersley, and European Molecular Genetics Quality Network (EMQN) MODY group, “Best practice guidelines for the molecular genetic diagnosis of maturity-onset diabetes of the young.,” *Diabetologia*, vol. 51, no. 4, pp. 546–53, Apr. 2008, doi: 10.1007/s00125-008-0942-y.

[25] K. M. Nkonge, D. K. Nkonge, and T. N. Nkonge, “The epidemiology, molecular pathogenesis, diagnosis, and treatment of maturity-onset diabetes of the young (MODY),” *Clin Diabetes Endocrinol*, vol. 6, no. 1, Dec. 2020, doi: 10.1186/S40842-020-00112-5.

[26] K. M. Nkonge, D. K. Nkonge, and T. N. Nkonge, “The epidemiology, molecular pathogenesis, diagnosis, and treatment of maturity-onset diabetes of the young (MODY).,” *Clin Diabetes Endocrinol*, vol. 6, no. 1, p. 20, Nov. 2020, doi: 10.1186/s40842-020-00112-5.

[27] B. S. Quintanilla Rodriguez, E. S. Vadakekut, and H. Mahdy, *Gestational Diabetes*. 2024. [Online]. Available: http://www.ncbi.nlm.nih.gov/pubmed/29370047

[28] E. Eyth, H. Basit, and C. J. Swift, *Glucose Tolerance Test*. 2024. [Online]. Available: http://www.ncbi.nlm.nih.gov/pubmed/22675678

[29] “Tests & Diagnosis for Gestational Diabetes - NIDDK.” Accessed: Jul. 08, 2024. [Online]. Available: https://www.niddk.nih.gov/health-information/diabetes/overview/what-is-diabetes/gestational/tests-diagnosis

[30] “Gestational diabetes - Symptoms & causes - Mayo Clinic.” Accessed: Jul. 08, 2024. [Online]. Available: https://www.mayoclinic.org/diseases-conditions/gestational-diabetes/symptoms-causes/syc-20355339

[31] J. F. Plows, J. L. Stanley, P. N. Baker, C. M. Reynolds, and M. H. Vickers, “The Pathophysiology of Gestational Diabetes Mellitus,” *Int J Mol Sci*, vol. 19, no. 11, Nov. 2018, doi: 10.3390/IJMS19113342.

[32] A. Sweeting *et al.*, “Epidemiology and management of gestational diabetes,” *The Lancet*, vol. 0, no. 0, Jun. 2024, doi: 10.1016/S0140-6736(24)00825-0.

[33] K. J. L. Bell, P. P. Glasziou, and J. A. Doust, “A call to reconsider the new diagnostic criteria for gestational diabetes mellitus.,” *CMAJ*, vol. 195, no. 38, p. E1307, Oct. 2023, doi: 10.1503/cmaj.148614-l.

[34] A. Dahl and S. Kumar, “Recent Advances in Neonatal Diabetes.,” *Diabetes Metab Syndr Obes*, vol. 13, pp. 355–364, 2020, doi: 10.2147/DMSO.S198932.

[35] S. A. W. Greeley, R. N. Naylor, L. H. Philipson, and G. I. Bell, “Neonatal Diabetes: An Expanding List of Genes Allows for Improved Diagnosis and Treatment,” *Curr Diab Rep*, vol. 11, no. 6, pp. 519–532, Dec. 2011, doi: 10.1007/s11892-011-0234-7.

[36] M. B. Lemelman, L. Letourneau, and S. A. W. Greeley, “Neonatal Diabetes Mellitus,” *Clin Perinatol*, vol. 45, no. 1, pp. 41–59, Mar. 2018, doi: 10.1016/j.clp.2017.10.006.

[37] J. Beltrand *et al.*, “Neonatal Diabetes Mellitus,” *Front Pediatr*, vol. 8, Sep. 2020, doi: 10.3389/fped.2020.540718.

[38] S. A. W. Greeley, R. N. Naylor, L. H. Philipson, and G. I. Bell, “Neonatal Diabetes: An Expanding List of Genes Allows for Improved Diagnosis and Treatment,” *Curr Diab Rep*, vol. 11, no. 6, pp. 519–532, Dec. 2011, doi: 10.1007/s11892-011-0234-7.

[39] M. S. Popoviciu *et al.*, “Diabetes Mellitus Secondary to Endocrine Diseases: An Update of Diagnostic and Treatment Particularities.,” *Int J Mol Sci*, vol. 24, no. 16, Aug. 2023, doi: 10.3390/ijms241612676.

[40] “Acromegaly | Johns Hopkins Diabetes Guide.” Accessed: Jul. 11, 2024. [Online]. Available: https://www.hopkinsguides.com/hopkins/view/Johns_Hopkins_Diabetes_Guide/547003/all/Acromegaly

[41] O. Alexopoulou, M. Bex, P. Kamenicky, A. B. Mvoula, P. Chanson, and D. Maiter, “Prevalence and risk factors of impaired glucose tolerance and diabetes mellitus at diagnosis of acromegaly: A study in 148 patients,” *Pituitary*, vol. 17, no. 1, pp. 81–89, Feb. 2014, doi: 10.1007/S11102-013-0471-7/METRICS.

[42] Y. Kinoshita *et al.*, “Impaired glucose metabolism in Japanese patients with acromegaly is restored after successful pituitary surgery if pancreatic β-cell function is preserved,” *Eur J Endocrinol*, vol. 164, no. 4, pp. 467–473, Apr. 2011, doi: 10.1530/EJE-10-1096.

[43] “Cushing’s Syndrome - NIDDK.” Accessed: Jul. 11, 2024. [Online]. Available: https://www.niddk.nih.gov/health-information/endocrine-diseases/cushings-syndrome

[44] G. Mazziotti, C. Gazzaruso, and A. Giustina, “Diabetes in Cushing syndrome: basic and clinical aspects,” *Trends in Endocrinology & Metabolism*, vol. 22, no. 12, pp. 499–506, Dec. 2011, doi: 10.1016/j.tem.2011.09.001.

[45] M. Barbot, F. Ceccato, and C. Scaroni, “Diabetes Mellitus Secondary to Cushing’s Disease,” *Front Endocrinol (Lausanne)*, vol. 9, Jun. 2018, doi: 10.3389/fendo.2018.00284.

[46] J. Herndon *et al.*, “The Effect of Curative Treatment on Hyperglycemia in Patients With Cushing Syndrome,” *J Endocr Soc*, vol. 6, no. 1, Jan. 2022, doi: 10.1210/jendso/bvab169.

[47] N. Reisch, M. Peczkowska, A. Januszewicz, and H. P. H. Neumann, “Pheochromocytoma: presentation, diagnosis and treatment.,” *J Hypertens*, vol. 24, no. 12, pp. 2331–9, Dec. 2006, doi: 10.1097/01.hjh.0000251887.01885.54.

[48] A. J. Carroll and O. E. Bogucki, “Depression and biomarkers of cardiovascular disease,” in *The Neuroscience of Depression*, Elsevier, 2021, pp. 239–249. doi: 10.1016/B978-0-12-817933-8.00018-9.

[49] T. Beninato *et al.*, “Resection of Pheochromocytoma Improves Diabetes Mellitus in the Majority of Patients,” *Ann Surg Oncol*, vol. 24, no. 5, pp. 1208–1213, May 2017, doi: 10.1245/S10434-016-5701-6.

[50] “Graves’ Disease - NIDDK.” Accessed: Jul. 11, 2024. [Online]. Available: https://www.niddk.nih.gov/health-information/endocrine-diseases/graves-disease

[51] E. Song *et al.*, “Risk of Diabetes in Patients with Long-Standing Graves’ Disease: A Longitudinal Study,” *Endocrinology and Metabolism*, vol. 36, no. 6, pp. 1277–1286, Dec. 2021, doi: 10.3803/EnM.2021.1251.

[52] J. B. Byrd, A. F. Turcu, and R. J. Auchus, “Primary Aldosteronism: Practical Approach to Diagnosis and Management.,” *Circulation*, vol. 138, no. 8, pp. 823–835, Aug. 2018, doi: 10.1161/CIRCULATIONAHA.118.033597.

[53] J. H. Scott, M. A. Menouar, and R. J. Dunn, *Physiology, Aldosterone*. 2024. [Online]. Available: http://www.ncbi.nlm.nih.gov/pubmed/25377117

[54] M. Moustaki, S. A. Paschou, E. C. Vakali, and A. Vryonidou, “Secondary diabetes mellitus due to primary aldosteronism,” *Endocrine*, vol. 79, no. 1, pp. 17–30, Aug. 2022, doi: 10.1007/s12020-022-03168-8.

[55] H. Komada *et al.*, “Insulin secretion and sensitivity before and after surgical treatment for aldosterone-producing adenoma,” *Diabetes Metab*, vol. 46, no. 3, pp. 236–242, Jun. 2020, doi: 10.1016/j.diabet.2019.10.002.

[56] T. J. O’Toole and S. Sharma, *Physiology, Somatostatin*. 2024. [Online]. Available: http://www.ncbi.nlm.nih.gov/pubmed/20629989

[57] “Diabetes Diagnosis & Tests | ADA.” Accessed: Aug. 29, 2024. [Online]. Available: https://diabetes.org/about-diabetes/diagnosis

[58] E. Eyth and R. Naik, *Hemoglobin A1C*. 2024. [Online]. Available: http://www.ncbi.nlm.nih.gov/pubmed/31411713

[59] D. H. Wasserman, “Four grams of glucose,” *American Journal of Physiology-Endocrinology and Metabolism*, vol. 296, no. 1, pp. E11–E21, Jan. 2009, doi: 10.1152/ajpendo.90563.2008.

[60] L. M. Jenkusky and K. S. Gawlik, “Glucose Tolerance Test,” *Laboratory Screening and Diagnostic Evaluation: An Evidence-Based Approach*, pp. 373–376, Apr. 2023, doi: 10.5005/jp/books/14203_21.

[61] N. A. ElSayed *et al.*, “2. Diagnosis and Classification of Diabetes: *Standards of Care in Diabetes—2024*,” *Diabetes Care*, vol. 47, no. Supplement_1, pp. S20–S42, Jan. 2024, doi: 10.2337/dc24-S002.

[62] A. D. Deshpande, M. Harris-Hayes, and M. Schootman, “Epidemiology of diabetes and diabetes-related complications.,” *Phys Ther*, vol. 88, no. 11, pp. 1254–64, Nov. 2008, doi: 10.2522/ptj.20080020.

[63] D. O. Soyoye, O. O. Abiodun, R. T. Ikem, B. A. Kolawole, and A. O. Akintomide, “Diabetes and peripheral artery disease: A review,” *World J Diabetes*, vol. 12, no. 6, pp. 827–838, Jun. 2021, doi: 10.4239/wjd.v12.i6.827.

[64] H. Wu *et al.*, “Diabetes and Its Cardiovascular Complications: Comprehensive Network and Systematic Analyses,” *Front Cardiovasc Med*, vol. 9, Feb. 2022, doi: 10.3389/fcvm.2022.841928.

[65] R. T. Varghese and I. Jialal, *Diabetic Nephropathy*. 2024. [Online]. Available: http://www.ncbi.nlm.nih.gov/pubmed/12800476

[66] “Diabetic nephropathy (kidney disease) - Symptoms and causes - Mayo Clinic.” Accessed: Jul. 19, 2024. [Online]. Available: https://www.mayoclinic.org/diseases-conditions/diabetic-nephropathy/symptoms-causes/syc-20354556

[67] “Diabetic Retinopathy | National Eye Institute.” Accessed: Jul. 19, 2024. [Online]. Available: https://www.nei.nih.gov/learn-about-eye-health/eye-conditions-and-diseases/diabetic-retinopathy

[68] W. Wang and A. C. Y. Lo, “Diabetic Retinopathy: Pathophysiology and Treatments.,” *Int J Mol Sci*, vol. 19, no. 6, Jun. 2018, doi: 10.3390/ijms19061816.

[69] Z. L. Teo *et al.*, “Global Prevalence of Diabetic Retinopathy and Projection of Burden through 2045: Systematic Review and Meta-analysis,” *Ophthalmology*, vol. 128, no. 11, pp. 1580–1591, Nov. 2021, doi: 10.1016/J.OPHTHA.2021.04.027.

[70] A. Berbudi, N. Rahmadika, A. I. Tjahjadi, and R. Ruslami, “Type 2 Diabetes and its Impact on the Immune System.,” *Curr Diabetes Rev*, vol. 16, no. 5, pp. 442–449, 2020, doi: 10.2174/1573399815666191024085838.

[71] O. Boyman and J. Sprent, “The role of interleukin-2 during homeostasis and activation of the immune system,” *Nat Rev Immunol*, vol. 12, no. 3, pp. 180–190, Mar. 2012, doi: 10.1038/nri3156.

[72] M. Saraiva and A. O’Garra, “The regulation of IL-10 production by immune cells,” *Nat Rev Immunol*, vol. 10, no. 3, pp. 170–181, Mar. 2010, doi: 10.1038/nri2711.

[73] E. P. Thong, E. Codner, J. S. E. Laven, and H. Teede, “Diabetes: a metabolic and reproductive disorder in women,” *Lancet Diabetes Endocrinol*, vol. 8, no. 2, pp. 134–149, Feb. 2020, doi: 10.1016/S2213-8587(19)30345-6.

[74] C. S. Marathe, C. K. Rayner, T. Wu, K. L. Jones, and M. Horowitz, “Gastrointestinal Disorders in Diabetes,” *Endotext*, Feb. 2024, Accessed: Aug. 17, 2024. [Online]. Available: https://www.ncbi.nlm.nih.gov/books/NBK553219/

[75] G. S. Aswath, L. A. Foris, A. K. Ashwath, and K. Patel, “Diabetic Gastroparesis,” *Music Educators Journal*, Mar. 2023, Accessed: Aug. 17, 2024. [Online]. Available: https://www.ncbi.nlm.nih.gov/books/NBK430794/

[76] T. Sözen, N. Ç. Başaran, M. Tınazlı, and L. Özışık, “Musculoskeletal problems in diabetes mellitus.,” *Eur J Rheumatol*, vol. 5, no. 4, pp. 258–265, Dec. 2018, doi: 10.5152/eurjrheum.2018.18044.

[77] X. Wang, C.-X. Yuan, B. Xu, and Z. Yu, “Diabetic foot ulcers: Classification, risk factors and management,” *World J Diabetes*, vol. 13, no. 12, p. 1049, Dec. 2022, doi: 10.4239/WJD.V13.I12.1049.

[78] X. Liao, S. H. Li, M. M. El Akkawi, X. B. Fu, H. W. Liu, and Y. S. Huang, “Surgical amputation for patients with diabetic foot ulcers: A Chinese expert panel consensus treatment guide,” *Front Surg*, vol. 9, p. 1003339, Nov. 2022, doi: 10.3389/FSURG.2022.1003339.

[79] A. Tuttolomondo, C. Maida, and A. Pinto, “Diabetic foot syndrome: Immune-inflammatory features as possible cardiovascular markers in diabetes,” *World J Orthop*, vol. 6, no. 1, p. 62, Jan. 2015, doi: 10.5312/WJO.V6.I1.62.

[80] “Diabetic Foot Problems: Symptoms, Treatment, and Care.” Accessed: Apr. 10, 2024. [Online]. Available: https://www.webmd.com/diabetes/foot-problems

[81] R. Sharma, R. Kapila, A. K. Sharma, J. Mann, and J. Resident, “Diabetic Foot Disease-Incidence and Risk Factors: A Clinical Study,” *The Journal of Foot and Ankle Surgery (Asia-Pacific)*, vol. 3, no. 1, pp. 41–46, doi: 10.5005/jp-journals-10040-1046.

[82] P. Zhang, J. Lu, Y. Jing, S. Tang, D. Zhu, and Y. Bi, “Global epidemiology of diabetic foot ulceration: a systematic review and meta-analysis †,” *Ann Med*, vol. 49, no. 2, pp. 106–116, Feb. 2017, doi: 10.1080/07853890.2016.1231932.

[83] S. P. Pendsey, “Understanding diabetic foot,” *Int J Diabetes Dev Ctries*, vol. 30, no. 2, p. 75, Apr. 2010, doi: 10.4103/0973-3930.62596.

[84] H. Deng *et al.*, “Mechanisms of diabetic foot ulceration: A review,” *J Diabetes*, vol. 15, no. 4, pp. 299–312, Apr. 2023, doi: 10.1111/1753-0407.13372.

[85] T. Thiruvoipati, C. E. Kielhorn, and E. J. Armstrong, “Peripheral artery disease in patients with diabetes: Epidemiology, mechanisms, and outcomes.,” *World J Diabetes*, vol. 6, no. 7, pp. 961–9, Jul. 2015, doi: 10.4239/wjd.v6.i7.961.

[86] W. W. Li, M. J. Carter, E. Mashiach, and S. D. Guthrie, “Vascular assessment of wound healing: a clinical review.,” *Int Wound J*, vol. 14, no. 3, pp. 460–469, Jun. 2017, doi: 10.1111/iwj.12622.

[87] L. M. Cucci, C. Satriano, T. Marzo, and D. La Mendola, “Angiogenin and Copper Crossing in Wound Healing,” *Int J Mol Sci*, vol. 22, no. 19, p. 10704, Oct. 2021, doi: 10.3390/ijms221910704.

[88] “Diabetes and Your Immune System | CDC.” Accessed: Apr. 19, 2024. [Online]. Available: https://www.cdc.gov/diabetes/library/features/diabetes_immune_system.html

[89] N. V. Vorobjeva and B. V. Chernyak, “NETosis: Molecular Mechanisms, Role in Physiology and Pathology,” *Biochemistry (Moscow)*, vol. 85, no. 10, pp. 1178–1190, Oct. 2020, doi: 10.1134/S0006297920100065.

[90] J. M. Raja, M. A. Maturana, S. Kayali, A. Khouzam, and N. Efeovbokhan, “Diabetic foot ulcer: A comprehensive review of pathophysiology and management modalities.,” *World J Clin Cases*, vol. 11, no. 8, pp. 1684–1693, Mar. 2023, doi: 10.12998/wjcc.v11.i8.1684.

[91] C. B. Thompson *et al.*, “A century of the Warburg effect.,” *Nat Metab*, vol. 5, no. 11, pp. 1840–1843, Nov. 2023, doi: 10.1038/s42255-023-00927-3.

[92] O. Niță *et al.*, “Evaluating Classification Systems of Diabetic Foot Ulcer Severity: A 12-Year Retrospective Study on Factors Impacting Survival,” *Healthcare 2023, Vol. 11, Page 2077*, vol. 11, no. 14, p. 2077, Jul. 2023, doi: 10.3390/HEALTHCARE11142077.

[93] F. Chuan, K. Tang, P. Jiang, B. Zhou, and X. He, “Reliability and validity of the perfusion, extent, depth, infection and sensation (PEDIS) classification system and score in patients with diabetic foot ulcer,” *PLoS One*, vol. 10, no. 4, Apr. 2015, doi: 10.1371/JOURNAL.PONE.0124739.

[94] J. D. Brocklehurst, “The Validity and Reliability of the SINBAD Classification System for Diabetic Foot Ulcers,” *Adv Skin Wound Care*, vol. 36, no. 11, pp. 1–5, Nov. 2023, doi: 10.1097/ASW.0000000000000050.

[95] P. Ansari *et al.*, “Hyperglycaemia-Linked Diabetic Foot Complications and Their Management Using Conventional and Alternative Therapies,” *Applied Sciences (Switzerland)*, vol. 12, no. 22, Nov. 2022, doi: 10.3390/APP122211777.

[96] T. I. Oliver and M. Mutluoglu, “Diabetic Foot Ulcer,” Aug. 2023, Accessed: Apr. 11, 2024. [Online]. Available: https://www.ncbi.nlm.nih.gov/books/NBK537328/

[97] M. A. Woodruff and D. W. Hutmacher, “The return of a forgotten polymer—Polycaprolactone in the 21st century,” *Prog Polym Sci*, vol. 35, no. 10, pp. 1217–1256, Oct. 2010, doi: 10.1016/j.progpolymsci.2010.04.002.

[98] A. B. Rosskopf, C. Loupatatzis, C. W. A. Pfirrmann, T. Böni, and M. C. Berli, “The Charcot foot: a pictorial review,” *Insights Imaging*, vol. 10, no. 1, Dec. 2019, doi: 10.1186/S13244-019-0768-9.

[99] “Amputation and diabetes: How to protect your feet - Mayo Clinic.” Accessed: Apr. 11, 2024. [Online]. Available: https://www.mayoclinic.org/diseases-conditions/diabetes/in-depth/amputation-and-diabetes/art-20048262

[100] E. P. Weledji and P. Fokam, “Treatment of the diabetic foot-to amputate or not?,” 2014, doi: 10.1186/1471-2482-14-83.

[101] “Clinical manifestations, diagnosis, and management of diabetic infections of the lower extremities.” Accessed: Apr. 19, 2024. [Online]. Available: https://medilib.ir/uptodate/show/7651

[102] “Diabetic Foot Exam: MedlinePlus Medical Test.” Accessed: Aug. 28, 2024. [Online]. Available: https://medlineplus.gov/lab-tests/diabetic-foot-exam/

[103] “Diabetic Wound Care: Monofilament Testing | WCEI.” Accessed: Apr. 19, 2024. [Online]. Available: https://blog.wcei.net/diabetic-wound-care-monofilament-testing

[104] E. Everett and N. Mathioudakis, “Update on management of diabetic foot ulcers,” *Ann N Y Acad Sci*, vol. 1411, no. 1, pp. 153–165, 2018, doi: 10.1111/NYAS.13569/FULL.

[105] “Diabetic Foot Exam: MedlinePlus Medical Test.” Accessed: Apr. 19, 2024. [Online]. Available: https://medlineplus.gov/lab-tests/diabetic-foot-exam/

[106] A. Llewellyn, J. Kraft, C. Holton, M. Harden, and M. Simmonds, “Imaging for detection of osteomyelitis in people with diabetic foot ulcers: A systematic review and meta-analysis,” *Eur J Radiol*, vol. 131, p. 109215, Oct. 2020, doi: 10.1016/J.EJRAD.2020.109215.

[107] E. Everett and N. Mathioudakis, “Update on management of diabetic foot ulcers”, doi: 10.1111/nyas.13569.

[108] Z. Ma, K. Shou, Z. Li, C. Jian, B. Qi, and A. Yu, “Negative pressure wound therapy promotes vessel destabilization and maturation at various stages of wound healing and

thus influences wound prognosis," *Exp Ther Med*, vol. 11, no. 4, pp. 1307–1317, Apr. 2016, doi: 10.3892/ETM.2016.3083/DOWNLOAD.

[109] V. Zaver and P. Kankanalu, "Negative Pressure Wound Therapy," *StatPearls*, Sep. 2023, Accessed: Apr. 19, 2024. [Online]. Available: https://www.ncbi.nlm.nih.gov/books/NBK576388/

[110] M. Y. Memar, M. Yekani, N. Alizadeh, and H. B. Baghi, "Hyperbaric oxygen therapy: Antimicrobial mechanisms and clinical application for infections," *Biomed Pharmacother*, vol. 109, pp. 440–447, Jan. 2019, doi: 10.1016/J.BIOPHA.2018.10.142.

[111] W. V. Sathyaraj, L. Prabakaran, J. Bhoopathy, S. Dharmalingam, R. Karthikeyan, and R. Atchudan, "Therapeutic Efficacy of Polymeric Biomaterials in Treating Diabetic Wounds—An Upcoming Wound Healing Technology," *Polymers (Basel)*, vol. 15, no. 5, Mar. 2023, doi: 10.3390/POLYM15051205.

[112] E. Grambow, H. Sorg, C. G. G. Sorg, and D. Strüder, "Experimental Models to Study Skin Wound Healing with a Focus on Angiogenesis," *Medical Sciences*, vol. 9, no. 3, p. 55, Aug. 2021, doi: 10.3390/medsci9030055.

[113] P. Martin and R. Nunan, "Cellular and molecular mechanisms of repair in acute and chronic wound healing," *British Journal of Dermatology*, vol. 173, no. 2, pp. 370–378, Aug. 2015, doi: 10.1111/bjd.13954.

[114] A. Grada, J. Mervis, and V. Falanga, "Research Techniques Made Simple: Animal Models of Wound Healing," *Journal of Investigative Dermatology*, vol. 138, no. 10, pp. 2095-2105.e1, Oct. 2018, doi: 10.1016/j.jid.2018.08.005.

[115] L. K. S. Parnell and S. W. Volk, "The Evolution of Animal Models in Wound Healing Research: 1993-2017.," *Adv Wound Care (New Rochelle)*, vol. 8, no. 12, pp. 692–702, Dec. 2019, doi: 10.1089/wound.2019.1098.

[116] A. Couturier, C. Calissi, J.-L. Cracowski, D. Sigaudo-Roussel, C. Khouri, and M. Roustit, "Mouse models of diabetes-related ulcers: a systematic review and network meta-analysis," *EBioMedicine*, vol. 98, p. 104856, Dec. 2023, doi: 10.1016/j.ebiom.2023.104856.

[117] B. L. Furman, "Streptozotocin-Induced Diabetic Models in Mice and Rats," *Curr Protoc*, vol. 1, no. 4, Apr. 2021, doi: 10.1002/cpz1.78.

[118] C. P. D. Kottaisamy, D. S. Raj, V. Prasanth Kumar, and U. Sankaran, “Experimental animal models for diabetes and its related complications—a review,” *Lab Anim Res*, vol. 37, no. 1, p. 23, Aug. 2021, doi: 10.1186/s42826-021-00101-4.

[119] H. Münzberg, P. Singh, S. B. Heymsfield, S. Yu, and C. D. Morrison, “Recent advances in understanding the role of leptin in energy homeostasis,” *F1000Res*, vol. 9, p. 451, May 2020, doi: 10.12688/f1000research.24260.1.

[120] R. Singh, M. Gholipourmalekabadi, and S. H. Shafikhani, “Animal models for type 1 and type 2 diabetes: advantages and limitations,” *Front Endocrinol (Lausanne)*, vol. 15, Feb. 2024, doi: 10.3389/fendo.2024.1359685.

[121] E. Malikmammadov, T. E. Tanir, A. Kiziltay, V. Hasirci, and N. Hasirci, “PCL and PCL-based materials in biomedical applications,” *J Biomater Sci Polym Ed*, vol. 29, no. 7–9, pp. 863–893, Jun. 2018, doi: 10.1080/09205063.2017.1394711.

[122] O. S. Manoukian *et al.*, “Biomaterials for tissue engineering and regenerative medicine,” *Encyclopedia of Biomedical Engineering*, vol. 1–3, pp. 462–482, Jan. 2019, doi: 10.1016/B978-0-12-801238-3.64098-9.

[123] J. C. Middleton and A. J. Tipton, “Synthetic biodegradable polymers as orthopedic devices,” *Biomaterials*, vol. 21, no. 23, pp. 2335–2346, Dec. 2000, doi: 10.1016/S0142-9612(00)00101-0.

[124] J. Ricardo, “AVALIAÇÃO DA APLICABILIDADE DE MEMBRANAS DE POLI (e – CAPROLACTONA) CARREGADAS COM FÁRMACOS NO TRATAMENTO DE FERIDAS,” Manaus, 2020.

[125] M. O. Christen and F. Vercesi, “Polycaprolactone: How a Well-Known and Futuristic Polymer Has Become an Innovative Collagen-Stimulator in Esthetics,” *Clin Cosmet Investig Dermatol*, vol. 13, p. 31, 2020, doi: 10.2147/CCID.S229054.

[126] M. Kurakula, G. S. N. K. Rao, and K. S. Yadav, “Fabrication and characterization of polycaprolactone-based green materials for drug delivery,” *Applications of Advanced Green Materials*, pp. 395–423, Jan. 2020, doi: 10.1016/B978-0-12-820484-9.00016-7.

[127] S. M. Espinoza, H. I. Patil, E. San Martin Martinez, R. Casañas Pimentel, and P. P. Ige, “Poly-ε-caprolactone (PCL), a promising polymer for pharmaceutical and biomedical applications: Focus on nanomedicine in cancer,” *International Journal of Polymeric Materials and Polymeric Biomaterials*, vol. 69, no. 2, pp. 85–126, Jan. 2020, doi: 10.1080/00914037.2018.1539990.

[128] “Weight-bearing mechanics of human joints. A central role for marrow fat.” Accessed: Apr. 21, 2024. [Online]. Available: https://researchfeatures.com/weight-bearing-mechanics-human-joints-central-role-for-marrow-fat/

[129] R. Dwivedi *et al.*, “Polycaprolactone as biomaterial for bone scaffolds: Review of literature,” *J Oral Biol Craniofac Res*, vol. 10, no. 1, p. 381, Jan. 2020, doi: 10.1016/J.JOBCR.2019.10.003.

[130] A. O. Mahmoud Salehi, S. Heidari Keshel, F. Sefat, and L. Tayebi, “Use of polycaprolactone in corneal tissue engineering: A review,” *Mater Today Commun*, vol. 27, p. 102402, Jun. 2021, doi: 10.1016/J.MTCOMM.2021.102402.

[131] A. Bhadran *et al.*, “Recent Advances in Polycaprolactones for Anticancer Drug Delivery,” *Pharmaceutics*, vol. 15, no. 7, Jul. 2023, doi: 10.3390/PHARMACEUTICS15071977.

[132] “Quill Monoderm VLM-1022 Suture - Henry Schein Medical.” Accessed: Apr. 21, 2024. [Online]. Available: https://www.henryschein.com/us-en/Shopping/ProductDetails.aspx?productid=1286186&cdivId=specialmarkets_d&name=Quill%20Monoderm%20Suture%202-0%20PGA/PCL%20Clear%2020cm%20Monofilament%2012/Bx&ShowProductCompare=true&FullPageMode=true

[133] “SXMD2B402-LATAMPT | Ethicon Latin America, Portuguese.” Accessed: Apr. 21, 2024. [Online]. Available: https://www.ethicon.com/latam/pt/epc/code/sxmd2b402?lang=pt-default

[134] X. Yang, Y. Wang, Y. Zhou, J. Chen, and Q. Wan, “The Application of Polycaprolactone in Three-Dimensional Printing Scaffolds for Bone Tissue Engineering,” *Polymers (Basel)*, vol. 13, no. 16, Aug. 2021, doi: 10.3390/POLYM13162754.

[135] P. Ginestra, E. Ceretti, and A. Fiorentino, “Electrospinning of Poly-caprolactone for Scaffold Manufacturing: Experimental Investigation on the Process Parameters Influence,” *Procedia CIRP*, vol. 49, pp. 8–13, Jan. 2016, doi: 10.1016/J.PROCIR.2015.07.020.

[136] R. A. Ilyas *et al.*, “Natural Fiber-Reinforced Polycaprolactone Green and Hybrid Biocomposites for Various Advanced Applications,” *Polymers (Basel)*, vol. 14, no. 1, Jan. 2022, doi: 10.3390/POLYM14010182.

[137] M. Serra, A. Casas, J. A. Teixeira, and A. N. Barros, “Revealing the Beauty Potential of Grape Stems: Harnessing Phenolic Compounds for Cosmetics,” *Int J Mol Sci*, vol. 24, no. 14, Jul. 2023, doi: 10.3390/IJMS241411751.

[138] J. Quero *et al.*, “Grape Stem Extracts with Potential Anticancer and Antioxidant Properties,” *Antioxidants*, vol. 10, no. 2, pp. 1–17, Feb. 2021, doi: 10.3390/ANTIOX10020243.

[139] M. Serra, A. Casas, J. A. Teixeira, and A. N. Barros, “Revealing the Beauty Potential of Grape Stems: Harnessing Phenolic Compounds for Cosmetics,” *Int J Mol Sci*, vol. 24, no. 14, Jul. 2023, doi: 10.3390/IJMS241411751.

[140] J. B. (Jeffrey B.) Harborne, *Phytochemical methods : a guide to modern techniques of plant analysis*. Chapman and Hall, 1998. Accessed: Jun. 29, 2024. [Online]. Available: https://link.springer.com/book/9780412572609

[141] V. L. Singleton, R. Orthofer, and R. M. Lamuela-Raventós, “Methods in Enzymology - Oxidants and Antioxidants Part A,” *Methods Enzymol*, vol. 299, pp. 152–178, Jan. 1999, doi: 10.1016/S0076-6879(99)99017-1.

[142] C. C. Chang, M. H. Yang, H. M. Wen, and J. C. Chern, “Estimation of total flavonoid content in propolis by two complementary colometric methods,” *J Food Drug Anal*, vol. 10, no. 3, p. 3, Jul. 2020, doi: 10.38212/2224-6614.2748.

[143] C. D. Stalikas, “Extraction, separation, and detection methods for phenolic acids and flavonoids,” *J Sep Sci*, vol. 30, no. 18, pp. 3268–3295, Dec. 2007, doi: 10.1002/JSSC.200700261.

[144] R. M. Silverstein, G. C. Bassler, and T. Morrill, “Chapter Three: Infrared Spectrometry,” *Spectrometric Identification of Organic Compounds, Fifth Edition*, pp. 91–164, 1991, Accessed: Jun. 29, 2024. [Online]. Available: https://www.wiley.com/en-ca/Spectrometric+Identification+of+Organic+Compounds%2C+8th+Edition-p-9780470616376

[145] F. J. Vázquez-Armenta *et al.*, “Antibacterial and antioxidant properties of grape stem extract applied as disinfectant in fresh leafy vegetables,” *J Food Sci Technol*, vol. 54, no. 10, p. 3192, Sep. 2017, doi: 10.1007/S13197-017-2759-5.

[146] M. Serra, A. Casas, J. A. Teixeira, and A. N. Barros, “Revealing the Beauty Potential of Grape Stems: Harnessing Phenolic Compounds for Cosmetics,” *Int J Mol Sci*, vol. 24, no. 14, Jul. 2023, doi: 10.3390/IJMS241411751.

[147] M. Miastkowska and E. Sikora, “Anti-Aging Properties of Plant Stem Cell Extracts,” *Cosmetics 2018, Vol. 5, Page 55*, vol. 5, no. 4, p. 55, Sep. 2018, doi: 10.3390/COSMETICS5040055.

[148] A. Teixeira *et al.*, “Natural Bioactive Compounds from Winery By-Products as Health Promoters: A Review,” *International Journal of Molecular Sciences 2014, Vol. 15, Pages 15638-15678*, vol. 15, no. 9, pp. 15638–15678, Sep. 2014, doi: 10.3390/IJMS150915638.

[149] “Nutricost, Extrato da Semente de Uva, 28.000 mg, 240 Cápsulas.” Accessed: Jul. 01, 2024. [Online]. Available: https://pt.iherb.com/pr/nutricost-grape-seed-extract-28-000-mg-240-capsules/129432?gad_source=1&gclid=CjwKCAjwhIS0BhBqEiwADAUhc4YdUbxH6XCZFgFAIY3YEZZ9Kl1KywjmdWe9w5xei1hkWJ88L6dZkhoCSZ8QAvD_BwE&gclsrc=aw.ds

[150] “Extrato de Semente de Uva Zumub na Zumub.” Accessed: Jul. 01, 2024. [Online]. Available: https://www.zumub.com/PT/-c-372/grape-seed-extract-90-capsulas?currency=EUR&gcpid=171&feedpid=10460&utm_source=google&utm_campaign=20672258808&utm_medium=cpc&utm_content=utm_term&gad_source=1&gclid=CjwKCAjwhIS0BhBqEiwADAUhc20-sdTTAizc2U_-GAV5mRMHXXRkgIW2UP3q8vVbBqt1g3yNbqfBqBoCmqAQAvD_BwE

[151] “Shop Farm Stay - Grape Stem Cell Wrinkle Lifting Cream - 50ml | STYLEVANA.” Accessed: Jul. 01, 2024. [Online]. Available: https://www.stylevana.com/en_EU/farm-stay-grape-stem-cell-wrinkle-lifting-cream-50ml25427.html?utm_source=google&utm_medium=organic&utm_campaign=freelisting&sonid=25407&___store=bwsveub_en&utm_source=google&utm_medium=cpc&utm_campaign=18174886948&utm_term=&utm_content=25407&device=c&gad_source=1&gclid=CjwKCAjwhIS0BhBqEiwADAUhc3ofM3SqReRSXbs02mbQReuxNesZjCzfln5wO-fixqNIeOzqw6MyGxoCmgEQAvD_BwE

[152] J. A. Nieto, S. Santoyo, M. Prodanov, G. Reglero, and L. Jaime, “Valorisation of grape stems as a source of phenolic antioxidants by using a sustainable extraction methodology,” *Foods*, vol. 9, no. 5, May 2020, doi: 10.3390/foods9050604.

[153] R. Adams and M. Hunt, “Structure of Cannabidiol, a Product Isolated from the Marihuana Extract of Minnesota Wild Hemp. I,” *J Am Chem Soc*, vol. 62, no. 1, pp. 196–200, Jan. 1940, doi: 10.1021/JA01858A058/ASSET/JA01858A058.FP.PNG_V03.

[154] “Differences Between CBD vs. THC.” Accessed: Jul. 01, 2024. [Online]. Available: https://www.webmd.com/pain-management/cbd-thc-difference

[155] “Cannabidiol | C21H30O2 | CID 644019 - PubChem.” Accessed: Jul. 01, 2024. [Online]. Available: https://pubchem.ncbi.nlm.nih.gov/compound/Cannabidiol

[156] M. D. Marks *et al.*, “Identification of candidate genes affecting Δ9-tetrahydrocannabinol biosynthesis in Cannabis sativa,” *J Exp Bot*, vol. 60, no. 13, p. 3715, Sep. 2009, doi: 10.1093/JXB/ERP210.

[157] S. Chayasirisobhon, “Mechanisms of Action and Pharmacokinetics of Cannabis,” *Perm J*, vol. 25, no. 1, p. 19, 2021, doi: 10.7812/TPP/19.200.

[158] M. Whirl-Carrillo *et al.*, “An Evidence-Based Framework for Evaluating Pharmacogenomics Knowledge for Personalized Medicine,” *Clin Pharmacol Ther*, vol. 110, no. 3, pp. 563–572, Sep. 2021, doi: 10.1002/cpt.2350.

[159] O. Devinsky *et al.*, “Cannabidiol: pharmacology and potential therapeutic role in epilepsy and other neuropsychiatric disorders.,” *Epilepsia*, vol. 55, no. 6, pp. 791–802, Jun. 2014, doi: 10.1111/epi.12631.

[160] “CBD Extraction Methods & Process Explained | Zebra CBD.” Accessed: Aug. 28, 2024. [Online]. Available: https://zebracbd.com/blogs/cbd-education/cbd-extraction-methods

[161] S. B. Hawthorne, C. B. Grabanski, E. Martin, and D. J. Miller, “Comparisons of Soxhlet extraction, pressurized liquid extraction, supercritical fluid extraction and subcritical water extraction for environmental solids: recovery, selectivity and effects on sample matrix,” *J Chromatogr A*, vol. 892, no. 1–2, pp. 421–433, Sep. 2000, doi: 10.1016/S0021-9673(00)00091-1.

[162] V. K. Madan, “Supercritical Carbon Dioxide as Greener Solvent of 21st Century,” *Asian Journal of Chemistry*, vol. 30, no. 4, pp. 719–723, 2018, doi: 10.14233/ajchem.2018.21150A.

[163] J. Dai and R. J. Mumper, “Plant phenolics: extraction, analysis and their antioxidant and anticancer properties.,” *Molecules*, vol. 15, no. 10, pp. 7313–52, Oct. 2010, doi: 10.3390/molecules15107313.

[164] F. J. Tiago, A. Paiva, A. A. Matias, and A. R. C. Duarte, “Extraction of Bioactive Compounds From Cannabis sativa L. Flowers and/or Leaves Using Deep Eutectic Solvents.,” *Front Nutr*, vol. 9, p. 892314, 2022, doi: 10.3389/fnut.2022.892314.

[165] K. Nedić Grujin, T. Lužaić, L. Pezo, B. Nikolovski, Z. Maksimović, and R. Romanić, “Sunflower Oil Winterization Using the Cellulose-Based Filtration Aid-Investigation of Oil Quality during Industrial Filtration Probe.,” *Foods*, vol. 12, no. 12, Jun. 2023, doi: 10.3390/foods12122291.

[166] B. N. Taylor, M. Mueller, and R. S. Sauls, “Cannaboinoid Antiemetic Therapy,” *StatPearls*, Aug. 2023, Accessed: Jul. 01, 2024. [Online]. Available: https://www.ncbi.nlm.nih.gov/books/NBK535430/

[167] E. and M. National Academies of Sciences, H. and M. Division, B. on P. H. and P. H. Practice, and C. on the H. E. of M. A. E. R. and R. Agenda, “Therapeutic Effects of Cannabis and Cannabinoids,” Jan. 2017, Accessed: Jul. 01, 2024. [Online]. Available: https://www.ncbi.nlm.nih.gov/books/NBK425767/

[168] S. Vučkovic, D. Srebro, K. S. Vujovic, Č. Vučetic, and M. Prostran, “Cannabinoids and Pain: New Insights From Old Molecules,” *Front Pharmacol*, vol. 9, no. NOV, Nov. 2018, doi: 10.3389/FPHAR.2018.01259.

[169] “CBD for Seizures- Use, Effectiveness, Side Effects, and More.” Accessed: Jul. 01, 2024. [Online]. Available: https://www.neurocenternj.com/blog/cbd-for-seizures-use-effectiveness-side-effects-and-more/

[170] K. Nichol, C. Stott, N. Jones, R. A. Gray, M. Bazelot, and B. J. Whalley, “The proposed multimodal mechanism of action of cannabidiol (CBD) in epilepsy: modulation of intracellular calcium and adenosine-mediated signaling (P5.5-007),” *Neurology*, vol. 92, no. 15_supplement, Apr. 2019, doi: 10.1212/WNL.92.15_SUPPLEMENT.P5.5-007.

[171] A. C. Parikh, C. S. Jeffery, Z. Sandhu, B. P. Brownlee, L. Queimado, and M. M. Mims, “The effect of cannabinoids on wound healing: A review,” *Health Sci Rep*, vol. 7, no. 2, Feb. 2024, doi: 10.1002/HSR2.1908.

[172] A. Oláh *et al.*, “Cannabidiol exerts sebostatic and antiinflammatory effects on human sebocytes.,” *J Clin Invest*, vol. 124, no. 9, pp. 3713–24, Sep. 2014, doi: 10.1172/JCI64628.

[173] I. Ahmed *et al.*, “Therapeutic Attributes of Endocannabinoid System against Neuro-Inflammatory Autoimmune Disorders,” *Molecules*, vol. 26, no. 11, p. 3389, Jun. 2021, doi: 10.3390/molecules26113389.

[174] P. Shah *et al.*, “Cutaneous Wound Healing and the Effects of Cannabidiol,” *Int J Mol Sci*, vol. 25, no. 13, p. 7137, Jun. 2024, doi: 10.3390/ijms25137137.

[175] “EPIDIOLEX® (cannabidiol) - FDA-Approved Prescription Cannabidiol (CBD).” Accessed: Jul. 03, 2024. [Online]. Available: https://www.epidiolex.com/

[176] “What Is Sativex? (Nabiximols) - MS Treatments | MS Society.” Accessed: Sep. 15, 2024. [Online]. Available: https://www.mssociety.org.uk/living-with-ms/treatments-and-therapies/cannabis/sativex

[177] T. Farias, “DESENVOLVIMENTO E CARACTERIZAÇÃO DE MEMBRANAS DE POLI (ε - CAPROLACTONA) ELETROFIADAS E MODIFICADAS COM HEPARINA E ÁCIDOS GRAXOS ESSENCIAIS PARA APLICAÇÃO BIOMÉDICA.”

[178] A. H. Fischer, K. A. Jacobson, J. Rose, and R. Zeller, “Hematoxylin and eosin staining of tissue and cell sections.,” *Cold Spring Harb Protoc*, vol. 3, no. 5, May 2008, doi: 10.1101/PDB.PROT4986.

[179] “Bancroft, J.D. and Gamble, M. (2008) Theory and Practice of Histological Techniques. 6th Edition, Churchill Livingstone, Elsevier, China. - References - Scientific Research Publishing.” Accessed: Sep. 12, 2024. [Online]. Available: https://www.scirp.org/reference/ReferencesPapers?ReferenceID=1582193

[180] “Van Gieson’s Stain - an overview | ScienceDirect Topics.” Accessed: Sep. 12, 2024. [Online]. Available: https://www.sciencedirect.com/topics/medicine-and-dentistry/van-giesons-stain

[181] S. Amin, P. Yang, and Z. Li, “Pyruvate kinase M2: A multifarious enzyme in non-canonical localization to promote cancer progression,” *Biochim Biophys Acta Rev Cancer*, vol. 1871, no. 2, pp. 331–341, Apr. 2019, doi: 10.1016/j.bbcan.2019.02.003.

[182] S. Y. Lunt and M. G. Vander Heiden, “Aerobic Glycolysis: Meeting the Metabolic Requirements of Cell Proliferation,” *Annu Rev Cell Dev Biol*, vol. 27, no. 1, pp. 441–464, Nov. 2011, doi: 10.1146/annurev-cellbio-092910-154237.

[183] “Lactate Dehydrogenase - an overview | ScienceDirect Topics.” Accessed: Sep. 12, 2024. [Online]. Available: https://www.sciencedirect.com/topics/neuroscience/lactate-dehydrogenase

[184] K. W. Finnson, S. McLean, G. M. Di Guglielmo, and A. Philip, “Dynamics of Transforming Growth Factor Beta Signaling in Wound Healing and Scarring,” *Adv Wound Care (New Rochelle)*, vol. 2, no. 5, p. 195, Jun. 2013, doi: 10.1089/WOUND.2013.0429.

[185] “Vasculotropin Receptor 2 - an overview | ScienceDirect Topics.” Accessed: Sep. 12, 2024. [Online]. Available: https://www.sciencedirect.com/topics/pharmacology-toxicology-and-pharmaceutical-science/vasculotropin-receptor-2

[186] A. E. Stoica, A. M. Grumezescu, A. O. Hermenean, E. Andronescu, and B. S. Vasile, “Scar-Free Healing: Current Concepts and Future Perspectives,” *Nanomaterials*, vol. 10, no. 11, p. 2179, Oct. 2020, doi: 10.3390/nano10112179.

[187] T. Bíró, B. I. Tóth, G. Haskó, R. Paus, and P. Pacher, “The endocannabinoid system of the skin in health and disease: novel perspectives and therapeutic opportunities,” *Trends Pharmacol Sci*, vol. 30, no. 8, pp. 411–420, Aug. 2009, doi: 10.1016/j.tips.2009.05.004.

[188] C. Leal *et al.*, “Potential application of grape (Vitis vinifera L.) stem extracts in the cosmetic and pharmaceutical industries: Valorization of a by-product,” *Ind Crops Prod*, vol. 154, p. 112675, Oct. 2020, doi: 10.1016/j.indcrop.2020.112675.

[189] A. Couturier, C. Calissi, J.-L. Cracowski, D. Sigaudo-Roussel, C. Khouri, and M. Roustit, “Mouse models of diabetes-related ulcers: a systematic review and network meta-analysis,” *EBioMedicine*, vol. 98, p. 104856, 2023, doi: 10.1016/j.ebiom.2023.104856.

[190] A. Jodheea-Jutton, S. Hindocha, and A. Bhaw-Luximon, “Health economics of diabetic foot ulcer and recent trends to accelerate treatment,” *The Foot*, vol. 52, p. 101909, Sep. 2022, doi: 10.1016/J.FOOT.2022.101909.

FACULDADE DE **MEDICINA**